Doctoral Dissertation
Doctoral Program in Chemical Engineering (30th Cycle)

Antimicrobial functionalization of technical textiles
for medical, aerospace and civil applications

By

Muhammad Irfan

******

Supervisors:
Prof. Monica Ferraris
Prof. Ada Ferri

Doctoral Examination Committee:
Prof. Giuseppe Rosace, Università di Bergamo, Italy
Prof. Simoncic Barbara, University of Ljubljana, Slovenia
Prof. Tanveer Hussain, National Textile University, Pakistan
Prof. Alberto Tagliaferro, Politecnico di Torino, Italy
Prof. Luigi Manna, Politecnico di Torino, Italy

Politecnico di Torino
2017

Declaration

I hereby declare that, the contents and organization of this dissertation constitute my own original work and does not compromise in any way the rights of third parties, including those relating to the security of personal data.

Muhammad Irfan

2017

I would like to dedicate this thesis to my loving parents whose prayers were always with me throughout my life

Acknowledgment

This journey to PhD started, five years ago, with the award of MS leading to PhD scholarship from Higher Education Commission (HEC) of Pakistan. Politecnico di Torino (PoliTo) Italy, one of the leading and reputable universities in the world, was the destination to start and finally finish this journey.

The invaluable, memorable and the most productive part of this journey was to work under the supervision of Prof. Monica Ferraris and Prof. Ada Ferri. Both of them are kind, affectionate, supportive and encouraging to all those working with them. I am highly thankful to them for providing me the opportunity to work under their supervision in an environment conducive for learning, growth and acquiring new skills. In fact, as supervisors, they will be my role model in my future academic career. I express my sincere gratitude to Dr. Sergio Perero and Dr. Cristina Balagna also, my immediate supervisors, for their indispensable support during this research work. I am grateful to Dr. Marta Miola also for her valuable support in conducting antibacterial tests for this study. The cooperation from Prof. Francesca Bosco and Dr. Chiara Mollea is also highly acknowledged, as part of the antibacterial tests were carried in their group. I am also thankful to Dr. Piela Roberta for her support during my activities at "Laboratorio Alta Technologia Tessile 1, Biella (LATT1)". I am grateful to numerous other colleagues and members of the group who helped me in my routine activities during last three years which helped successfully accomplishing this PhD thesis.

Most importantly, the moral support and encouragement from my family (my parents, wife and my little daughters) was crucial in accomplishment of this task. Especially my wife, Namrina Tubassam, who proved a source of strength not only for me but also for my entire family.

Abstract

Textiles, today, are no more just traditional textiles. With the advancements in nano and fiber technology, they find various technical applications and are known as technical textiles. Antimicrobial functionalization is an integral requirement for some of these applications that include medical textiles, aerospace textiles and textiles used in filtration. Various organic and inorganic antimicrobial agents are being explored for antimicrobial functionalization of textiles with the objective to obtain effective, durable and broad spectrum antimicrobial properties. However, these antimicrobial agents may have their own advantages and disadvantages. Some of them may lack broad spectrum antimicrobial properties as well as complex method of their synthesis and application which may not always be environmental friendly.

Silver is well known inorganic antimicrobial agent with effective antimicrobial action against broad spectrum of microbes. Silver is being intensively studied in nano particle form for the functionalization of textiles. However, mostly the synthesis and application of silver nano particles to textiles is carried through wet routes. These may have environmental considerations due to possible use of toxic reducing and stabilizing agents. In addition their solution or colloidal based application to textiles is intense in water and energy consumption along with production of waste water and necessitating its treatment. This may not help reduce environmental burden of textile industry which is regarded as one of the most polluting industrial sector of the world. Therefore, along with providing antimicrobial protection, the process of obtaining antimicrobial textiles itself should not create adverse environmental impact.

In this context, ecofriendly processes for textile industry have always been in focus of research. The objective of this thesis was to achieve "antimicrobial functionalization of technical textiles for medical, aerospace and civil applications"

via a simple and single step environment friendly technique known as radio frequency "co-sputtering". Sputtering is a plasma based process and is mostly used in automotive, tools and electronics industry. It is not yet fully explored in textile industry. This study aimed at obtaining antimicrobial textiles via co-sputtering and exploring some of the its key strengths and weaknesses for textiles.

In the adopted co-sputtering technique, an antimicrobial silver nano clusters/silica composite coating was deposited on four different textile substrates. The deposition parameters of both silica and silver were controlled independently such that silica constituted the matrix of the composite coating and silver was deposited in the form of nano clusters embedded in the silica matrix. The four textile substrates used in this study were: cotton fabric intended for medical applications, high performance Kevlar® and Vectran® fabrics for aerospace applications and activated carbon fabric (ACF) to be used in air filtration.

The morphology and composition of the deposited coating was investigated in detail using FESEM, EDX and XPS which showed that silver nano clusters (25-50 nm) were uniformly distributed and firmly embedded in the silica matrix. Total silver concentration in the composite coating was evaluated through ICP_MS and was found to be dependent on deposition time and thus on coating thickness. Silver ion release test in water and in artificial sweat showed a progressive and gradual release of silver ions, beneficial for prolonged antimicrobial activity. The nature of the fabric substrate was also found to influence the release of silver ions. The coating showed effective antimicrobial properties against Gram positive (*S. aureus, S. epidermidis*), Gram negative (*E. coli*) bacteria and fungus (*C. albicans*) with varying intensity of the action depending upon the microbe as well as silver ion release profiles. Water contact angle and sorption tests revealed hydrophilic nature of the coating. Moisture management properties evaluated by Moisture Management Tester showed that coating imparted fast absorbing and quick drying characteristic to the fabric. The coating was highly conformal and did not altered air permeability of the substrates which is a highly desirable characteristic to preserve thermo physiological comfort of

the fabric as well as maintain filtration capacity of ACF. However, the washing stability of the coating was found not to be completely satisfactory.

The work was carried with in the frame wok of an Italian regional project with several other project partners. Some results from these partners, duly acknowledged, are also discussed in this thesis and summarized in conclusion.

Overview of the Thesis

↓

Abstract

↓

Chapter 1
This chapter highlights the need for antimicrobial coating on textiles for different applications foreseen for the textile substrates used in this study and defines the objective of the thesis

↓

Chapter 2
This chapter describes the state of the art about different most commonly used antimicrobial agents for textiles and their application techniques. Emerging coating techniques were also in focus that are currently at research scale but have potential to be commercialized

↓

Chapter 3
This chapter provides the "Experimental" part of the thesis discussing briefly the textile substrates used in this study, coating deposition technique and all the characterizations performed

↓

Chapter 4
All the results of the thesis are presented in this chapter. Results are grouped separately for each textile substrate used in this study and are annexed with a combined discussion at the end

↓

Conclusion and future insights

Contents

List of Figures

List of Tables

Chapter 1

Objective of the thesis

This chapter describes briefly the necessity to impart antimicrobial properties to textiles for various technical applications and objective of the thesis. The need for antimicrobial properties for various textiles, used in this study (natural and high performance fabrics), is discussed with respect to the intended applications. The importance of the processes for achieving antimicrobial functionalization is highlighted with respect to environment friendliness of process as well as impact of the process on bulk properties of textiles.

1.1 Need for antimicrobial textiles

Microbial contamination is key issue of concern in various areas including health care infrastructures, medical devices, food packaging and storage, personal and protective clothing and other house hold products [1]. Microbes are found everywhere and can grow easily when suitable moisture, temperature and nutrient media is available. Textiles provide conducive environment for their growth. Natural fibers, for example wool (proteins) and cotton (carbohydrates), are more susceptible to microbial attacks than synthetic fibers as they can provide nutrients and source of energy to the microbes under favorable conditions. Microbial attack can develop bad odor, discoloration of the textile and potentially deteriorate the textile itself [2].

Other than inherent ability of textile materials to absorb moisture, textile structures offer high surface area and hence ability to retain moisture [3] that put even synthetic fibers susceptible to microbial attacks and biofilm formation. Today, with the invention of high performance fibers and advancements in nano technology as well as improved performance of traditional fibers and textiles due to wide variety of functional and protective coatings, textiles find their

applications in wide range of technological fields rather than being simple traditional textiles. These textiles are better known as technical textiles as their primary function is to deliver technical value and their aesthetic and decorative properties are not important [4]. Some categories of these textiles requiring antimicrobial properties are discussed below.

1.1.1 Medical textiles

Medical textiles are one of the categories of technical textiles. Combination of strength and flexibility of textiles have been utilized to design products that can meet the requirements of medical and surgical end use. Medical textiles include products that range from simple yarns (mono and multifilament) and fabrics (woven, knitted and nonwoven ets) to complex composite structures [5]. Medical textiles can be broadly classified into four categories: (1) non implantable materials, e.g bandages, plasters, wound dressings, (2) implantable materials, e.g sutures, artificial joints, vascular grafts, (3) extra corporeal devices, e.g artificial kidney and liver ets, (4) healthcare and hygiene products, e.g clothing, bed sheets, gowns and wipes [5].

Clothing and gowns of the nursing staff is one of the possible source of contamination and infection to other patients as they can carry bacteria [5]. It is estimated that nosocomial infections cause three million deaths per year and 1 out of 10 patients in Europe get hospital acquired infections [6]. Since textile products are common in the hospital environment and are also in close contact with patients and health care personals, they can easily be contaminated with different microbes originating from different body fluids of patients and transported with the carrier to others [6].

1.1.2 High performance textiles for aerospace applications

The application of textiles in various high tech areas including aerospace, automotive, protective clothing, textile reinforced composites and wind mills etc, has also increased with the development of high performance fibers. High performance fibers have excellent mechanical properties, thermal and chemical resistance combined with flexibility which is characteristic of textile materials and structures. Kevlar®, Vectran®, Spectra® and Zylon® are some of the examples of these fibers [7].

Light weight, strong and flexible structures are of particular importance when it comes to space missions and protection from microbes is of great importance in aerospace applications of high performance textiles. Inflatable habitat module for space stations is an excellent example exploiting these properties of high performance polymeric fibers. This module is designed to occupy small room and

has minimal payload on the rocket during launch and after being in space can be expanded to provide more volume to the astronauts to live and work. The first inflatable habitat module known as "Bigelow Expandable Activity Module (BEAM)" shown in Figure 1, has been attached in April 2016 to the International Space Station (ISS) [8]. It consists of aluminum structure with two metal bulkheads and multiple layers of fabrics with spacing between the layers protecting an internal restraint layer. Vectran® and Kevlar® are ideal candidates to be used in its construction [9]. This module will undergo investigations over a period of two years of test mission. During this period, astronauts will spend few hours from time to time to collect sensor data and surface samples to evaluate its performance regarding protection against solar radiation, extreme temperatures and space debris. The surface samples collected by the crew will be analyzed to assess microbial growth in the inflatable module [10].
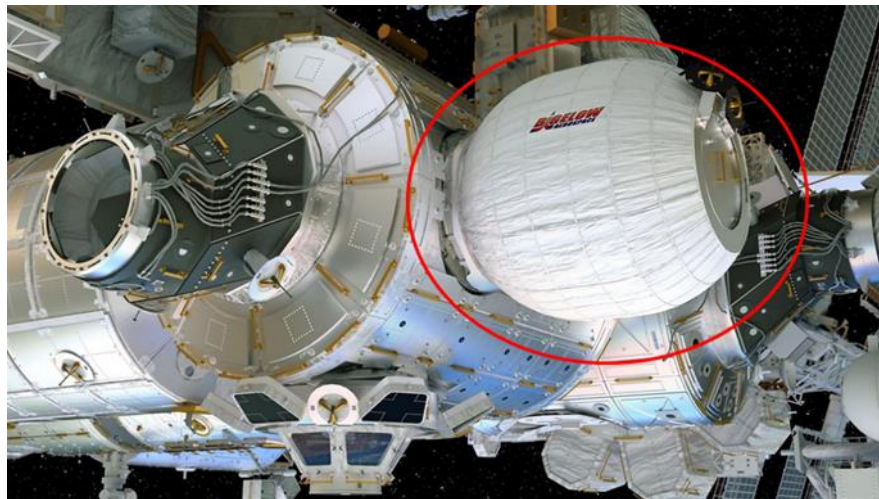
Figure 1: Inflatable habitat module "Bigelow Expandable Activity Module (BEAM)" attached to the ISS in 2016, image source NASA website [8]

Several studies have confirmed the presence of different types of bacteria in space. The presence of bacteria can pose not only health threats to the astronauts but can trigger degradation of different materials of the space station including polymers. *Novika et al.* [11] reported the results of a six year study, conducted on 554 samples collected from air and surfaces of ISS, for the presence of bacteria. They reported a total of 36 bacterial species recovered from surface samples whereas 15 bacterial species were found in the air samples. Various fungal species were also found in the samples collected from surfaces and air of the ISS. 32 fungal species were detected in the samples from the surfaces whereas 5 fungal species were recovered from air samples. Some of the species that can cause polymer deterioration and be corrosive for metals were also detected, however,

the concentration of all of these bacterial and fungal species have been reported to be less than the permissible limits [11].

Several factors can increase the threat of infection caused by microbes during space missions. Bacterial growth may increase in microgravity and may require increased minimum inhibitory concentration of antimicrobial agents. Human immune system may also change during space travel [12]. Most of the water as well as air is reclaimed in space stations and relative crowded conditions can further increase the risk of microbial infection [13]. Most of these studies address disease causing (pathogen) bacteria. However, the ability of these pathogenic bacteria to survive and affect a host or the others is also partly dependent on the existence of nonpathogenic bacteria in the host or the others. It was reported that most of the human related built environment associated nonpathogenic bacteria behave similarly, regarding their growth patterns, both on earth and onboard International Space Station (ISS). *Coil D.A. et al.* [14] studied the growth of 48 nonpathogenic bacterial strains on ISS that were collected from different built environments on earth and sent to the ISS via Falcon 9 v1.1 rocket in April 2014. They reported that 45 out of 48 bacteria showed similar growth behavior and kinetics both on earth and at ISS. Since environmental conditions in ISS are maintained close to that of on earth, vast majority of bacteria behaved similarly in space and on earth [14].

Bacterial and fungal species found in space station may have the potential to deteriorate polymeric materials. Polymeric materials used in electronics circuits and fiber reinforced composites are susceptible to bio deterioration as they can support bio film formation by providing organic carbon as a nutrition source. Biofilm formation and possible deterioration of polymeric materials have been assessed using qualitative tests but loss of mechanical integrity has not yet been assessed as currently available methods for mechanical characterization are not applicable due to very slow biodegradation rates [15].

Despite these microbial threats, continuous improvements and effective measures have contributed to provide safe environment in the space stations [13]. Therefore, the increased use of textile fabrics, made of high performance fibers, in aerospace applications highlights the importance of antimicrobial coatings on these fabrics to provide biologically safe environment in space. The Kevlar® and Vectran® woven fabrics used in this study were intended to be used in aerospace applications, especially in the inflatable habitat module. However, very little has been reported on antimicrobial functionalization of fabrics made of high performance fibers as most of the work in literature is focused on antimicrobial coating of traditional textiles made of cotton, polyester, nylon etc.

1.1.3 Textiles in filtration

Various types of textile based woven and non-woven materials are used in water and air filtration. Among these materials, activated carbon fibers and fabrics constitute an important category. Activated carbon fibers and fabrics (ACF) are known for their high specific surface area as a result of surface porosity and excellent adsorption capabilities due to which they are widely used in waste water treatment and air filtration. However, ACF may support the growth of different microbes on its surface which reduces its adsorption capacity as well as becoming itself a source of contamination [16]. The intended application of the activated carbon fabric used in this study was air filtration to improve the quality of air for personal use, in various transportation systems and particularly closed environments like space stations.

1.2 Antimicrobial functionalization of textiles: Process perspective

Various antimicrobial agents and coating techniques have been studied for antibacterial functionalization of textiles as are described in detail in the next chapter. Most of these textile treatments and coating techniques involve wet processes. These processes rely on heavy water and energy consumption and hence produce waste water containing potential hazardous chemicals. This implies additional costs for waste water treatments or danger of being released to the environment. Moreover, subsequent drying process for the textiles becomes compulsory and this increases the overall cost of the process.

Among all industrial sectors, textile industry is known to be the most polluting sector in terms of high volumes of water consumption and waste water production. Waste water produced by textile processes is complex and diverse due to wide variety of fibers, dyes, process auxiliaries, and finishing treatments [17]. Additionally, concern over environment friendliness of textile processes has increasingly grown up as guidelines by environment control authorities has become more and more stringent [18]. This provides a driving force for innovations in textile processes and technologies.

Most of the water consumption takes place in dyeing and finishing of textiles which may vary from 70 - 250 l/kg fabric depending on textile process being applied. The amount of chemicals used may vary from 10% to 100% on the weight of the fabric whose residues end up in the waste effluent of textile processes raising environmental concerns. Textile processes also produce other hazardous solid and air pollution. However, waste water production stands high

among all other waste streams in textile industry [19]. Therefore, more research efforts are focused on textile process improvements and innovations.

The focus of process developments shifted from pre-2000 approach of mass production, consistency and profitability to the process innovations having less impact on environment. The terms "carbon and water footprints" replaced old terminology, for examples "liter per kilogram" for water consumption, to express environment friendliness of textile processes to quantify the impact on environment so that everything cannot be dressed up as green. This will finally lead to lowering the overall costs as process innovations will reduce the costs related to heavy water and energy consumption, waste water treatment and air emissions [20].

It is due to this reason that projects focusing on innovations in textile manufacturing and finishing processes with respect to water and energy consumption are increasingly gaining funding from public and private organizations. A project by North Carolina State University College of Textiles was awarded recently with research grant from Walmart Foundation. The project aims at designing a sustainable commercial textile dying method with 95% saving in water and energy without producing effluent. The fabric will be dyed in single step by converting the dye bath into a foam and eliminating the need of washing and drying [21]. Companies advertise the ability of their textile processing machinery to eliminate the need of additional processes as their competitive edge. Albergo digital textile printer by Kornit is an example [22]. The company claims to challenge the textile industry status quo as their roll to roll digital printer can print the fabric in a single step with no need of pretreatment and post printing washing. The fabric can be printed in shortest possible time saving water and energy and thus bringing the whole printing line in a single step.

Summing up, more research has been focused on ecofriendly processes that can potentially replace traditional processes. In this regard research addresses following main areas: (1) reduction in water and energy consumption, (2) heat recovery, (3) water reuse in textile processes, (4) efficient utilization of materials and avoiding hazardous chemicals. Since presence of some species in textile waste water, as highlighted in literature, may lead to problems in waste water treatment plants due to inhibition of microbial activity. Therefore, research is also addressing the substitution of hazardous chemicals with nonhazardous or at least chemicals with relatively less hazard potential to be used in textile processes [19]. In addition, presence of metal nano particles, from residual textile processes, may affect the efficiency of biological treatment plants leading to their failure. On the contrary, with the advancements in nano technology, the use of metal

nanoparticles has increased in textile products to achieve desired properties. This has exaggerated the risk of more contaminants in textile waste streams. Therefore, other than substitution of hazardous chemicals and wet processes improvements to reduce water consumption and waste water production, completely dry processes are of particular interest especially for finishing treatments of textiles. Plasma based processes are one of the most attractive emerging alternatives for traditional wet textile finishing treatments that can deliver promising benefits regarding these issues.

Plasma based processes has long been used to modify and functionalize the surfaces of various substrates. Wide variety of plasma processes are available both at low and atmospheric pressures. Initially in the field of textiles, plasma was used primarily to activate the surface of the textiles by generating radicals to assist and promote subsequent wet chemical processes. Today, single step plasma based processes have been developed that can be used to apply different textile finishes and coatings thus eliminating the need of additional processes. In addition, chemical inertness and high crystalinity of some high performance fibers like Kevlar$^®$ and Vectran$^®$ may make it difficult to apply finishes through traditional processes involving organic reactions [23]. However, plasma processes can easily modify or functionalize the inert surfaces and are limited to top 100 nm of the surface and thus bulk properties of the textiles are preserved [24]. Depending upon the type of the plasma gases and precursors that are fed, different surface treatments ranging from mere surface etching to physical sputtering to plasma polymerization can take place on the surface of the textile substrates [24].

Plasma etching, surface functionalization and plasma polymerized coatings are intensively studied and equipment can be found commercially, although not widely accepted, for textile industry. However, plasma based metallic deposition techniques, for example sputtering, are not yet fully exploited in the field of textiles. Sputtering is a Physical Vapor Deposition (PVD) technique, extensively used to deposit a variety of coatings ranging from thin films in electronics to hard coatings. Sputter depositions, although widely reported on metallic and glass substrates, were rarely reported on textiles [25] [26]. However, an increase in number of publications on textile functionalization using sputtering has been observed during past few years due to its environment friendly nature and diversity of functional coating that can be applied. Nevertheless, the number of these publications are far less than those reported for textile functionalization using wet processes. This thesis work focuses on antimicrobial functionalization of *technical textiles* via sputtering.

1.3 Requirements for antimicrobial coatings

Ideally, antimicrobial coating or finish should fulfill the following key requirements [2]: (1) it should be effective against a wide variety of microbes including various bacterial and fungal species, (2) it should be nontoxic to humans, (3) the coating should be durable to laundering, (4) it should not deteriorate textile properties (5) coating method should be environment friendly. Practically it is difficult to combine all these characteristics in single process. Especially, durability to repeated washing is perhaps the greatest challenge. However, it is equally important for the coating process to be environment friendly as it should not release harmful and toxic substances to the environment. Moreover, the process should be efficient in water usage and energy consumption.

1.4 Objective of the thesis

The objective of this study was to achieve effective antimicrobial coating on technical textiles, while preserving typical bulk properties of textiles, via an ecofriendly Radio Frequency (RF) co-sputtering technique. The research work of this thesis was partially carried in the frame work of an Italian project named

"MARTe- Materiali Antibatterici (per) Rivestimento (di) Tessuti (PAR FSC 2013 Asse I- Innovazione e P.M.I. Interventi a sostegno dei Poli di Innovazione)"

The deposited coating was a composite coating comprised of silver nano clusters embedded in the silica matrix obtained via co-sputtering. Different metals in free state or in the form of compounds exhibit antimicrobial effect against microbes at very low concentrations. Silver has antimicrobial performance reported against a wide variety of microbes and has also been known and used as antibacterial agent throughout history [27]. Silica was used to provide the matrix of the composite coating as it has good thermal stability, biocompatibility and it is nontoxic and inert. These properties of silica make it ideal candidate to be used as matrix to achieve additional functionalities by incorporating active agents in it [28]. Additionally, embedding functional agents in the silica matrix can provide stability against chemical attacks, light and heat [29] whereas polymeric antibacterial agents may reduce the thermal stability of the treated fabric [30].

Silver can either be applied on the surface of natural and synthetic fibers during finishing and coating or it can be incorporated into the polymer matrix of the synthetic fibers before extrusion. Incorporation of silver in the matrix of the fibers can limit its availability for biocidal action whereas surface treatments of textiles with metals through wet process also have serious technical and environmental considerations [2]. Moreover, most of the surface treatments of

textiles with metal nanoparticles are multistep processes [6] involving synthesis of metal nanoparticles and their application method which are not always environmental friendly. Most of these processes involve reducing agents, stabilizers and other chemical auxiliaries that may be hazardous along with necessity of high water usage and thus waste water production. In addition, application of Ag NPs from a solution may not give uniform results depending upon the nature of the textile substrates. Silver uptake from a solution is favored by amorphous structure and the presence of functional groups on fiber surface. Due to this reason hydrophilic fibers can absorb greater amount of silver particles than hydrophobic fibers [31]. Coating by sputtering may offer solution to these problems and this work will provide an evidence that uniform application of silver nanoclusters on different fabric surfaces can be achieved irrespective of the nature of fabric substrate. This thesis work will exploit the potential of the silver nanoclusters/silica composite coating on textile substrates and explore the key strengths and weaknesses of the deposition technique on textiles. The coating is obtained through novel co-sputtering technique of silver and silica originally developed by "GLANCE" group at Politecnico di Torino and previously studied on other substrates.

Chapter 2

Antimicrobial textiles: state of the art

This chapter will provide a state of the art description of the different types of antimicrobial agents most commonly used in the textile industry. The merits, demerits and possible mechanism of action of these agents is highlighted. Various textile surface modification processes are also described. An attempt has been made to incorporate latest advancements and research trends in the application of these antimicrobial agents to textiles. Since silver was the antimicrobial agent used in this study, therefore, it has been discussed in detail. Latest trends in the synthesis of silver nano particles for textile applications, their release behavior from textiles in different types of fluid (water, artificial sweat, soap etc) has been discussed with reference to available literature.

2.1 Two broad categories of antimicrobial coatings

Antimicrobial coatings can be broadly divided into two categories namely leaching and non-leaching type of coating depending upon whether the antimicrobial agent leaches from the coating or is permanently attached to the surface. In leaching type of antimicrobial materials, the agent responsible for the antimicrobial action is leached into the surrounding for killing the pathogens through chemical interaction. These kind of antimicrobial agents require minimum inhibitory concentration (MIC) of the leached antimicrobial agent for the antimicrobial action to occur. Below this concentration no antimicrobial action occurs and antibiotic resistance can develop in microorganisms after repeated exposure to these antibiotics. Leached agents can also cause sensitization to the

patient when applied in medical applications [32]. Another disadvantage of leaching antimicrobial agents is that these are not usually chemically linked to the fabric surface, therefore, they cannot withstand repeated washing processes and their antimicrobial efficiency is dependent on the concentration of these agents present on the textile surface [33].

In non-leaching type of antimicrobial materials, the antimicrobial agent or additive is bound to the surface or the polymer. These bio active materials work only when the microbes come in direct contact with the surface of these materials. Their mode of action depends on the physical interference with the bacterial structures that destroys bacterial cell wall and cell structure due to direct contact of the bacteria to the antibacterial surface. However, their exact mode of action is not exactly known. Another benefit of non-leaching antimicrobial materials is that they are not yet reported to increase microbial resistance [32]. Majority of the antibacterial agents used in textile industry are of leaching type. Consequently, antibacterial activity is not durable due to gradual release of active agent from the coating leading to decrease in its concentration on the textile and finally loss of the antibacterial action [34]. Even in case of non-leaching agents, the antimicrobial activity may decrease due to several reasons including presence of dirt and dead microorganisms [33]. Majority of the coatings applied to textiles are of leaching type where antimicrobial agent leaches from the coating and cause bactericidal action.

2.2 Different antimicrobial agents for textile functionalization

2.2.1 *N*-Halamines

N-Halamines started to be studied as an effective biocidal agent in 1980s. They are interesting as they are nontoxic to humans and are rechargeable [35]. N-Halamines are generally formed by the halogenation of amine, imide or amide groups so that one or more covalent bonds are formed between the halogen and nitrogen. Biocidal activity of these N-Halamines depends on the oxidative properties of these N-halogen bonds. The oxidative reaction occurs when microorganisms come in contact with N-Halamines that leads to inactivation of these microorganisms [36]. Direct transfer of halogen from N-Halamines to the cell membrane of the microorganisms can lead to cell death [33]. There is a variety of N-Halamines but they can be represented by a general structure as follows [37]

```
              X
              |
              N
            /   \
          R1     R2
```
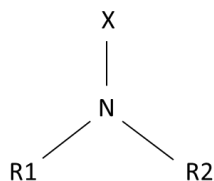
where R1 and R2 can be an organic or inorganic group, Cl, Br or H and X is Cl, Br or I.

The advantage of using N-Halamines is that the consumed halogens can be recharged by another halogenation treatment. It has been shown that the coating recharged even for 50 times exhibit the same level of antimicrobial action as that of freshly applied coating. It is due to this reason that N-Halamines are widely used as disinfectants in different fields [36]. The chlorine loading was found to decrease from 0.35% from unwashed coated cotton to 0.09% after 50 washes for which 51% chlorine loss was restored upon rechlorination [35]. They can be regenerated after treatment with solution of sodium hypochlorite. Their stability in aqueous solutions is very good and are considered to be effective against wide spectrum of microbes [33].

The limitations of traditional wet processes for N-halamine applications, as wet processes consume excessive amounts of monomer resulting in high cost, pollution and health and safety problems, have driven efforts to search for other application routes of N-Halamines on textiles. *Xi G et al.* [33] fabricated N-Halamine coating on plasma activated polyester fabric in a solvent free vapor phase assisted polymerization (VAP) process. In VAP, the initiator is immobilized on the solid surface and monomer is gasified to deposit a thin polymer layer on the surface. The monomer for N-Halamine, 3-allyl-5,5-dimethylhydantoin (ADMH), was heated to vaporize in a vacuum flask in which polyester fabric was hanged. After VAP, the fabric was treated with NaClO solution to obtain halogenized fabric. The treated fabric resulted in 80 % reduction in the growth of *S. aureus* and *E. coli*. More than 60 % bacterial reduction was retained after 30 washing cycles [33]. N-Halamine coating on cotton fabric have also been achieved via LbL coating as will described in the respective section below. The rate of antibacterial activity of so coated cotton fabric has been reported to be higher than other antibacterial agents. It was also shown by the authors that cationic and anionic N-halamine polymers were not irritant to rabbit skin and therefore, suggested to be safe antibacterial agents [35]. In another study N-Halamine chitosan derivative was prepared which was further quaternized to prepare cationic polyelectrolyte which was deposited by LbL method on cotton

fabric. The treated cotton showed 100% bacterial reduction against *S. aureus* and *E. coli* in one minute contact time [38].

N-Halamines, both monomeric and polymeric (cyclic as well as acyclic) have demonstrated durable and regenerable antibacterial functions. However, it has been found that acyclic halamine structure was more vulnerable to hydrolysis during repeated washing as more than 70% of the amide groups were hydrolyzed after 50 washing cycles. Copolymers containing N-halamines have also been synthesized in order to obtain ideal water soluble compounds with improved antibacterial efficacy. Water solubility can make the application process easy and relatively ecofriendly [39]. Various types of N-Halamines having polyacrylate, polystyrene, polysiloxane and poly(oxyethylene)s as polymeric backbones have been reported to be used [40]. *Liu et al.* [39] grafted cotton fabric with a water soluble N-Halamine precursor monomer (3-acrylamidopropyl) trimethylammonium chloride), containing both N-H and quaternary ammonium groups, via radical polymerization. The N-H was then converted to N-Cl by chlorination. Quaternary ammonium compounds themselves have antimicrobial effect and are used as antibacterial agents in textile modifications. Therefore, treated cotton fabric showed bacterial reduction of 96.08 % for *S. aureus* and 48.74% for *E. coli O157:H7* within 30 min contact time which increased to 100 % within contact time of 5 min upon chlorination. The bactericidal action based on oxidative chlorine transfer from N-Halamine to bacteria was much stronger than bactericidal action based on electrostatic interaction between positively charged quaternary ammonium group and negatively charged bacterial cell surface. The advantage of this combination is that a certain level of antibacterial effect, although moderate, will be there because of quaternary ammonium groups even if all the chlorine of N-Halamine is consumed [39].

2.2.2 Chitosan

Chitosan is a biopolymer extensively used for antibacterial functionalization of textiles. It is synthesized from chitin, a polysaccharide and main component of crustaceans shells. Deacetylation of chitin produces chitosan by converting acetyl amine to primary amino groups [41]. The chemical structure of chitosan is given below [42]
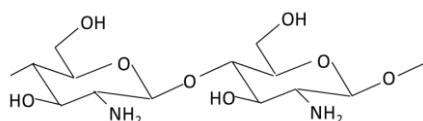
It is known for its unique properties as it is biocompatible, biodegradable, nontoxic and bioactive. Its antibacterial action depends on protonization of its

amino groups due to which it acquires positive charge. The electrostatic interaction between positive charge of the polymer and negative charge on bacterial membrane is considered to be responsible for antibacterial action. Therefore, it displays its antibacterial properties at low pH (<6). In addition, its aqueous solubility is also limited to low pH. This limits its antibacterial properties in alkaline and neutral medium [43]. Moreover, chitosan coatings on textiles have poor durability. Sometime crosslinking agents are used to improve durability of chitosan coatings on textiles [41]. However, crosslinking agents can deteriorate the mechanical properties of natural fibers like cotton [44].

Chemical modification of chitosan can improve its bioactivity and aqueous stability. Quaternization of the amino group of chitosan is one such modification. Quaternary ammonium derivatives can impart positive charge permanently on the polymer backbone. The presence of permanent charge on polymer can improve the binding with the negative charge on the bacterial cell membrane leading to its disruption and cell death. *N,N,N*-trimethyl chitosan (TMC), a quaternary ammonium derivative, was applied to polypropylene and polylactide nonwovens by layer-by-layer (LbL) technique. The fiber surface was first grafted with acrylic acid to give negative charge to the surface to develop electrostatic interaction with TMC. Antibacterial properties of the treated nonwoven fabrics were verified against *S. aureus* [43]. Quaternization of chitosan is also reported with quaternary ammonium compounds (QAC). The grafting of QAC on chitosan may result in increased number of quaternary ammonium groups per chitosan unit. A quaternary ammonium compound, Poly[2-(acryloyloxy)ethyl]trimethyl ammonium chloride, was grafted on chitosan backbone and applied to wool fabric. Wool fabric was first treated with Polystyrene sulphonate to introduce anionic cites on the surface for further grafting cationic chitosan derivative. The treated wool fabric was found effective against *S. aureus* and *Klebsiella pneumoniae*. Pretreatment of wool fabric with styrene sulphonate was important. Without styrene sulphonate pretreatment, the application of chitosan derivative was removed within 5 washing cycles whereas pretreated fabric was reported to maintain antibacterial effect up to 5 washing cycles [45].

In another study, chitosan was modified to chitosan phosphate and applied to cotton fabric in combination with TiO_2 NPs. The treated fabric showed good antimicrobial properties against the tested microbial strains and synergistic effect of both TiO_2 and chitosan phosphate was observed on each other's antimicrobial properties [44]. As antibacterial effect of chitosan alone is not as prominent as other antibacterial agents, its efficiency can be enhanced by combining it with some other antibacterial agents. In this regard, chitosan derivatives with N-Halamines were reported to be very effective in achieving 100 % bacterial reduction in 1 minute contact time [38]. Chemical structure of chitosan is similar

to that of cellulose, another polysaccharide, with the difference that acetylamine group replaces one of the hydroxyl groups in cellulose. Therefore, it is studied a lot for antibacterial functionalization of cotton fibers to obtain tailor made properties but it can cause yellowing and impart stiffness to the fabric due to high weight add on [41].

Generally, chitosan is applied by impregnating the fabric in chitosan solution and then thermally curing it. Environmental considerations in textile finishing has driven the research attention to process innovations that are green and consume relatively less water and energy. *Ferrero F. et al.* applied UV radiation to cure chitosan replacing thermal curing [41]. Cotton fabric coated with UV cured chitosan showed good antibacterial properties. UV curing also improved durability of the chitosan coating. First, the curing was done on dried samples and in inert atmosphere as is required for radical curing because presence of oxygen and wet conditions are considered worse for radical reactions. Later, curing was also done on wet samples and in air in a scaled up process. Total bacterial reduction was achieved with these samples and antibacterial activity remained unvaried even after 30 washing cycles. The authors suggested UV grafting of chitosan as a sustainable process.

2.2.3 Quaternary ammonium compounds

Quaternary ammonium compounds (QACs) are known to have antimicrobial activity since 1930. QAC can induce structural and functional changes in the cell wall and leakage of intracellular components. QACs exhibit antibacterial action by adsorbing and penetrating through bacterial cell wall, binding to lipid and protein members of cell membrane, leakage of intracellular components, protein and nucleic acid degradation and release of autolytic walls [46]. They are reported to be effective over wide pH range and against Gram positive, Gram negative bacteria, molds and yeast [47]. An example of QAC (mono quaternary ammonium salt: alkyltrimethylammonium bromide) is shown below [42]
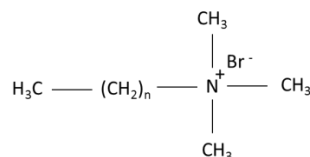
The length of the alkyl chain can influence the antibacterial properties of QACs. The silk fabric coated with quaternary ammonium salt (QAS), via graft radical copolymerization, having alkyl chains of different lengths (C8, C12 and C18) showed different levels of bacterial reduction against *S. areus* and *E. coli* [48]. QAS with longer alkyl chains showed higher level of biocidal action.

Bacteria can adsorb on fabric surface, treated with these cationic biocides, through ionic interaction and alkyl chains can penetrate the cell membrane resulting in inactivation of bacteria. Phospholipids and membrane proteins, with alkyl chain lengths of C12-C20 with two fatty acid ends, are the two main components of the cytoplasmic membrane of the microbes. Due to this reason, longer chain alkyls of QAS can be attached to the surface of microbes in a self-assembled manner through hydrophobic affinity between alkyl chains and phospholipids of bacterial cell membranes leading to higher antibacterial action for QAS with longer chains.

In another study, cotton fabric coated with long chain quaternary ammonium salt hexadecyltrimethyl ammonium bromide was found effective against five fungal strains [29]. Whereas cotton fabric treated with glycidyltrimethyl ammonium chloride (GTAC), a shorter molecule, was not as effective against *P. aeruginosa* (Gram-negative multidrug resistant bacteria) as it was against *S. aureus* (Gram-positive) and *S. typhimurium* (Gram negative) in antibacterial test conducted by colonies forming unit (CFU) method. Further, no inhibition zone was observed in any case in disk diffusion test. However, additional treatment of GTAC treated cotton fabric with silver NPs with a cross linking agent improved the antibacterial efficacy to the extent that it completely killed all the tested bacteria in CFU method and a clear inhibition halo was observed against all the tested bacterial strains in disk diffusion method [30]. This shows that synergy in moderate antibacterial effect of QAS can be achieved by combining them with silver NPs. Possibly, longer chain QAS inactivate bacteria both by binding them to the surface as well as by penetrating the bacterial cell structure [48]. Longer alkyl chains promote hydrophobicity and can have enhanced penetration through hydrophobic bacterial membranes through hydrophobic interaction [47]. On the other hand, shorter QAS may inactivate bacteria mainly by adhering them on the treated surface due to interaction between positive charge on QAS and negative charge on microbial surface [30]. This may lead to less significant antibacterial action of shorter chain QAS which can be improved by Ag NPs incorporation as they can penetrate bacterial cell membrane and thus enhance cell permeability concurrently providing synergy in the effect.

In another study, zinc oxide sol containing diallylmethyl alkyl ammonium bromides, with four different alkyl chain lengths (C12, C14, C18, C18), was applied on cotton fabric [49]. The antibacterial activity, opposite to what was reported in [48], was found to decrease with increase in alkyl chain length of QAS with minimum level for C18-ZnO. The authors attributed the difference in antibacterial effect to particle size and dispersity of ZnO sol and dissolution of ZnO from treated fabric which was found to vary with alkyl chain length. Therefore, longer chain length of QAS may not be the sole cause of decreasing

level of antibacterial effect. Alkyl chain lengths may show different effect on antimicrobial activity of different QACs. A review by *Tischer M* et al discussed in detail the structure-activity relationship of various QACs towards different microbes. The review mentioned that antibacterial activity of QACs vary considerably against different bacterial species and may increase, decrease or have no correlation with varying alkyl chain lengths [46].

QAC have also been applied in combination with other inorganic NPs. Antibacterial finish comprising QAC based TiO_2 was applied via sol-gel route to cotton fabric. The treated fabric showed strong antibacterial effect against Gram positive and Gram negative bacteria, however, washing stability of the coating was not satisfactory [47]. Washing stability of the biocidal coatings is the main issue confronted by almost all types of antimicrobial agents including QAS [30] as QAC may be easily removed by diffusion of water [49]. Washing stability can be improved by formation of non-hydrolysable covalent bond between QAC and the fiber surface. An antimicrobial finish comprising sodium aliginate – QAC complex nano particles applied to cotton fabric was reported to maintain significant antibacterial effect (99% bacterial reduction) after 30 washing cycles. Nano sized colloidal of sodium alginate (SA) and 3-(trimethoxysilyl)propyl-octadecyldimethylammonium chloride (TSA), a quaternary ammonium compound, was synthesized using ionic gelation method with $CaCl_2$ and applied to cotton fabric via pad-dry-cure method. The authors attributed the improved adhesion to covalent bond formation between hydroxyl groups on cotton fiber and silanol groups of SA-TSA nanoparticle complex formed due to partial hydrolysis of trimethoxysilyl groups. In addition authors reported enhanced antibacterial efficiency which they linked to NP formation. NPs of SA-TSA complex may result in high positive charge density for improved electrostatic interaction with negative surface of bacteria and long chain of QAC may promote hydrophobic interaction with cytoplasmic cell membrane [50].

Incorporating the functional agent in organosilicon is one of the approaches to impart some durability to the coating as organosilicon coatings are considered to bind well to the fibers. Applying the same approach, cotton fabric was modified with quaternary ammonium salt and Tetraethoxysilane (TEOS). The treated fabric showed high hydrophobicity due to siloxane layer formed on the surface of cotton fabric but the reported washing stability was not necessarily as good as claimed by the authors [29]. The other potential disadvantage of QAS is that tensile strength of fabrics treated with QAS may be decreased. High temperature curing of QAS can cause a decrease in the tensile strength of the protein fibers like silk due to breakage of peptide bonds at high temperature [48]. Cellulosic fibers were also found to lose tensile strength upon treatment with QAS [29].

2.2.4 Triclosan

Triclosan, diphenyl ether derivative known as 5-chloro-2-(2,4-dichlorophenoxy) phenol, is another synthetic antibacterial agent used in a wide variety of personal care and household cleaning products including textiles. Triclosan is reactive towards chlorine and ozone and photo unstable. As an antibacterial agent, its activity is attributed to the inhibition of lipid synthesis enzymes in microbes whereas some bacteria can also inactivate triclosan and hence it is regarded as biodegradable also [51]. Triclosan is a synthetic odorless chlorinated bisphenol with chemical structure given as follows [42]
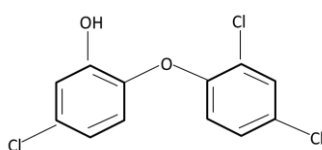
In a comparative study, cotton fabric modified with tetraethoxysilane along with triclosan exhibited higher biocidal activity against five molds than that was shown with tetraethoxysilane alongwith QAC treatment. However, washing performance of the fabric modified with triclosan was very poor as no activity was observed after 5 washing cycles [29].

Although antibacterial properties of triclosan are reported against a range of Gram positive and Gram negative bacteria, it has poor water solubility [51] that can give rise to problems in its formulations and subsequent application to textiles. To improve the solubility and to enhance the binding of triclosan with the fabric, cotton fabric has been treated with triclosan together with a β-cyclodextrin derivative. The modification was carried in two ways. In one cotton fabric was first grafted with monochlorotriazinyl β-cyclodextrin having vynilsulphonic functional group and then soaking the so obtained fabric in triclosan solution. In second approach, solutions of both triclosan and the b-cyclodextrin were mixed first and then grafted on the fabric surface. The fabric modified using second approach was more resistant to washing whereas significant loss of antibacterial activity was observed after two washing cycles for the fabric modified using first approach [52].

The binding of triclosan with synthetic fibers can also be increased after plasma pretreatment of the fabric surface. Plasma treatment can produce surface roughening and induce functional groups on fiber surface that may increase wettability with the applied coating material. Plasma pretreatment of polyester (PET) fabric resulted in increased wet pick up of the triclosan solution and hence increased antibacterial activity was observed compared with the fabric coated with triclosan without plasma treatment [53]. Another approach to increase durability

of the applied finish is to use cross linking agents which are usually small molecules. Crosslinking agents may contain several functional groups which can chemically react with other functional groups on polymeric materials. However, crosslinking agents, for example formaldehyde based, may not be safe and environment friendly. Two polycarboxlic acids, 1,2,3,4-butanetetracarboxylic acid (BTCA) and citric acid (CA), were used as crosslinking agents in the finishing of cotton fabric with triclosan to increase the durability of the finish [54]. The durability of the finish applied using BTCA was much higher than the finish applied with CA as it was able to show 100 % bacterial reduction after 50 washing cycles. BTCA has four carboxlic groups and resulted in high cross linking yield as compared to CA. However, cross linking agents decreased the breaking strength of the cotton fabric. The disadvantage of triclosan is that its higher dosage and long term exposure can cause bacterial resistance to increase. Moreover concerns has been raised over by products obtained by degradation of triclosan in the environment [51].

2.2.5 Natural antimicrobial agents

Natural antimicrobial agents are also gaining attention of the researchers due to different undesired environmental and toxic effects associated with synthetic agents. They are considered to be less toxic and environment friendly as they are biodegradable. They can be obtained from natural resources and include plant extracts, natural dyes and spices. However, they are reported to have non standardized antibacterial effect and are not available in quantities to fulfill industrial requirements. Some of them may also be smelly [45]. Natural antibacterial compounds include polyphenols and phenolics, alkaloids, essential oils, polypeptide, polyacetylenes, lactins and terpenoids [34] [55] [56]. Chitosan, one of the famous antibacterial agents used for textile functionalization, also belongs to this category [45]. With the passage of time, bacterial susceptibility to existing antimicrobial agents is decreasing resulting in evolution of multidrug resistant bacteria [55]. Whereas, antibacterial resistance has not yet been reported against natural agents probably due to their antibacterial action based on multiple mechanisms. Although exact mechanism of action of these agents is not yet fully known, various inhibition mechanisms have been proposed [56].

Various plant based antibacterialextracts have been reported to be used for textiles. Cotton fabric was finished with Aloe vera gel with 1, 2, 3, 4-butanetetracarboxlic acid (BTCA) as cross linking agent and antibacterial properties were verified against *S. aureus* and *E. coli*. High weight add on (7%) of Aloe vera was required for bacterial reduction of up to 99%. At 3% weight add on, bacterial reduction was 90%. Antibacterial activity was decreased to 50% after 8 repeated washing cycles. Other than high weight add on, 44% decrease in the

tensile strength of the fabric was observed [57]. In another study, cotton fabric treated with curcumin (1,7- bis(4-hydroxy-3-methoxyphenyl)-1,6-heptadiene-3,5-dione), a turmeric based natural compound, exhibited antibacterial properties against *S. aureus* and *E. coli* [58]. Extract of Ocimum sanctum leaves (Tulsi) was also applied to cotton and cotton/polyester blended fabric using glutaraldehyde as crosslinking agent and sodium hypophosphite as catalyst. A maximum of 95% and 85% bacterial reduction was achieved against *S. aureus* and *E. coli* respectively. The washing durability of the fabric was reported to be poor [59].

Various plant based dyes also possess antimicrobial properties. Natural dyes rich in naphthoquinones and tennins have been shown to exhibit antifungal and antibacterial properties [34]. Although many of the plants used to extract dyes are described as medicinal, the study of antibacterial potential of the dyes used for textile purposes was not usually considered in the past. Antibacterial properties of 5 different natural dyes available commercially in powder form were evaluated by *Singh et al.* against five common bacteria. Some of the dyes were effective against all the tested bacteria, some were selective in antibacterial action and one showed no activity against any bacterium. However, when these dyes were applied to the wool fabric, the level of their antibacterial effect exhibited in solution form decreased greatly. The authors suggested that dye concentration on fabric could be less than the minimum inhibitory concentration (MIC) of 5-40 μg whereas maximum dye concentration on fabric was reported to be 9.2% on weight of fabric [60]. There are also some disadvantages associated with natural dyes as they impart poor quality colors and show poor fastness properties due to heterogeneity and complexity of their structures. It is also difficult to reproduce different shades [61]. Natural based colors are rich in diverse active compounds including tannins, alkaloids, curcuminoids, quinines and flavonoids. Various plant based extracts based on these active compounds along with various anchoring agents for application to textiles and current challenges have been discussed in a comprehensive review [62].

2.2.6 Metal nano particles

Heavy metals are known to be toxic for microbes at very low concentrations. They can be used either in metallic state or in the form of salts [2]. Since properties of materials change dramatically at nano metric scale, extensive research is being made to exploit unique properties of metal nano particles (NPs). Consequently large number of studies report functionalization of textiles with metal nano particles to achieve antibacterial properties.

Textiles coated with metal NPs also undergo coloration due to localized surface plasmon resonance (LSPR) of metal NPs. Conduction electrons of noble

metal NPs oscillate locally at particular frequency upon interaction with light and is known as LSPR. Since LSPR is sensitive to morphologies of metal NPs, the color of the fabrics can be tuned by controlling this factor. The color of the bamboo pulp fabrics treated with gold and silver NPs varied with the size, content and shape of metal NPs as was reported by *Tang B. et al* [63]. Colors imparted by metal NPs are different from those imparted by dyes. Colors of dyed fabrics originate from chromophores present in the structure of dye molecules where as those of metal NPs are due to LSPR. This can be interesting as dyes are sensitive to photo degradation and hence photo fading whereas metal NPs are expected to be stable to sunlight exposure [63]. Antimicrobial performance of textiles finished with silver, gold, copper and platinum NPs have been investigated [64].

Metal oxide nano particles have also been reported to demonstrate antibacterial properties [6]. TiO_2 NPs are well known for their photo catalytic activity and have chemical and thermal stability. They have been studied for their antibacterial, UV protection and self-cleaning properties [44]. It has been suggested that the surface defects of some metal oxides, e.g MgO and ZnO, are reactive in nature and in wet condition can produce reactive oxygen species (ROS) that can impair the cell structure of the microbes. The generation of ROS by metal oxides can be enhanced at nano metric scale due to increased surface to volume ratio thus making the metal oxide NPs effective antibacterial agents. Cotton fabrics coated with ZnO and CuO NPs showed good antimicrobial properties [6]. CuO NPs are reported to exhibit higher antibacterial effect than that of ZnO [65] and TiO_2 NPs [66]. For some other metal oxide NPs, for example alumina (Al_2O_3), the electrostatic positive charge can possibly disrupt the bacterial membrane thus causing cytotoxic action. However, antibacterial properties of textile fabric coated with Al_2O_3 have been found to be less significant than textiles coated with other metal oxide NPs [67]. Synergy in the antibacterial effect can be achieved by combination of different metal oxide NPs. Cotton fabric treated with TiO_2/CuO/citric acid/polyethylene glycol nano composite showed enhanced antibacterial effect compared to what was observed when CuO an TiO_2 were applied individually [66].

Since silver was used as antimicrobial agent in this study, therefore, detailed discussion has been done in the following section about possible mechanism of antimicrobial action of silver NPs, their synthesis with reference to textile applications and their release from nano silver containing textiles in different relevant fluids (water, artificial sweat and washing solutions).

2.2.6.1 Silver

Among metal NPs, Ag NPs are the most widely used for antibacterial functionalization of textiles as well as in majority of other consumer products [68]. Silver nano particles show highest antimicrobial efficiency compared with other metallic biocides like copper, zinc and titanium [69] and have highest share in consumer products among all other engineered nano materials [70]. Antimicrobial properties of silver against wide variety of microbes are extensively reported in literature. Silver is considered to have relatively low toxicity towards human cells and does not cause skin irritation, argyria and does not disturb the balance of microflora of healthy human skin [31]. However, there is also some evidence of toxicity found to be associated for silver NPs [71].

There has been increased interest in the development of nanoparticles based antibiotics over past few decades. The exact mechanism of antibacterial action of Ag NPs is not yet completely known, however, it is reported to be due to several mechanisms including binding to the cell walls and disrupting them, damaging intracellular and nuclear membrane, damaging respiratory system and denaturing DNA and RNA [72]. The mechanism of Ag NPs toxicity has been found dependent on reactive oxygen species (ROS) generation and oxidative stress. There is debate in literature whether these are Ag NPs or Ag^+ responsible for the toxicity. Ag NPs release Ag^+ in aqueous media therefore, some studies suggest that Ag NPs deliver Ag^+ and these silver ions are responsible for the toxicity whereas other studies find both silver ions and silver nano particles responsible for the toxic action [70]. The generation of reactive oxygen species may be accelerated by Ag NPs and Ag^+ as shown in the following reaction [31].

$$H_2O + \frac{1}{2}O_2 \xrightarrow{Ag\ NP,\ Ag^+} H_2O_2 \rightarrow H_2O + ROS$$
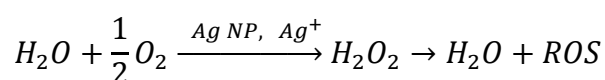
Although ROS are produced normally as by products during cell respiration, their large amount causes oxidative stress which can lead to cell destruction . *He W. et al.* [73] studied the generation of hydroxyl radicals and oxygen produced by decomposition of H_2O_2 induced by Ag NPs at different pH values. Since H_2O_2 is produced continuously in the cells and tissues at micro molar levels, the study gives an insight into the interactions between H_2O_2 and Ag NPs. The study used electron spin resonance spectroscopy (ESR) with spin trapping which was reported to be the most reliable and direct method to identify short lived free radicals. ESR spectroscopy showed that the hydroxyl radicals (•OH) were generated when decomposition of H_2O_2 occurred with Ag NPs under acidic conditions. Whereas little hydroxyl radicals were generated (equivalent to control) when $AgNO_3$ was present indicating that Ag^+ had no significant activity in generating hydroxyl radicals from decomposition of H_2O_2. No appreciable effect

on ESR signal was observed even at higher concentrations of $AgNO_3$. The generation of hydroxyl radicals in presence of Ag NPs was found to be heavily dependent on the pH with more hydroxyl radicals at lower pH (1.2). The hydroxyl radicals generation decreased to the level of control when pH increased to 4.6. Under alkaline conditions, H_2O_2 again reduced Ag^+ to Ag^0 thus forming a cyclic reaction between elemental silver and silver ions [73]. Keeping in view these literature insights, it can be suggested that antimicrobial activity of Ag NPs can be due to these mechanisms involved simultaneously as also suggested in [74]: (1) penetration through bacterial cell wall and thus collapse of cell structure, (2) formation of free radicals that can damage cell membrane, (3) release of silver ions from silver NPs that can bind with thiol groups of proteins and inactivate enzymes functions.

Many consumer products like sprays, fabrics, cosmetics and other house hold appliances contain silver nano particles. Physicochemical parameters like size, shape and specific surface area are potential factors that affect mechanism of toxicity, uptake and exposure dose [75]. Ag nano particles may lose their bactericidal effect if their interaction and uptake by bacteria is hindered. Ag NPs showed no antibacterial activity against *Pseudomonas fluorescens*, a Gram negative bacterium, when a thin layer of humic acid was formed around them by adding humic acid in the suspension of silver NPs [75]. The basic difference in numerous studies reported in literature, for the functionalization of different fabrics with Ag NPs, lies in the synthesis of NPs. Therefore, latest trends and approaches in Ag NP synthesis will be discussed separately in the next section.

Silver NPs can also be combined in a composite coating where matrix of the composite coating is made of different material and silver NPs are embedded in this matrix. This approach can possibly offer several advantages as embedding the metallic NPs in the matrix can avoid direct contact of the NPs with the skin and matrix can also be selected to reduce Ag^+ in situ on the fabric surface. Using this approach *Lu Z. et al.* functionalized silk fabric with silver NPs where the fabric was first coated with polydopamine which provided the matrix and also acted as reducing agent to reduce silver ions. Functionalized silk fabric, containing 4 wt % silver NPs, showed excellent antibacterial properties against *E. coli* and *S. aureus* [76]. Embedding Ag NPs in a different matrix can also control the release of silver NPs from the coating.

Silver containing antimicrobial textiles can also be produced by incorporating silver into the bulk of synthetic fibers or filaments before extrusion process. This method can result in high consumption of silver and less antimicrobial efficiency as most of the silver is entrapped within the fiber material and is not available for

biocidal action. However, this technique can be of interest for wound dressings where innovative new fiber materials are being studied for improved wound healing and antimicrobial protection. *Masood R. et al.* developed a new silver containing fiber, Psyllginate, based on natural polymers. The fiber was formed by coextruding Psyllium with sodium/calcium alginate. Alginate is biocompatible and biodegradable polysaccharide used in wound care applications. Psyllium is also a natural polysaccharide used in herbal medicines and possess excellent gelation properties. The resultant fiber showed slow rate of silver release and good capabilities to gel and absorb body fluids, higher in comparison with commercially available silver containing dressings [77].

Along with imparting excellent antibacterial properties, silver NPs treated textiles can also provide UV protection thus giving multifunctional textiles. Cotton fabric coated with silver NPs have been found to demonstrate improved ultra violet protection as well as increased electrical conductivity [78]. Silver NPs loading on cotton fabric can reduce UV transmittance to 90 % where as 25 % reduction was observed for wool [79]. Ultra violet protection factor (UPF) of bamboo pulp fabrics was increased to 80 (from18) after treatment with silver NPs [63].

Other than silver NPs, silver nano wires also possess interesting properties and have been used for antibacterial functionalization of textiles. Cotton fabric loaded with silver nano wires showed significant antibacterial effect against *E. coli* and *S. aureus* [80]. Excellent UV protection of cotton fabric was also achieved as ultra violet protection factor (UPF) increased from 4 to 113 after silver nano wires loading. The white color of the cotton fabric changed to green as silver nano wires have plasmon absorption peak at about 390 nm which is different than that of silver NPs. Silver NPs absorb at wave lengths higher than 400 nm and impart yellow or brown color to white textile substrates [80]. New silver containing compounds are being synthesized and studied for their potential use as antibacterial agents in textile finishing. Silver abietate, a silver containing complex, was synthesized from the reaction of $AgNO_3$ and abietic acid. After synthesis, silver abietate was applied to cotton fabric by padding and was found to be effective against six tested bacteria. Antibacterial effect was maintained after 20 washing cycles. It was proposed that silver abietate has no environmental hazard and difficult to get on the skin [81].

The increased use of silver nano particles has also raised the concern about their impact on human health. A review by *Ahamed M. et al* [70] evaluated the risk of possible exposures to silver nano particles and their cytotoxicity presented in different studies. An exposure to nano particles can occur through dermal

contact, inhalation and ingestion. The review reveals that most of the studies have been done to evaluate toxicity occurring through inhalation, ingestion and dermal contact of damaged skin (e.g wound dressing) whereas there is lack of reports dealing with silver nano particle exposure through intact skin via textiles [70]. In another study, *Larese F.F. et al* studied the penetration of the Ag NPs through intact and damaged human skin in an in vitro diffusion cell system. The penetration of the Ag NPs were found to be five time higher through damaged skin than through intact skin. The permeation through intact skin was just above or below the analytical detection limit suggesting that Ag NPs absorption through intact human skin was low [82].

2.2.6.2 Silver nano particle's synthesis

For application to textiles, silver nano particles can be synthesized via various methods. $AgNO_3$ is the most commonly used precursor for synthesis of silver NPs. Upon dissolution of $AgNO_3$ in solution, Ag^+ can be reduced to Ag NPs using a reducing agent. The size of the NPs depend on whether strong or weak reducing agent has been used. Stronger reducing agents yield smaller size as they result in large number of nucleation cites and thus avoid agglomeration [31]. The selection of reducing agent and functionalization of synthesized NPs can be done according to the chemistry of textile substrates on which they have to be applied. Generally, a stabilizing agent is required to avoid agglomeration of silver NPs in case long term stability is required. Stabilizers are not always ecofriendly and their presence can also diminish antibacterial properties of silver NPs. Therefore, recent research focuses on the synthesis of silver NPs using ecofriendly reducing agents that can also act as stabilizers [83].

Dextran, synthesized using dextransucrase, has been used to synthesize silver NPs assisted with microwave power. Dextransucrase was synthesized using microorganism *Leuconostoc mesenteroides* T3 and resulted silver NPs had bimodal size distribution of 15 nm and 50 nm [83]. Carboxymethyl cellulose (CMC) has also been used both as reducing agent and as stabilizer in the synthesis of silver nano particles. CMC has alcoholic and aldehydic groups that can reduce Ag^{1+} to Ag^0 and polymeric chains of CMC can stabilize these NPs and avoid their aggregation [78]. In situ synthesis of silver NPs on the fabric surface is also being reported increasingly. Trisodium citrate has been used as reducing, stabilizing and crosslinking agent to synthesize silver NPs in situ on fabric surface. Complexes may form between Ag^+ and chelating groups of cotton (COOH and OH) and wool (COOH, NH2 and SH) upon impregnation of the fabric in the silver nitrate solution. The addition of trisodium citrate can reduce silver ions into silver NPs while citrate being oxidized to acetone carboxylate. Finally, functional groups of cotton and wool and citrate may chelate produced silver NPs and stabilize them. The size of synthesized NPs was different on cotton and wool with

wide range of size distribution. The difference of size of Ag NP was suggested to be due to difference in electrostatic interaction between silver NPs and the substrate [79].

Starch, a biocompatible polysaccharide, has reducing aldehyde groups and, therefore, has been used as reducing as well as stabilizing agent to synthesize Ag NPs in situ on cotton fabric under autoclave conditions at 103.42 kPa and 121 °C. Reduction of silver ions may be linked to oxidation of aldehyde groups of starch to carboxylic acid. Upon impregnation, Ag^+ can adsorb on –OH groups of cellulose and can be reduced to Ag NPs by starch at high temperature and pressure [84]. Cellulose itself can also be used as reducing agent due to presence of hydroxyl groups. This can be of interest particularly for cellulosic fibers as metal ions can be reduced to metal NPs due to abundant reducing hydroxyl ends in the fibers. Silver and gold NPs were synthesized in situ on bamboo pulp fabric without using any other reducing agent and without the need of high temperature unlike the reduction by starch as in [84]. Contrary to the gold NPs, alkaline conditions were required for the synthesis of silver NPs [63]. Polydopamine (PDA) has also been used to reduce Ag^+ to Ag NPs in situ on silk fibers. Polydopamine is biocompatible and is formed by polymerization of dopamine which is a neurotransmitter in human body. It is also suggested that PDA can adhere on almost every kind of surface. Catechol moiety of polydopamine can reduce Ag^+ to Ag NPs [76].

The interest in biological synthesis of silver nano particles has also increased because of no use of toxic chemicals and no high temperature and pressure requirements. In this regard both microbes and plants are being studied for large scale synthesis of silver nano particles. *Kumar P. et al* has reported successful synthesis of silver nano particles using seaweeds *Ulva lactuca* [85] that can be applied to textiles.

2.2.6.3 Silver leaching in water, artificial sweat and washing solutions

Nano technology has also raised environmental concerns related to silver release in various forms from silver coated products including textiles. Research studies are being conducted dealing with release of silver from treated textiles in water, artificial sweat and during washing.

Liu J. and *Hurt R.H.* [71] studied the kinetics of silver ion release in aqueous nano silver colloids. They studied the effect of dissolved oxygen, pH, temperature, ocean salts and natural organic matter in the aqueous media on the kinetics of ion release. In the absence of dissolved oxygen in deionized water, the release of ionic silver was inhibited completely. This indicates that dissolved oxygen in water plays an important role in the initiation of oxidation of nano

silver. Ag^+ release is strongly pH dependent and was found to be higher at lower pH (acidic) values than at higher pH (basic) values. However, the role of dissolved oxygen is important even at lower pH as in the absence of dissolved oxygen, Ag^+ release was significantly reduced compared with that of in the presence of dissolved oxygen at pH 4. Sea salts were found to have only minor effect on silver ion release whereas ionic release in sea water was less than that of in deionized water [71].

In a study, textiles were treated with a variety of silver containing additives including conventional and nano silver and were characterized for the quantity and form of silver released during washing process [86]. Textiles that were surface treated were found to release more Ag in washing liquid compared to that where silver was contained in the fiber bulk. Furthermore, the nano treated textiles yielded much lower amount of silver during washing compared to the conventional or bulk treated textiles. This was suggested to be due to the higher amount of silver usually deposited during bulk treatments. It was also found that conventional treated textiles (not containing nano Ag) also released nano silver into the washing solution at a concentration higher than that of released from nano treated textiles indicating that conventional treatments also release nano sized silver during practical conditions. Silver can exist in different forms in washing effluent depending upon (1) the form of the silver deposited on textile (2) washing bath composition and (3) washing conditions [86]. In another study, 8 different silver containing commercial textiles were studied for their silver release behavior in washing liquid. It was found that not all the products contained silver as claimed on their label and silver was released in different forms. Only one textile released metallic silver whereas AgCl (nano and larger particles) and nano Ag_2S were also released. The study suggested, therefore, not to focus only on the metallic but other forms of silver also while studying release of silver nano particles from the textiles [87].

Benn T.M and *Westerhoff P.* [88] studied the leaching of the nano silver from 6 different commercially available socks in the washing liquid without detergent. The socks contained silver contents from 2 to 1360 µg/g of the sock weight were found by ICP-OES. Socks containing higher amount of nano silver did not necessarily leached more silver into the washing liquid. This was due the different manufacturing process for socks. The rate of silver release was also found to be different among the tested socks. The socks washed with domestic tap water released 15 µg of silver compared to 155 µg when the same socks were washed in ultrapure water. This suggested that the ultra-pure water is more aggressive than domestic tap water in stripping the metal nano particles from the textiles [88].

While in another study, 13 consumer products for children use were investigated for their potential release of silver in different fluids, like tap water, synthetics sweat, saliva, urine and milk and orange juice. In this study the silver release was also measured in saline (185 mM NaCl) and HCl solutions. Most of the products released $1 - 6$ % silver of their total silver mass. The silver release, from all the products, was found to be the highest in sweat and urine compared to other liquid media. The lowest silver release was found in tap water. The authors suggested that the presence of chloride (Cl^-) can accelerate the release of silver as similar quantities (like sweat) were found in saline and HCl solutions. The effect of the individual ingredients of the artificial sweat was also investigated on the leaching of silver and it was found that slightly less amount of silver was released in the absence of NaCl whereas other ingredients had no effect. The study suggested that the level of silver exposure of these products during normal use can be considered low, as the ingested nano silver dose for slight liver damage in a 10 Kg child was reported to be 1230 mg of silver per day, and bioavailable silver is mostly in ionic form rather than particulate form. [89].

Textiles are in direct contact with the skin, therefore, silver release behavior in artificial sweat from silver coated textiles is important to study as silver exposure may have risk of inflammation and accumulation. Sweat is a body fluid that comes in direct contact with the textiles used in medical or apparel. It contains electrolytes, ionic species (Cl-, S-, SO_4^{-2}), organic acids and sebum [90]. Since metal nano particles are considered to be toxic above certain concentrations, the potential risk of dermal exposure to any toxicity of the metal nano particles is dependent on physical (during wear) or chemical (by sweat) mobilization of the nano particles from treated textiles. *Goetz N.V et al* studied the Ag and TiO_2 release in artificial sweat under worst case scenario and reported maximum dermal exposure level of silver at 17.1 and 8.2 µg/kg body weight for total and particulate Ag. They suggested that under realistic conditions, much lower exposure was expected [91].

Stefaniak A.B et al. studied dermal exposure potential of silver nano particles from textiles. It was found that silver ions immediately formed silver chloride, that is Ag^+ reacted immediately with available Cl^-, in artificial sweat as observed through EDX. Moreover, UV-Vis spectroscopy of the solid particles obtained as a result of interaction with artificial sweat showed no surface plasmon resonance (SPR) absorption in the wave length range 390-420 nm confirming the EDX results as AgCl does not exhibit SPR. The study confirmed the absence of Ag NPs as no SPR absorption peak was observed in UV-Vis spectroscopy due to formation of AgCl. In this study, silver release behavior was found to be similar both in simple formulation of artificial sweat and the more complex one. It was

suggested that the physiological factors of the body fluids (composition, pH, and temperature) have little influence on the silver release from textiles, whereas the way textiles have been treated with Ag nano particles (surface treated or incorporated in the bulk) has the greatest influence [90]. However, in this study the variation in pH of the two sweat formulations over which silver release was evaluated was narrow (4.5 vs 5.3).

Yan et al. [92] studied the silver dissolution into three different sweat formulation over a wide pH range, acidic sweat (pH 3), basic sweat (pH 8.5) and salt simulated sweat (pH 8). The silver dissolution rate was found to be different in the three formulations over a period of 4 hours and silver concentration in acidic sweat after 4 hours was found to be much higher (0.9 mg/L) compared to that of in the basic sweat (0.32 mg/L). Whereas in salt simulated sweat, the silver solubility was found to be in between (0.65 mg/L) that of acidic and basic sweat formulations [92]. The authors also investigated the form of silver, whether free Ag^+ or Ag NPs, present in the three sweat solutions. In acidic sweat, silver was initially released as Ag^+ but after reaching a maximum further silver was released as NPs. In the basic sweat, 85% of the total silver was released as free Ag^+ whereas very small amount of free Ag^+ was detected in salt simulated sweat even after 4 hours while total amount of silver released was high. The authors suggested that the silver was largely released as NPs.

Summing up the discussion, the difference in the nature of released silver species in any given fluid, as found in different studies in literature, could be due to dynamic behavior of Ag NPs in aqueous solutions that can be attributed to the medium redox potential of the silver (0.80 V) enabling both oxidation and reduction of silver in aqueous solutions. The same is true for studies dealing with environmental effect of silver NPs where it is suggested that after being released to the environment from the Ag NP containing products, Ag NPs undergo many chemical and morphlgical transformations depending upon the chemical environment they pass through during transportation that determine their ultimate bio availability and toxicity [93].

2.3 Different textile surface modification/coating techniques

This part of the chapter describes different textile surface modification techniques. Particularly effort has been made to highlight recent research trends in each discussed technique. Some of the techniques reported here are still at research stage but are environmental friendly and have potential to be scaled up or adopted commercially.

2.3.1 Sonochemical coating

A sonochemical pilot plant development has been reported by *Perelshtein I.* [6] and colleagues that can operate in a continuous mode to deposit metal oxide nanoparticles on textiles. The pilot plant can process a 40 cm wide fabric at a speed of 1-3 m/min in a roll-to-roll process with 160 L capacity of the sonochemical tank. The plant has been developed and evolved after a series of studies reported by the same research group. The sonochemical process involves the synthesis and simultaneous application of metal oxide nano particles on textiles. Metal oxide nano particles were synthesized by the basic hydrolysis of the corresponding metal acetates. Initially, the synthesis of NPs was carried in ethanol:water mixture, later on ethanol was eliminated for being not suitable for industrial plants and synthesis was carried only in water. However, synthesis in water resulted in lesser amount of metal oxide nano particles on textiles but the particle size was also reduced thus giving same level of antibacterial effect. Continuous addition of the concerned metal acetate and ammonia solution is needed to compensate the depletion of the metal acetate and to maintain the pH (pH 8) of the solution respectively, to ensure homogeneous coating on the fabric [6].

The authors reported in situ synthesis of ZnO NPs and their simultaneous application to textile material via sonochemical process. During synthesis, ammonia acts as a catalyst in hydrolysis of zinc acetate and ZnO is produced via zinc ammonium complex formation [94]. Since the synthesis of some of the metal oxide NPs, for example MgO and Al_2O_3, could be impossible through sonication of the corresponding metal acetates due to amorphous metal hydroxide formation, the authors have reported successful application of already synthesized (commercially available) metal oxide NPs through sonication [67]. However, it was also reported that using water as solvent can result in partial hydrolysis of MgO NPs and thus did not result in any coating on the fabric. Instead, a combination of ethanol and ethylene glycol yielded good deposition of metal oxide on the fabric that was reported to be sufficient for a good antibacterial action. However, this implies an important limitation of the process as it requires suitable combination of solvents for the process that could be undesirable for an industrial level plant. Pure ethanol has high vapor pressure and may not lead to formation of acoustic bubbles that were proposed to play key role in deposition according to the authors. Pure ethylene glycol has high viscosity and it is not suitable for ultrasound irradiation. The proposed deposition mechanism lies in the asymmetric collapse of the cavities (acoustic bubbles), that are formed due to ultrasound irradiation of the liquid suspension containing fabric, near the solid (fabric) surface. After collapse, the potential energy of the bubble is converted

into kinetic energy of liquid jets that can impinge nano particles on the fabric surface with high speed resulting in a coated fabric [67].

This mechanism may result in strong adhesion of the NPs as they get effectively embedded in the fabric. In another study by the same research group, the authors have reported cotton fabric coated by CuO NPs through sonochemical treatment that was able to withstand 65 washing cycles and still able to retain its antibacterial properties [65]. Silver nano particles has also been synthesized and applied on cotton, polyester and nylon fabric via the same sonochemical process. $AgNO_3$ was used as precursor and ethylene glycol as reducing agent. The deposited coating was able to withstand 20 washing cycles as no reduction of Ag contents was reported after repeated washing [27]. Later on, an improvement in the adhesion of ZnO NPs was achieved due to enzyme activation of the cotton fabric in a single step sonochemical − enzymatic coating process. Significant enzymatic activation of cotton fabric was achieved as only 10 to 20 % enzyme activity loss was observed due to ultrasonic radiation [95]. Recently, a nano composite solution comprising TiO_2/CuO/citric acid/Polyethylene glycol was applied on cotton fabric via ultrasonic sol-gel method. The sols were prepared separately, mixed together and then applied via sonication under different conditions. Antibacterial activity of the composite coating was higher than that of individual TiO_2 and CuO NPs. Significant decrease in antibacterial activity was observed after 3 washing cycles [66].

2.3.2 Pad-dry-cure method

In this technique the fabric is dipped in the prepared coating formulation and then passed through the wringer or padder to obtain a desired wet pickup on the fabric. The fabric is then dried and cured under proper conditions to obtain the final coated fabric [78]. This method of coating application to textiles is so simple that even formulations that involve complex multistep and time consuming preparation procedure, for example as presented in [28], can be applied easily. Therefore, a variety of antimicrobial agents comprising metal NPs, polymers, metal NPs/polymer composites etc can be applied via pad-dry-cure method [44]. Moreover, emerging textile finishing techniques, like UV curing of polymers, can be integrated easily with this technique [41]. This method is also adopted for sol-gel finishing of the textiles where textile is impregnated with a sol, dried after padding and then cured at desired temperature [49].

2.3.3 Layer by Layer assembly method

Layer-by-layer (LbL) deposition technique is based on electrostatic interaction between oppositely charged species. LbL assembly can be achieved by stepwise

dipping of solid substrate in the corresponding solutions containing these oppositely charged species. Substrate can be charged properly before dipping in the solution first time and intermediate rinsing steps can be carried. The technique was initially employed to deposit multilayer coating of oppositely charged polyelectrolytes (polycations and polyanions) but later on a wide variety of nano metric sized charged species have been deposited using LbL technique. Other than electrostatic interaction, hydrogen bonding, covalent bonding, charge transfer and other types of interactions have been studied to achieve LbL assemblies on various substrates [74]. N,N,N-trimethyl chitosan (TMC) was applied on the surface of polypropylene nonwovens by LbL technique and antibacterial properties were investigated against *S. aureus*. The surface of polypropylene fibers was first grafted with acrylic acid to impart negative charge to the surface to develop electrostatic interaction with positively charged TMC. Although nano scale precision can be obtained using LbL [74], it may be difficult to achieve homogeneous coating on some substrates as was found in [43] where full surface coverage was not obtained on polypropylene nonwovens.

N-Halamines, rechargeable antibacterial agents, containing positive or negative charge bearing species on polymer have also been self-assembled on textiles substrates. *Liu Y. et al.* [35] synthesized N-Halamine cationic and anionic homopolymers via free radical polymerization and applied them on bleached cotton fabric via LbL method. The surface of bleached cotton fabric is negatively charged due to large number of carboxylate groups (–COO) and hydroxy groups (–OH) and therefore, can attract polymer of opposite charge. The fabric was coated by alternately immersing it into oppositely charged solutions of N-Halamine polyelectrolytes. The coated fabric was chlorinated by immersion in NaClO solution. About 50% of oxidative chlorine of thus coated cotton was retained during storage in dark at ambient temperature and the loss was regained by rechlorination [35]. Metallic NPs can also be deposited using this technique. A multilayered nano composite film comprising polyethyleneimine (PEI), a polycation, and negatively charged silver NPs were obtained on silicon wafers and studied for their antibacterial properties [74].

2.3.4 Sol-gel method

Using sol-gel method a variety of functional coatings, consisting of hybrid organic-inorganic networks can be applied on textiles. Sol-gel process is based on the preparation of the appropriate colloidal suspensions called "sols". Majority of the precursors used include metal oxides or metal or semimetal–silicon containing alkoxides, also known as organometallics. The hydrolysis of these compounds results in the formation of corresponding hydroxides in acidic medium which are unstable and further undergo condensation process to form nano sized particles

[96]. The size of the nano particles is usually less than 50 nm with solid contents in the range 4-20 wt%. Sols prepared using alcohol as solvent have high long term stability but the recovery of inflammable solvents using textile processing equipment may be difficult. Therefore, it is advantageous to work either with aqueous nano sols or obtaining sol from other precursors, for example, hydrolysis of other metal salts like metal halides [97].

The sol formation is influenced by pH, temperature, concentration and solvent type. Textiles are impregnated in these sols and are dried at elevated temperature to condense them to form three dimensional network called lyogel layer [96] [97]. These gels contain high water content and further drying at high temperature leaves a porous coating on the fibers or fabrics. The cross linking in this coating is up to the level of xerogels which is required for textiles to retain some elasticity. The conditions of hydrolysis and thermal treatment determine mechanical properties, porosity and density of the deposited layer [97]. Intense thermal treatments up to 600 °C may lead to highly cross linked and hard gel coating. Lower temperature thermal treatments are required for textiles to avoid degradation but results in less cross linked coating (xerogel) having less hardness but higher elasticity [96]. Usually thermal treatments for textiles are kept below 180 °C [97].

In sol-gel application, under thermal treatments for textiles may result in insufficient adhesion of the coating with the textile substrates. The adhesion can be improved by appropriate precursors and heat treatments. An additional treatment on prepared sol may be helpful in improving the adhesion if activation of the functional groups in the sol can be achieved. It was demonstrated that solvothermal treatment of the SiO_2 sol, modified by 3-glycidyloxypropyltriethoxysilane, before application to the fabric can improve the adhesion of the resultant coating with the textiles. The solvothermal treatment was carried in the autoclave at temperature 100-180 °C and at pressure 2-18 bar. Solvothermal treatment at temperature 120-140 °C resulted in increased adhesion which was attributed to the activation of the glycidyloxypropyl group under these autoclave conditions. Solvothermal treatment at 180 °C may result in degradation of certain sol modifying additives [98]. High temperature curing of applied coating may also degrade base textile materials as was reported for silk fabric [48].

Mostly sols are obtained from metal alkoxides by hydrolysis and polycondensation of alkoxy groups [77]. Various antibacterial agents including QACs [47] [49], triclosan [29], silver NPs [99] natural biocidal agents [58] have been applied on textiles via sol-gel route. Other than antimicrobial, functional coatings imparting hydrophobic, oil and soil repellent, anti-adhesive, improved

electrical conductivity and coatings with other desired properties can be applied to the textiles via sol-gel method [97]. After preparation of sols of interest, it can be applied at high speed with almost all conventional textile coating methods [97]. Applying the sol by pad-dry-cure method is the most common method [49] [49] [58]. Dip coating and spray coating [98] can also be used to apply the sols to the textiles. Inorganic sols containing TiO_2 and CuO NPs have also been applied via sonication [66]. The main demerits of sol-gel technique include necessity of thermal treatment that can possibly degrade fibers materials, inhomogeneous coating and possibly poor adhesion of the coating with the substrate [100].

2.3.5 Chemical vapor deposition technique (CVD)

In chemical vapor deposition, chemicals in vapor form are reacted to deposit films on solid substrates. The precursors used are in gaseous state unlike physical vapor deposition (PVD) where the precursors are in solid form. Different variations of the CVD involve atmospheric pressure, low pressure, plasma enhanced chemical vapor depositions and some other variations. CVD does not alter the porosity of the substrates, therefore, textiles can be coated maintaining their breathability [101].

Plasma enhanced chemical vapor deposition (PECVD) is most commonly used for modification of textile surfaces. When precursors are fed to the plasma chamber, they get energized through inelastic collision with the high energy species in the plasma. This leads to breaking and formation of new bonds and deposition of solid thin films on the substrates. Since this process is limited to the top most layers of the surface, bulk properties of the substrates can be maintained while imparting new functionalities to the surfaces. Like other plasma based processes, PECVD offers the advantages of less material consumption, no effluent production and being environment friendly compared with other textile surface modification techniques [102].

A wide variety of monomeric precursors having polymerisable bonds can be deposited on different substrates. Uniform coatings can be deposited on substrates with complex geometries and shapes due to conformal nature of the deposited coatings [103] as demonstrated in [104]. In addition, plasma deposited films can easily be tailored with respect to type and density of functional groups and surface topologies can be engineered. [104]. However, contrary to other polymerizing techniques where regular (real) polymeric chains are obtained, plasma polymerization result in deposition of oligomeric fragments [103] [105]. Therefore, the term plasma polymerization may not qualify the true definition of polymerization process. However, a plasma polymer is a material that is formed as a result of an electric discharge in an organic gas. Plasma polymerization yields

a polymer that consists of randomly branched short chains with a high cross linking density [106].

PECVD can also be attractive for modification of inert surfaces, e.g surfaces of high performance fibers like Kevlar® and Vectran®, that are relatively difficult to modify through usual chemical formulations. It has been shown that the friction among the yarns in woven Kevlar® fabric was increased by plasma polymerization of Dichlorodimethylsilane $((CH3)_2Cl_2Si)$ with reactive nitrogen plasma. Kevlar® has very low coefficient of surface friction. Friction among the fibers in the woven fabrics in protective clothing is important to slow down and deform the penetrating projectile or bullet to provide enhanced ballistic protection [24]. Self-cleaning and hydrophobic TiO_2 coatings have been obtained through radio frequency (RF) PECVD on cotton fabric using titanium chloride $(TiCl_4)$ as a source of titanium. Deposition process parameters including RF power and flow rate of plasma gas (oxygen) was found to have strong effect over the properties of the coating and the treated fabric [100].

A right mix of properties can be achieved by polymerization or deposition of more than one monomers by feeding them simultaneously in the plasma chamber. Fluorine containing polymers are used to render hydrophobic properties to the textiles but intermolecular forces between the polymeric chains are weak which may lead to poor mechanical properties of films comprising these fluoro-alkyl polymers. The durability of the fluorinated acrylate films has been found to increase when the precursor (2,2,3,4,4,4 hexafluoro butyl acrylate (HFBA)) was co deposited with glycidyl methacrylate (GMA). Plasma induced cross linking may occur between epoxide and fluorine containing functional groups leading to durable film deposition. However, co polymerization triggered by PECVD conditions may not lead to real expected co polymer, rather irregularly structured fragments of co polymers may be deposited [103].

Recently, PECVD has also been exploited to produce reactive polymeric films on substrates that can be useful for further modification of the surface for added functionality. *Gilabert-Porres et al.* combined PECVD with Tollen's method for in situ reduction of silver ions with reductive sugars to fabricate an antibacterial layer with increased hydrophobicity. First, the PECVD deposition of pentafluorophenyl methacrylate (PFM) was carried on prosthesis made of polydimethylsiloxane (PDMS) and on silicon wafers, resulting in reactive film due to the presence of ester groups which are highly reactive. The samples were then incubated with glucoseamine (a reducing sugar) solution for six hours and finally treated with Tollen's reagent (silver ions complex with ammonia) for in situ reduction of silver ions to metallic silver upon completion of the reaction. The

modified surfaces showed complete bacterial reduction and were biocompatible when tested against animal cell (COS-7 cells) [104].

Most of the PECVD coatings reported in literature involve low pressure plasma as they are carried in vacuum. However, recently the interest in atmospheric pressure plasma has gained momentum because of its benefits of being economic and easy processing. *Yim et al.* obtained antimicrobial coating on spectra and nylon/cotton fabric by atmospheric pressure plasma polymerization of 1,1,3,3-tetramethylguanidine, a monomer derived from guanidine. The coating deposited on nylon/cotton fabric exhibited 5 log reduction of bacteria whereas that deposited on spectra did not show satisfactory bacterial reduction. This difference was attributed to different adhesion of the coating on different substrates. The coating on spectra was suggested to be removed when subjected to ethanol/water rinse before the antimicrobial test [105]. A double layer organosilicon film has been applied on polyester fabric through atmospheric pressure plasma process using hexamethyldisiloxane (HMDSO) precursor. Three antibacterial agents, namely silver, copper and zinc oxide nanoparticles, were incorporated in between the two films in a three step process. The fabric was first deposited with an HMDSO layer which was then immersed in NPs suspension and dried. Finally, the fabric hosting NPs was again deposited with HMDSO to serve as a barrier layer. Enhanced washing stability of the NPs was observed on the fabric deposited with barrier layer compared to that of without barrier layer [107].

2.3.6 Physical vapor deposition techniques (PVD)

Physical vapor deposition (PVD) is another technique to modify and structure the surfaces of the materials at nano level. The surface of the metals (or targets) is evaporated in vacuum and the evaporated material is deposited on the required substrate. PVD has the advantage, like other plasma based techniques, that the process is dry and ecofriendly compared with other wet chemical treatments that produce waste water with hazardous chemical compounds. The following section describes some of these techniques to modify and functionalize the surfaces of textiles.

2.3.6.1 Sputtering

Sputtering was first developed in late 1970s. Sputtering has been used to produce thin films of metals and their oxides on a wide variety of substrates. Sputtering process is carried in vacuum where a high voltage is applied across a gas (inert or reactive) to create plasma. Plasma consists of high energy electrons, ions or radicals that can extract atoms from a target of desired coating material. The extracted atoms from the target have sufficient kinetic energy and orientation to travel to and condense on a substrate to deposit a thin functional film. The rate of

deposition depends on number of excited species hitting the surface of the target material to extract the atoms. Magnetron sputtering (with magnets placed parallel to the target surface) was developed to confine the plasma and increase the plasma density on the target surface and hence to increase the deposition rate [108]. The magnetic field in front of cathode (target surface) can trap free electrons and hence the probability of ionizing the neutral gas atoms or molecules is increased by an order of magnitude [109]. Other techniques include direct current (DC) sputtering, reactive sputtering and radio frequency (RF) sputtering. DC sputtering is used for metals and RF for insulating materials to avoid charge build up. In reactive sputtering, the deposited layer is a result of chemical reaction between the target material and reactive gas used as plasma source. Argon is used normally for non-reactive sputtering [108].

The use of sputtering to deposit coating on metals, glasses and ceramics is not new, but sputter coating of textiles is relatively new and has increased over the past years because of its solvent free and ecofriendly benefits [25]. Depositions of various metals have been reported in literature enhancing the desired functionality for a particular application. Sputtering has been reported to produce more uniform metallic coating on textiles compared with other textile metallization methods. A blended cotton fabric (90% cotton, 10 % spandex) was more uniformly coated with sputter deposition compared with metal powder printing and metal foil laminating. The coating resulted in uniform silver grains over fiber surface and mechanical properties of the fabric were also not degraded [110].

Different sputtering process parameters can influence the structure and morphology of the deposited film. *Wu et al.* investigated the effect of working pressure on the thickness and growth of Lanthanum hexaboride (LaB6) thin films on the polyester (PET) fabric. Film thickness increased with increase in working pressure, due to increased deposition rate, up to certain level and then decreased. At higher working pressures, the density of the argon gas is increased resulting in decrease in mean free path of colliding particles. This can lead to decrease in deposition rate with reduced film thickness. Ultra violet protection factor of the PET fabric increased from 6 for uncoated fabric to 18 for coated fabric [111].

Various metals have been deposited on different fabrics and evaluated for their different functional properties. Glass fabrics have been deposited with thin layers (300 nm) of copper, silver, gold, platinum and platinum/rhodium using magnetron sputtering and studied for their antimicrobial and electrical properties. Antimicrobial properties were studied against two bacterial strains: *S. aureus* and *K. pneumonia* and three fungal strains: *Aspergillus niger, Chaetomium globosum and Penicillium funiculosum*. Silver and copper were found to be effective against both the bacteria compared with gold, platinum and platinum/rhodium layers [64].

In another study, cotton fabric was deposited with silver and silver/platinum alloy (1% Pt) and evaluated for its antibacterial properties against air born bacteria. Silver was found effective against air born bacteria whereas no synergistic effect was observed due to platinum. Minimum sputtering time of 60 s was required to get minimum silver quantity (0.0026 wt% on cotton) sufficient for bactericidal effect. Below 60 s no bactericide effect was observed. However, at increased sputtering time, the presence of Ag(II)O was also observed via XPS. The oxidized species were found to be present only on the surface with Ag° as the major coating component [109]. At increased sputtering time, thicker silver coating is obtained resulting in higher amount of silver ions that can be released for antibacterial action as was also reported by *Wang H. et al*. Antimicrobial performance and electrical conductivity of polypropylene nonwoven deposited with silver increased with the increase in sputtering time and coating thickness [25]. A nano structured layer of Ag was also deposited on polyester fabric by sputtering and evaluated for its morphology, wettability and antimicrobial properties. The layer consisted of dense silver aggregates uniformly distributed over the fabric surface. Water contact angle on the fabric surface was increased after silver deposition. Untreated fabric showed a contact of 0° due to loose fabric structure that increased to 132.2° after 30 minutes deposition due to roughness created by nano structure and air entrapment [112].

Cotton fabric deposited with metallic layer of copper has also been found to exhibit good antibacterial properties. The coating was reported to retain antibacterial properties up to 30 washing cycles. Surprisingly, the antibacterial activity of the coated fabric was found to increase with increasing number of washing cycles as the size of the inhibition halo increased after multiple washings. The authors attributed this effect to the formation of Cu complexes with the soap while providing no further experimental evidence and explanation [26].

Electrically conductive textiles can also be obtained by metallic depositions via sputtering. *Wang RX. et al*. deposited silver thin films on nylon and polyester plane woven fabrics. The electrical conductance of the films was found different on both the textiles. The electrical conductivity of the silver film on the nylon was found to be $2.4*10^3$ S/m compared to bulk silver ($6.3*10^7$ S/m) whereas that of silver film on polyester fabric was six orders of magnitude less than that of on nylon fabric. This was attributed to the discontinuous film formation on polyester fabric. Silver coated nylon fabric, when used as an electrode, produced the similar signal for human heart beat in electrocardiograph as that of produced by commercial electrode. However, the washing performance of the silver coated fabric was not satisfactory. The electrical conductivity of silver coated textile decreased significantly even after one washing [113]. Polyamide nanofibers

produced via electrospinning have also been deposited with TiO$_2$ [114] and silver [115] to improve their wettability and electrical conductivity respectively.

Polymers can also be deposited using sputtering. Co-sputtering has been used to deposit metal NPs in polymeric matrix where polymer matrix was obtained by sputtering from solid polymer target. *Liu et al.* fabricated Polymer-metal composite film by co sputtering polytetrafluoroethylene (PTFE) and gold from independent targets and studied their electrical and optical properties as a function of metal contents. The influence of post deposition heat treatment was also studied on optical properties of the coating [116]. In another study, silver and gold nano particles were co-sputtered with polytetrafloroethylen (PTFE) to produce metal/polymer composite antimicrobial coating. The metal nano clusters were embedded in the polymer matrix and coating showed good antimicrobial properties against different microbes. The metal filling factor (MFF) was reported to be 30% in a coating of 100 nm thickness. The obtained coatings demonstrated antibacterial efficiency at extremely low metal contents: about 0.1 mgm^{-2} for silver and 1 mgm^{-2} for gold NPs. [108].

Washing performance of the coatings deposited on textiles via sputtering has been reported not to be satisfactory. Efforts have been made to increase the adhesion of the sputter coatings on the textiles. *Wei et al* studied the effect of plasma pretreatment and heating of the substrate on the adhesion of copper coating deposited on the polypropylene non-woven. The improvement in adhesion was evaluated by abrasion and peel test methods and was reported to be increased both after plasma pretreatment and heating during sputtering. The increase in adhesion was attributed to surface roughening by plasma treatment and diffusion during heating [117]. However, the resistance of the coating against repeated laundering, which is usually found to be poor, was not evaluated.

2.3.6.2 Room temperature pulsed laser deposition

Pulsed laser deposition (PLD) is another physical vapor deposition technique in which a high power laser beam is focused periodically on the surface of the targets to evaporate it and ionize the surface atoms making dense plasma inside the evaporated environment. These plasma species travel under vacuum and hit the surface of the substrate to nucleate and grow thin films having chemical composition as that of evaporated material. With this technique Ti, TiN, Ti(C,N) and diamond like carbon coating have been deposited on flexible polymer (polyurethane). The coatings were reported to be dense, less porous, uniform in thickness and highly elastic compared with the coatings deposited by other deposition techniques like sputtering [118]. PLD can be used to apply thin films

of high melting point materials. The film structure can be tailored from layer to layer in case of multiple layer structure [119].

Over the past years, research output reporting the deposition of thin films using PLD has increased. ZnO thin films were applied on cotton/polyester fabric using PLD. It was shown that depending upon the deposition chamber environment varying it from oxygen to vacuum, wettability of the textile surface with ZnO thin film can be tuned from hydrophilic to hydrophobic [120]. Thin films comprising polytetrafluoroethylene (PTFE) have also been deposited on cotton fabric using this technique. The fabric was rendered with super hydrophobicity after the deposition as water contact angle increase from 0° to 151° [119]. In another study, CO_2 lasers have been used to deposit thin films on textile substrates. CO_2 lasers have received less attention due to their poor pulse ability, however, carbon fiber fabrics have been reported to be deposited successfully with anatase TiO_2 using CO_2 lasers [121]. Metal oxide thin films can be grown through reactive PLD if reactive gas is used for metallic targets. *Dellasega et al.* obtained silver oxide thin films on cellulosic substrates by employing oxygen atmosphere during PLD. The films demonstrated superior antibacterial properties towards *E. coli* [122].

2.3.6.3 PVD combined with CVD

The two processes of PVD (sputtering) and PECVD (plasma polymerization) have also been investigated together to obtain the combined benefits of the two processes. The advantage of the combination of the two process is that different metal NPs can be embedded in different polymeric matrices to tailor the properties of the obtained coating [106]. Using this approach silver clusters were embedded in polymeric matrices of vinyltrimethylsilane (VTMS) and tetraethoxysilane (TEOS) prepared by simultaneous polymerization and sputtering. The mean diameter of silver clusters was found to be between 1.3 nm and 4.5 nm in the matrix from VTMS and between 4.2 nm and 6.2 nm in the matrix from TEOS. The influence of the size and filling factor on the optical and structural properties of the silver clusters in polymer matrix was studied. It was suggested that the polymeric matrix around the clusters protects them against oxidation. The deposition was carried out in an apparatus where metal cluster source was separated from the plasma discharge region [123].

Peter et al. reported the successful combination of magnetron sputtering technique and plasma polymerization process for the deposition of Ag nanoclusters in the polymer matrix over different substrates. Ag nano clusters were obtained through sputtering whereas hexamethyldisiloxane (HMDSO) was plasma polymerized on the substrates. Spherical shaped Ag nanoclusters were distributed in the polymer matrix with in size range of 2 to 12 nm. The effect of

different process parameters was studied on the deposition rate of Ag nanoclusters and plasma polymerization rate. At low power, Ag sputtering was found to be less effective than plasma polymerization but at higher power coating composition remained almost same but deposition rate was found to be changed [124].

The literature shows that a difficult to achieve, if not impossible, balance is required to be established between the two processes (sputtering and plasma polymerization) if they are going on simultaneously in the same deposition chamber. Metal target poisoning with the polymeric material is an important problem to overcome but it can be avoided by optimization process parameters. *Despax and Raynaud* obtained polysiloxane thin films containing Ag nanoclusters by an RF asymmetrical discharge on silicon substrate and characterized their composition and morphology. The films were deposited by a combination of silver sputtering and plasma decomposition of hexamethyldisiloxane (HMDSO). The authors showed that control of flow of HMDSO was crucial to have balance between cathode coverage and silver sputtering. Too high flow of HMDSO in the sputtering chamber covered the silver target completely and deposited only $SiC_xO_yH_z$ over the substrate. The control was achieved by pulsation of the HMDSO flow. The polymer matrix composition was found to be a function of RF power and silver volume fraction [125].

Nano composite coatings containing silver nano particles can also be prepared through plasma polymerization of ethylene and carbon dioxide to obtain the polymer matrix as reported by *Drabik et al. (2015)..* The size of the metal nanoparticles changed from 6 nm to about 60 nm as the power was varied from 30 W to 60 W. Optical properties of the films were dependent on the microstructure and an absorption peak was observed at 500 nm due to surface plasmon resonance (SPR) of the Ag nano particles. The aging of the films in air and in water was studied in detail. The microstructure and the optical properties of the films were found to be changed with aging both in air and in water [106]. In another study, the effect of input power and varying ratio of CO_2/C_2H_2 was studied on Ag contents. The films were characterized for Ag quantity and Ag release in deionized water. Initial film growth contained higher silver contents that later on decreased due to Ag target poisoning by polymer deposited on the target. However, homogeneous deposition is possible after reaching a steady state. The authors observed that the deposition with unclean Ag target, target that was used for previous processes, resulted in more homogeneous silver distributions as the process was already in steady state relatively [126].

The aging behavior of polymer/metal composite films deposited under various conditions of simultaneous plasma polymerization and sputtering has been

studied in detail by *Hlídek et al*. Aging behavior was analyzed by FTIR measurements for which reflection/absorption infrared spectroscopy (RAIRS) method was used. IR spectra was acquired immediate after the deposition without exposure to air (in vacuum chamber) and after 5 min and 1day. Oxidation of the polymer/metal composite film occurred after 5 min and 1 d exposure to ambient air. Surface oxidation behavior was also determined by subjecting the films to individual gases of the environment in the process chamber. Nitrogen was found to have no effect and aging was suggested to proceed without contribution from this gas. Oxygen caused the same aging effects as caused by the ambient air with a minor difference. RAIR spectra showed that silver surface was oxidized by carboxylate and carbonate groups bound to the silver particles [127]. Although polymer/metal composite thin films obtained through combination of sputtering and plasma polymerization are relatively new for textiles, it is particularly promising for environmental friendly surface functionalization of textiles. A successful scale up of any such process can provide a diverse and flexible alternative to traditional processes to obtain either pure polymeric, metallic or composite thin films possibly in a roll-to-roll batch process.

Chapter 3

Experimental

This chapter provides brief introduction of the textile substrates used in this study, the description of the co-sputtering process of silver nano clusters/silica composite coating and all the characterizations performed in this study. The key properties of textile substrates and their intended applications are highlighted. Not all the characterizations presented in this chapter has been performed on each textile.

3.1 Fabric substrates

Four types of woven textile fabrics, composed of natural as well as high performance fibers, were used in this study. These include Cotton, Kevlar[®], Vectran[®], and Activated Carbon Fabric (ACF). Cotton is composed of natural cellulose fibers. Kevlar[®] and Vectran[®] are two high performance polymeric fibers. ACF was a Kynol based activated carbon fabric used in filtration. A brief description of key properties of each of these fibers along with general and intended applications of this study are described in the following section.

3.1.1 Cotton

Cotton is a natural fiber composed of cellulose molecules. Its molecular structure consists of crystalline and amorphous regions in the ratio 2:1 respectively. Cellulose with its native crystal structure is known as cellulose I. The structure of the cellulose is modified after mercerization with NaOH (and some other treatments also) and is termed as cellulose II. The glucose molecules in the cellulose are joined in long chains that render cotton fiber its natural structure composed of microfibrils of thickness 4 nm. These fine microfibrils are crystalline and combine to yield flat sheet or lamellae that finally result in ribbon like, long

and convoluted cotton fibers. The hydroxyl groups (–OH) present in the molecular chain can result in hydrogen bonding with (-OH) groups of other fibrils [128].

The presence of the hydroxyl groups makes cotton a highly hygroscopic fiber. Moisture absorbance, breathability and other desirable characteristics of the cotton fibers have always made it an attractive choice for clothing and apparel. Cotton fabrics have been found to have good comfort properties compared to other synthetic or blended fabrics [129]. However, porous and hydrophilic structure of cotton fibers is able to retain moisture and oxygen thus providing a good nutrient media for bacterial and fungal growth [26] [109]. Cotton is extensively used in medical applications in different forms including wound care, gauzes, lint, bandages, wadding, plasters, bedding and surgical clothing and hosiery goods [5].

Cotton fabric used in this study was plain woven fabric intended to be used as gown in medical wear. Surgical gowns are normally made of cotton fabric and can be a potential source of pollution in hospital wards and operating theaters. These gowns can carry bacteria which can be transferred to other patients as they generate and shed high level of polluted particles in the form of lint [5]. The count of the yarn (warp and weft) used in the fabric was 24/1 resulting in fabric weight (gram per square meter value: GSM) of 290-300 g/m^2.

3.1.2 Kevlar®

Kevlar® is high performance polymeric aramid fiber chemically composed of poly(*p*-phenylene terephthalamide) (PPTA). Its synthesis involves polycondensation of terephthaloylchloride with *p*-phenylene diamine in the reaction shown in Figure 2
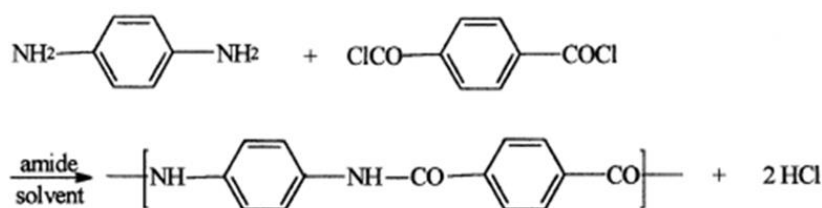
Figure 2: Synthesis of poly(p-phenylene terephthalamide) from polycondensation of terephthaloylchloride and p-phenylene diamine [130].

It was originally developed by DuPont^{TM}. The polymer has rigid rod like molecular chains that form crystals in solution form known as liquid crystals. The crystallinity of the fiber is reported to be 100%. In the fiber crystallographic structure, crystallites are formed from the molecular chains through hydrogen bonding that develop in the radial direction of the fiber. The orientation of these crystallites along the fiber axis is known to impart high stiffness to the these

fibers. The crystallites join together through hydrogen bonding to form fibrils which are further connected to each other through hydrogen bonding to form the core of the fiber [131].

The fiber possesses high tenacity and modulus and exhibits anisotropy in mechanical properties. It has high tensile strength, modulus, thermal stability and chemical inertness [132] [133]. Because of its excellent properties it finds its application in various fields demanding high performance and lighter weights. Aerospace, rail and marine industries exploit high strength and light weight characteristics of Kevlar® to achieve light weight and fuel efficiency. Kevlar® is used in cabin floors and overhead bins of aircrafts where, in addition to light weight, low electrical conductivity, fire resistance, thermal and sound insulation fulfill safety requirements and contribute to passenger comfort. Kevlar® is also used in the production of landing gear doors, honey combs for wing-to-body fairings, filament wound oxygen pressure bottles, aircraft tires and rotor blades of the aircrafts [134].

High mechanical strength, thermal stability and fire resistance properties of Kevlar® make it excellent candidate in multipurpose protective clothing [36]. Low density and high energy absorption properties make it a good candidate for flexible body armor along with other high performance fibers. Protective vests made of multilayered woven Kevlar® fabrics are used for ballistic protection of soldiers in military [135]. Because of its ability to retain its strength at high temperature, internal tendons in the airbag landing system of the Mars Pathfinder were made of Kevlar® fibers [136]. Kevlar® is widely used as reinforcement in high performance polymer composites but due to its chemical inertness and smooth surface, these composites exhibit poor interface adhesion between the fiber and the resin matrix. Interfacial adhesion between fiber and matrix can be improved by chemical as well as plasma treatments [133]. However, chemical inertness and high crystalinity of Kevlar® fibers may make it difficult to treat the fiber surface through traditional processes involving organic reaction [23]. Whereas plasma processes can easily modify or functionalize the inert surfaces and are limited to top 100 nm of the surface and thus bulk properties of the fibers are preserved [24].

By antimicrobial functionalization of the Kevlar® fabric, an additional protection (biological) can be achieved in protective clothing made of Kevlar® along with other protections including thermal, chemical and cut resistance. The Kevlar® fabric used in this study was intended to be used in aerospace applications, especially in inflatable habitat module. The fabric was coated with antibacterial coating to provide biologically safe environment to the astronauts.

The count of the yarn used in the plain woven Kevlar[®] fabric was 26/2 Nm, warp and weft density 16.5 and 15.5 yarns/cm of fabric and fabric weight, in gram per square meter (GSM), of $250 \pm 5\%$ g/m^2.

3.1.3 Vectran[®]

Vectran[®] is a high performance thermotropic liquid crystal polymer fiber. It is an aromatic co polyester of p-hydroxy benzoate (HBA) and 2-hydroxy-6-naphthoic acid (HNA) with following chemical structure
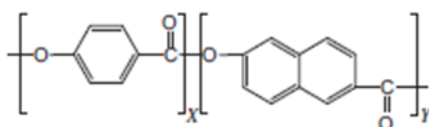
It is melt spun into fiber at high temperatures. The liquid crystal polymer domains in the melt state become highly oriented along the fiber axis during extrusion through the spinnerets resulting in a fiber with high tensile properties [137]. High orientation of the molecular chains in non-crystalline domains can yield the highest obtainable modulus [138]. Along with high mechanical properties, Vectran[®] also possess thermal stability over wide temperature range, excellent chemical resistance, low moisture take up and no creep when loaded up to 50% of its breaking strength [139]. Vectran[®] exhibits much higher specific strength compared to titanium, stainless steel and aluminum. Because of these excellent properties, it finds its applications in diverse areas like ropes and cables, protective clothing, aerospace and medical [140].

In aerospace applications Vectran[®] is used in astronauts' gloves [140] and in inflatable habitat systems. Air bags of Mars Pathfinder, in 1997 mission to help landing, were made of Vectran[®] fabric [141]. Flex-crack and abrasion resistance properties of Vectran[®] fibers are superior than those of Kevlar[®] fibers. Vectran retains its full strength at low temperature. These properties led to its selection to be used as bladder fabric layer in a multilayered airbag used in the landing system of the Mars pathfinder [136]. Bumper shields designed using Vectran[®] fibers can provide lighter weight and thinner protection system from the space debris [142]. Medical applications include catheter reinforcement, actuation cables and device delivery systems [141]. Many of these applications require antibacterial protection. Woven Vectran fabric used in this study was intended to be used in inflatable habitat module for aerospace applications. The count of the yarn used in the plain woven Vectran[®] fabric was 26/2 Nm, warp and weft density 16 and 12 yarns/fabric cm respectively and fabric weight, in gram per square meter (GSM), of $240 \pm 5\%$ g/m^2

3.1.4 Activated carbon fabric (ACF)

Activated carbon fabric (ACF) used in this study was Kynol[®] Activated Carbon Fabic (ACF). It is based on Kynol novoloid precursor fibers and textiles. Precursor fibers and fabrics are carbonized and activated to form activated carbon fibers or fabrics. ACF finds its application in air and water filtration, solvent recovery and in electronics applications as double layer capacitors. The manufacturer reported specific surface area of ACF fabric used in this study was more than 1300 m^2/g with GSM (gram per square meter) value of 120 g/m^2. Due to high specific surface area as a result of surface porosity and excellent adsorption capabilities, activated carbon fibers and fabrics are widely used in waste water treatment and air filtration [16].

3.2 Method

3.2.1 Coating deposition by co-sputtering

Antibacterial silver nano clusters/silica composite coating was deposited by means of co-sputtering on the four textile substrates namely Cotton, Kevlar[®], Vectran[®] and ACF. The novelty of the deposition lies in the co-sputtering of two targets (silica and silver) in a way where silica is deposited as a matrix of the composite coating while silver is deposited and embedded in the silica matrix in the form of nanoclusters. The technique has been originally developed by the same (GLANCE) research group and previously studied on other substrates [143] with deposition parameters that can be varied keeping in view the intended application. The desired composition of the coating is obtained by manipulating and controlling the flux of the material to be extracted from the targets and deposited on the substrates.

Sputtering is carried in vacuum where plasma is created by applying high voltage across a gas. Bombardment of high energy species of plasma (ions, radicals, electrons) can extract atoms from the desired target material that can be deposited on a substrate. The sputtering equipment used in this study was Microcoat™ MS450 which is equipped with two cathodes: one 6" diameter and other one 1" diameter. Silica target used in this study was of 6" dia (99.9% purity) supplied by Franco Corradi S.r.l.™ while silver target was of 1" dia, (99.9% purity) and supplied by Sigma-Aldrich™. A simple schematic representation of the co-sputtering process carried in this study is shown in Figure 3.
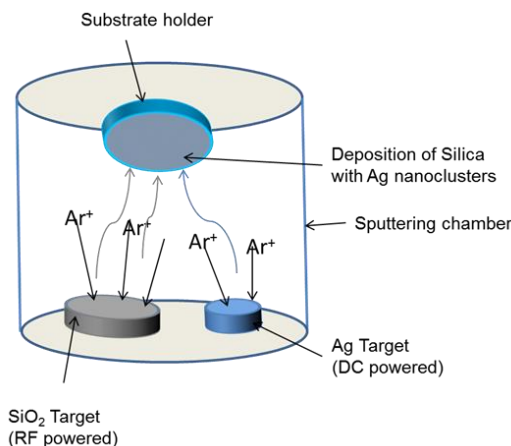
Figure 3: Schematic representation of the co-sputtering process.

Before deposition, sputtering chamber was evacuated to 70 μPa and working pressure was maintained at 5.5 dPa with argon as plasma gas. Silica target was supplied a power of 200 W RF (radio frequency 13.56 MHz) and silver target was supplied a power of 1 W DC (direct current). Since silver deposition rate (108 nm/hr) was quite high compared with that of silica (88 nm/hr) even at an applied power of 1 W (Figure 4 vs Figure 5), a 6 s plasma duty cycle was defined in which silver target was switched on intermittently for 2 second while silica target was switched on continuously. In preliminary investigations, various duty cycles starting from 6 s to 24 s were investigated in order to lower the silver concentration to figure out where there would be the minimum effect on the color of the substrates due to surface plasmon resonance associated with silver nano clusters. The samples were inspected visually after coating to analyze the color effect. It was possible to achieve relatively transparent coating at longer duty cycles (with lower silver concentrations) preserving the aesthetic look of the original textile substrate. However, finally considering the technical applications for the textile substrates used in this study, where functional performance of the fabric was more important than aesthetic value, aesthetic properties were given less priority and shorter duty cycle (comprising 6 s) was selected. With this duty cycle, although the color of the substrates changed after deposition but long term antibacterial activity was expected due to higher silver concentration   when combined with long term supply of silver ions for antibacterial action in addition to controlled and progressive silver ion release properties of the composite coating which will be described in detail in the next chapter. Three depositions were carried for 15, 40 and 80 minutes resulting in coating thickness of about 60, 150 and 300 nm respectively. The deposition rates of silica and silver were calculated from the graphs shown in Figure 4 and Figure 5 respectively. The graphs report coating thickness versus deposition time at specific applied power.
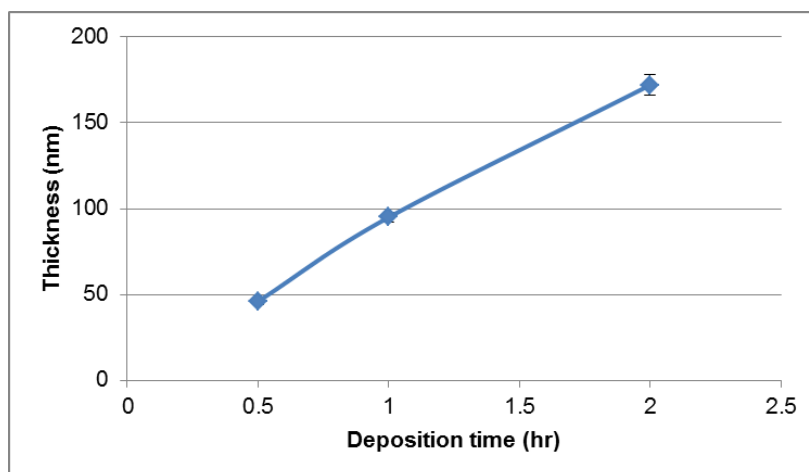
Figure 4: Coating thickness of silica versus deposition time at an applied power of 200 W RF

The deposition rate of silica at 200 W RF was calculated to be 88 nm/hr.
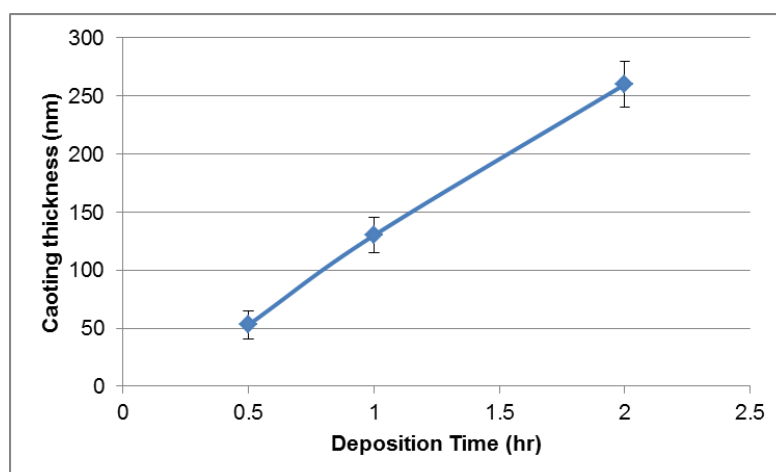
Figure 5: Coating thickness of silver versus deposition time at an applied power of 1 W DC

The deposition rate of silver at an applied power of 1 W DC was calculated to be 108 nm/hr.

The overall deposition parameters are summarized in Table 1.

Table 1: Deposition parameters of silver nanoclusters/silica composite coating

Process Parameters	Values	
Atmosphere	Ar	
Vacuum pressure	70 μPa (0.7 pbar)	
Working pressure (deposition pressure)	5.5 dPa (5.5 μbar)	
Power to silica target (6 inch dia)	200 W RF	
Power to Ag target (1 inch dia)	1 W DC	
Plasma duty (sputtering) cycle	6 s	
	Si	Ag
Plasma ON interval	6 s	2 s
Plasma OFF interval	0 s	4 s
Deposition time	Three depositions	
	1. 15 min	
	2. 40 min	
	3. 80 min	

The schematic representation of the silver nanoclusters/silica composite coating is given in Figure 6.
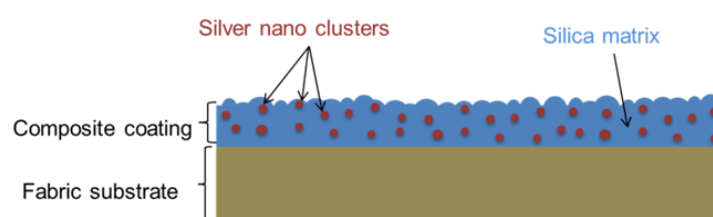
Figure 6: Schematic representation of the silver nanoclusters/silica composite coating

3.2.2 Coating morphology and composition (FESEM, EDX, XPS)

The morphology of the composite coating deposited on four textiles was investigated using field emission scanning electron microscope (FESEM) by QUANTA INSPECT 200, Zeiss SUPRATM 40™. To analyze the specimen, FESEM uses a focused beam of electron to scan across a specimen to produce an image. Semi quantitative elemental analysis was performed using Energy Dispersive Spectroscopy, (EDS, EDAX PV 9900™).

Detailed compositional analysis of the coating on four textiles was performed using x-ray Photoelectron Spectroscopy (XPS, Phi 5000 Versa Probe™). XPS is photoelectric technique and is also known as electron spectroscopy for chemical analysis (ESCA). XPS is highly surface sensitive and is extensively used to investigate surface compositions. Incident X-rays can excite atoms on the surface of specimen which results in ejection of en electron known as photoelectron. The spectral lines of XPS are identified by the particular shell from which these photo

electrons are ejected. The core level vacancy, created by the emission of the photoelectron, is filled by an electron from another shell. This results in emission of another electron, known as auger electron, which is emitted by the atom to conserve energy. The analysis of the kinetic energies of the emitted photo electrons yields important information about composition and chemical states of the elements present on the surface.

For XPS, monochromatic Al Kα x-ray source with photon energy of 1486.6 eV at 15 kV and 1 mA was used. The binding energy scale was calibrated by setting the carbon C1s (C-C) binding energy at 284.5 eV. The operating condition was 21.7 W for the x-ray source and tilt angle for analyzer was 45°. The survey scans were taken at pass energy of 187.85 eV with a step size of 1 eV whereas high resolution scans at pass energy of 23.50 eV with a step size of 0.1 eV. The morphological and compositional analysis was performed both on coated and uncoated fabric samples.

3.2.3 Total silver content by ICP-MS

The concentration of the silver in the composite coating was determined through inductively coupled plasma mass spectroscopy (ICP-MS) by Thermo Scientific iCAP™ Q ICP-MS. Fabric samples of known weight were dissolved in a mixture of 15 ml of nitric acid (65%) and 2 ml of H_2O_2 (30%). After dissolution, the liquor was filtered in a flask of 25 ml. Deionized water was used to fill the flask to the final volume and was distilled through evaporation. For calibration, solutions containing silver at concentrations of 125, 250, 500 and 1000 ppb were used.

3.2.4 Silver release in water

Ionic silver release from the composite coating was assessed by silver ion release test in water. Test was carried in milliQ water. Coated fabric samples of dimension 1x1 cm^2 were immersed in 25 ml of milliQ water. The amount of ionic silver released in water was analyzed through silver photometer by Hanna Instruments™ after 3, 24 and 72 hours of immersion. Separate liquors and fabric samples were tested for each duration and test was performed in triplicate for each duration.

Silver photometer is based on adaptation of 1-(2-pyridylazo)-2-naphtol (PAN) method. Four silver reagents from Hanna Instruments™ are used in the analysis. When added, a reaction between silver and the reagents takes place that causes an orange tint to the water containing silver. The reagents are added in a sequence defined by the instrument manufacturer. First, 1 ml of "Reagent A" (HI93737A-0) was put in control beaker containing only milliQ water and 1 ml of "Reagent B" (HI93737B-0) in the beaker containing water in which fabric samples were

immersed and swirled gently. After 2 minutes, "Reagents C" (HI93737C-0) was added in both the beakers and mixed gently. After another two minutes, silver fixing "Reagent D" (HI93737D-0) was put in both the beakers and put for two minutes. For the measurements, 10 ml from both the beakers was put in two separate cuvette, one for control and one for the specimen. The control cuvette was inserted in the photometer to set the instrument to "0" and then cuvette containing test liquor was tested for the measurement. Silver meter displays reading in mg/l which was converted to $\mu g/cm^2$.

3.2.5 Silver release in artificial sweat

Silver release behavior from the composite coating in artificial sweat was analyzed. Artificial sweat was prepared by dissolving sodium chloride (0.5% mass), lactic acid (0.1% mass) and urea (0.1% mass) in milliQ water [144]. The pH of the resulting sweat solution was 3. Fabric samples of 1x1 cm^2 were immersed in 30 ml of artificial sweat and incubated at 37 °C to simulate body temperature. One ml of the sweat solution was picked after 3, 24 and 72 hours and analyzed through inductively coupled plasma mass spectroscopy (ICP–MS NEXION 350D, Perkin Elmer Waltham, MA, USA).

3.2.6 Antimicrobial tests

Antibacterial performance of the coated textiles was evaluated through inhibition halo test (disk diffusion or Kirby Bauer test) following the procedure described in NCCLS M2-A9 standard [145]. Antimicrobial properties were evaluated against four microbial strains namely: *Staphylococcus aureus* (*S. aureus*, a Gram positive bacterium), *Escherichia coli* (*E. coli*, a Gram negative bacterium), and *Candida Albicans* (*C. albicans*, a fungus). For some cases *Staphylococcus epidemidis* (S. epidermidis, a Gram positive bacterium) was also used

The procedure of inhibition halo test involves preparing a microbial suspension by dissolving respective microbial strains in physiological solution (0.9 % sodium chloride). The concentration of microbes was adjusted with the help of McFarland index using an optical instrument (Phoenix Spec BD McFarland). The instrument measures the turbidity of the solution caused by bacterial suspension. Standard microbial suspensions of 0.5 McFarland index were prepared for all the tested microbes which correspond to approximately 1-2 x 10^8 colonies forming units of bacteria per ml of solution (CFU/ml). An inoculum from this suspension was streaked uniformly on Muller Hinton agar plates. Both control and coated fabric samples of size 1x1 cm^2 were placed on agar surface with coated side in contact with bacteria. Agar plates were incubated at 35°C for 24 hours. Microbes grow on the agar surface during incubation

leaving only the region around the samples where antimicrobial activity is present. This region is known as inhibition halo and is a semi quantitative measure of antimicrobial activity of antimicrobial agents.

In some cases, antimicrobial performance was also evaluated through counting number of colonies forming unit method (CFU), also known as broth dilution test. Broth dilution test is comparatively difficult and time consuming than inhibition halo test but provides quantitative information about antimicrobial efficacy [26]. Broth dilution test was performed only against *S. aureus* and was used to evaluate the efficacy of the antimicrobial coating in terms of bacterial proliferation in the broth as well as bacterial adhesion on the sample surface. For the test, a 0.5 McFarland index bacterial suspension was prepared as above. From this solution, an aliquot of 25 µl was mixed in 5 ml solution in the Mueller Hinton broth tube thus obtaining a bacterial suspension of approximately 5×10^5 CFU/ml. In total six such broths were prepared, three for uncoated and three for coated fabric samples. Fabric samples of size 0.5×2 cm^2 were immersed in these broths and incubated at 35˚C for 24 hours. After incubation, the McFarland index of each broth was measured. The difference in the McFarland index of broth tubes containing uncoated and coated specimens is a semi-quantitative measure of antimicrobial activity in terms of bacterial proliferation. However, bacterial proliferation as well as adhesion were more precisely assessed by counting the number of CFU.

In order to estimate the bacteria proliferated in the broths, a series of dilutions were performed after incubation. An aliquot of 500 µl was drawn from each of the above incubated broths and put in another tube containing 500 µl of fresh physiological solution (0.9% sodium chloride) making the total volume 1 ml. From this first dilution, an aliquot of 100 µl was drawn again and put in another tube containing 900 µl of fresh physiological solution. The process was repeated up to 7 dilutions. From each of the last diluted solutions, a dose of 100 µl was spread on six blood agar plates (three for uncoated and three for coated fabric samples), thus making 8 dilutions in total. The agar plates were then incubated at 35˚C for 24 hours to allow the growth of colonies of bacteria. After incubation, the colonies forming units (CFU) were counted on each agar plate and compared to assess the bacterial proliferation in the broths that contained uncoated and coated samples.

The second part of the broth dilution test was to assess the bacterial adhesion on the surface of uncoated and coated fabric samples. For this purpose, the uncoated and coated fabric samples that were drawn from the Mueller Hinton broths were put in separate tubes containing 3 ml of physiological solution (0.9%

sodium chloride) and vortexed for 1 minute at 50 Hz to detach any bacteria on the sample surface. From this solution, 300 µl was drawn and mixed in 700 µl of physiological solution. From this first dilution, an aliquot of 100 µl was drawn and put in another tube containing 900 µl of fresh physiological solution and process was repeated up to 5 dilutions. From the last dilutions, 100 µl was spread on blood agar plates (making the 6th dilution) and incubated at 35˚C for 24 hours. After incubation the CFU were counted on each agar plate and results of uncoated and coated samples were compared. The number of CFU counted both in proliferation and adhesion was multiplied by the number of their respective dilutions to obtain the number of CFU in the original solution.

3.2.7 Water wettability and Moisture management properties

Three types of tests, namely water contact angle, water sorption and moisture management tests, were performed to asses water wettability characteristics before and after coating. "Kruss DSA 100" with drop shape analyzer was used for water contact angle measurements. A 5 µl water droplet was introduced on the fabric surface with the help of a syringe. The image of the drop was captured with the help of integrated camera after 10 seconds and contact angle was noted with the help of software. An average of 6 readings is reported both for coated and uncoated samples.

Water sorption test was performed to analyze water absorbing behavior of textile substrate before and after coating using Kruss tensiometer. Fabric samples (6 cm x 1 cm) were fixed in clamps of the apparatus and lowered gently to a depth of 0.1 mm in the distilled water as shown in Figure 7. Test lasted for two minutes during which the instrument records water uptake (mass) by the sample. An average of three measurements is reported both for coated and uncoated samples.
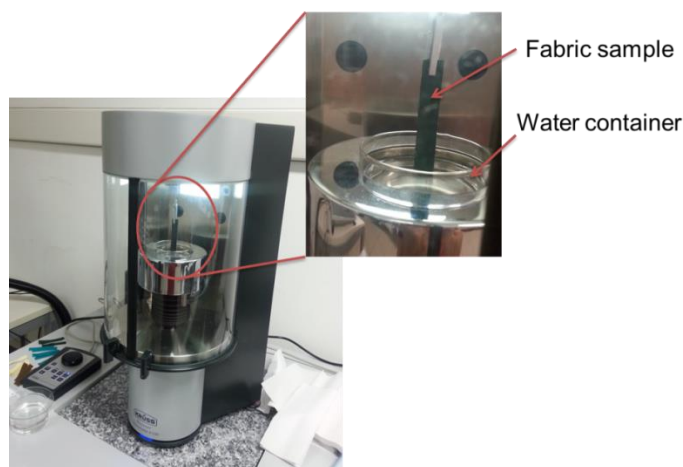
Figure 7: Water sorption test on Kruss tensiometer in "Laboratorio Alta Technologia Tessile 1, Biella (LATT1)"

Moisture management properties of the fabric were measured using moisture management tester by Atlas (MMT M290, SDL Atlas) according to AATCC195-2011 [146]. Liquid transport properties in three dimensions of the fabric are known as moisture management properties. The measuring head of the instrument consists of upper and lower moisture sensors which are arranged in concentric circles as shown in Figure 8. These sensors sense and record the transport of the test liquid, introduced on the surface of the fabric, in three dimensions. These include (1) spreading the liquid outward on top surface of the fabric (2) transfer through the fabric thickness and (3) transfer outward on the lower surface of the fabric. The conductivity of the test liquid (water) was adjusted to 16 ± 0.2 mS by dissolving approximately 9 g of NaCl to 1 L distilled water. Approximately 0.21 ± 0.01 g of this test liquid was introduced on top surface of an 8 cm^2 fabric sample and dynamic liquid transport properties were measured by the sensors. The test was carried under controlled laboratory atmosphere at temperature 20 ± 2 °C and relative humidity (RH) 65 ± 2 %. The samples were conditioned to the laboratory atmosphere before measurements and test was carried in triplicate for coated and uncoated fabric samples.
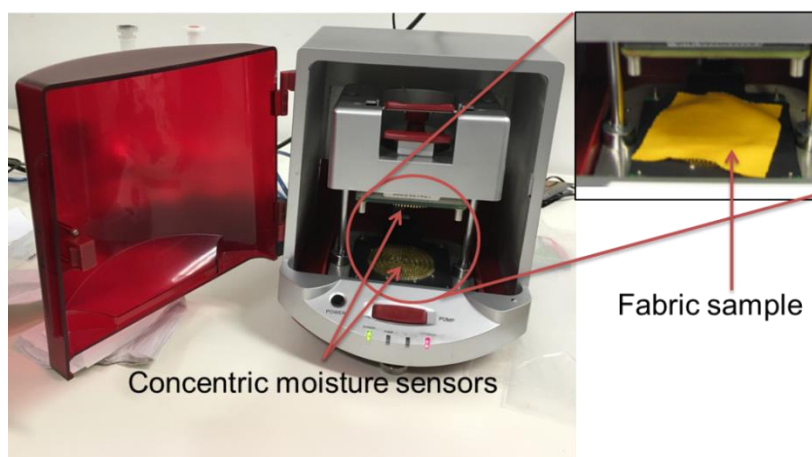
Figure 8: Analyzing moisture management properties of fabric on Moisture management tester in "Laboratorio Alta Technologia Tessile 1, Biella (LATT1)

3.2.8 Air permeability

Air permeability of the fabric, before and after coating, was determined using Branca Idealair™ according to ASTM D737-96 standard. The instrument measures the air flow rate through a known area by setting a defined air pressure difference across the fabric to be tested. The instrument was first calibrated

according to the procedure described by the manufacturer using standard plates with circular air inlets. For the measurements, fabric samples of 10 cm^2 were placed between two metal plates and fixed horizontally as shown in Figure 9. Metal plates have holes of known area for air passage. The instrument measured the volumetric air flow rate through the fabric section when a pressure differential of 100 Pa was created across the fabric. Air permeability, expressed in terms of air velocity (mm/s) through the fabric section, was noted from the instrument display. Five samples of both coated and uncoated fabric were tested.
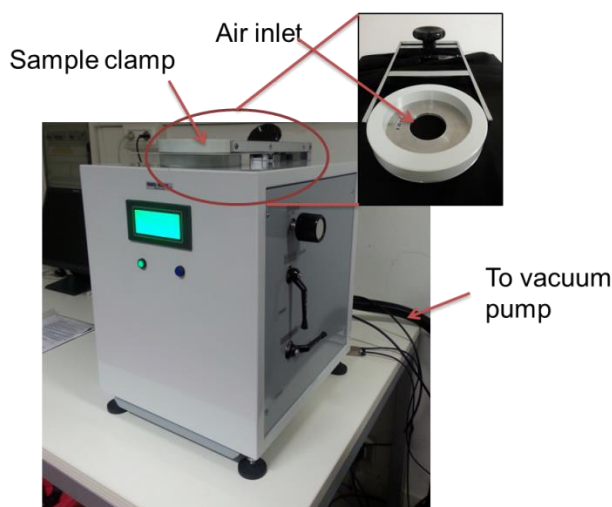
Figure 9: Air permeability testing through Branca Idealair™ in "Laboratorio Alta Technologia Tessile 1, Biella (LATT1)

3.2.9 Washing fastness

Washing fastness of coating was assessed through multiple washing cycles. Washing was done with two soap solutions, one was commercial Castile soap and the other one was AATCC standard detergent without optical brightener (WOB). Coated samples of size 2.5 cm x 2 cm were washed in solution containing 100 ml of MilliQ water and 2 g/l of one of the detergents. Washing was carried for 30 minutes at 60 °C in a thermo stat bath with oscillation set to 150 rpm. After washing, the samples were rinsed thoroughly with distilled water and dried at room temperature. FESEM and EDS was performed on washed samples to analyze coating stability on fabric substrates.

Chapter 4

Results and discussion

In this chapter the results of characterization of silver nano clusters/silica composite coating are presented. The results of these characterizations are presented and grouped separately for each textile substrate which are accompanied by a discussion at the end of the chapter. The discussion also highlights some results that were obtained by other project partners of the study and were published jointly. Some of the results presented in this chapter have been published in two publications [147] [148].

4.1 Cotton

4.1.1 Coating morphology and composition (FESEM, EDS, XPS)

The morphology of the uncoated cotton fabric surface and that coated with silver nanoclusters/silica composite coating was investigated with FESEM and is shown in Figure 10 at low and high magnifications. The coated cotton samples are named by adding the deposition time to the acronym "Cot" (Cot_15, Cot_40 and Cot_80).

Since cotton fibers are composed of micro fibrils [128] [80], therefore, the smooth and longitudinal fibrillar structure of the uncoated cotton fibers is visible at high magnification in Figure 10. After deposition, the presence of the coating can be observed on the fiber surface, however, pronounced roughness and typical morphology of the sputtered coating is relatively more visible at longer deposition time (Cot_80). Silver nanoclusters are uniformly distributed and embedded in the silica matrix. Silver nanoclusters, with an average size ranging from 25 to 50 nm, are clearly visible at lower deposition times (Cot_15, Cot_40). Since silver nano

clusters are expected to be embedded in the silica matrix according to the co-sputtering scheme, their presence on the surface may not always be observed at increased deposition time (Cot_80). After 80-minutes deposition (Cot_80), the typical granular morphology of the sputtered layer becomes clearly visible and the underlying longitudinal cellulose fibrils are no more visible. The roughly spherical and conjoined grains (Cot_80) are composed of silica and provide matrix to host silver nano clusters. The evolution of the nano structure on the fiber surface, coating morphology and increment in coating thickness with the deposition time can be seen from FESEM images and EDS spectra shown in Figure 10 and Figure 11 respectively.

The elemental analysis of the uncoated and coated cotton fabric was performed with EDS and is shown in Figure 11. Since cellulose is the structural unit of cotton fibers, the EDS spectrum of the uncoated cotton fabric (Cot_uncoated) is composed of carbon (C) and oxygen (O) peaks only. The presence of chromium (Cr) is due to Cr coating required to give necessary conductivity to the nonconductive cotton surface for FESEM analysis. Silicon (Si) and silver (Ag) peaks appeared on coated samples (Cot_15, Cot_40 and Cot_80) with intensity of the peaks increasing with increased deposition time. From the elemental composition obtained through EDS, the ratio Ag/Si with respect to atomic percent was calculated and is shown in the respective EDS spectrum in Figure 11. The Ag/Si ratio is approximately the same, within narrow distribution range, for all the three depositions suggesting same composition of the coating with increasing coating thickness.

The color of the cotton fabric also changed after coating due to well-known localized Surface Plasmon Resonance (L-SPR). The green color of the dyed cotton fabric changed from light to dark brown, as shown in Figure 12, depending upon deposition time and hence silver content.
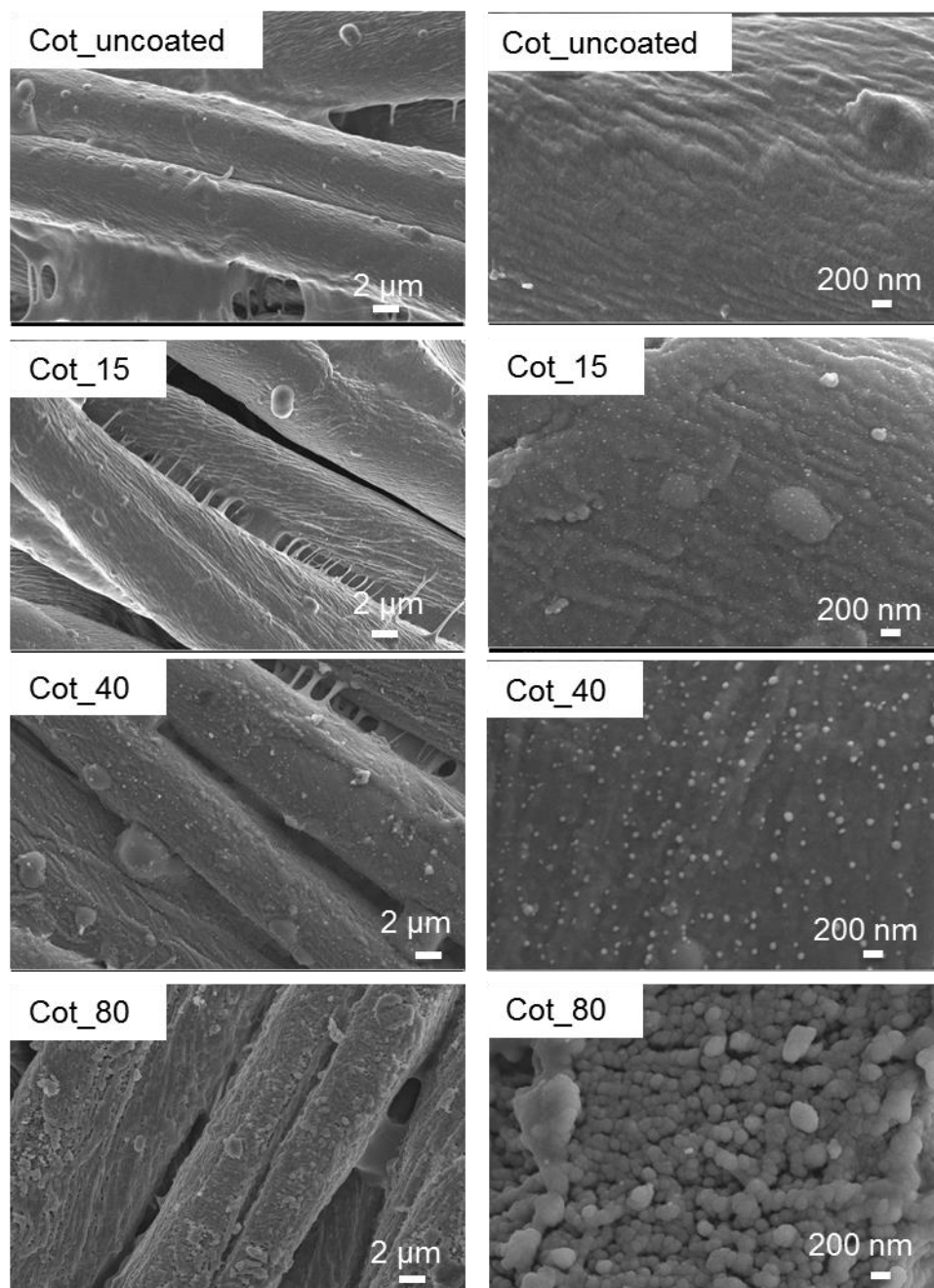
Figure 10: FESEM surface morphology of uncoated (Cot_uncoated) and coated (Cot_15, Cot_40 and Cot_80) cotton fabric at low and high magnification
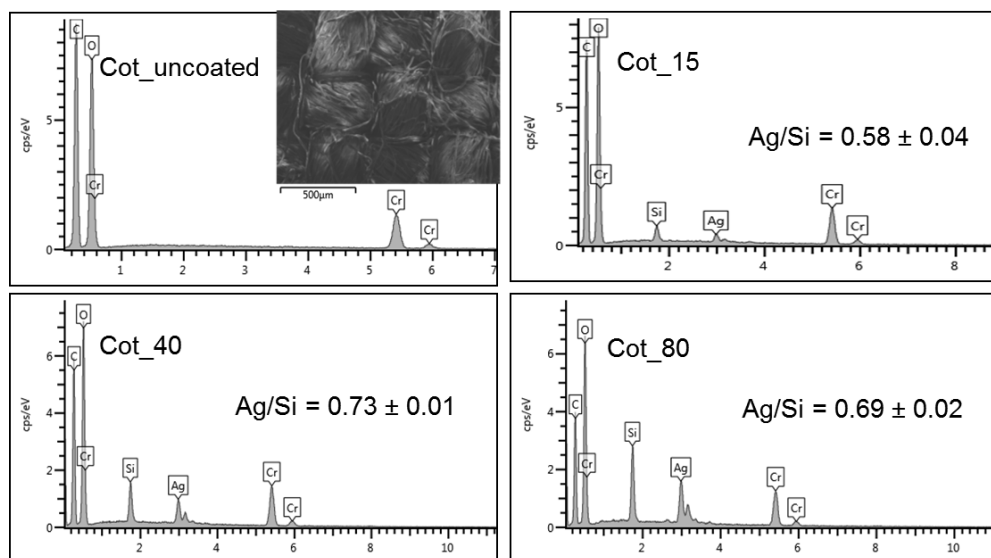
Figure 11: EDS spectra of the uncoated (Cot_uncoated) and coated cotton fabric (Cot_15, Cot_40 and Cot_80) and corresponding Ag/Si (at. %) ratio
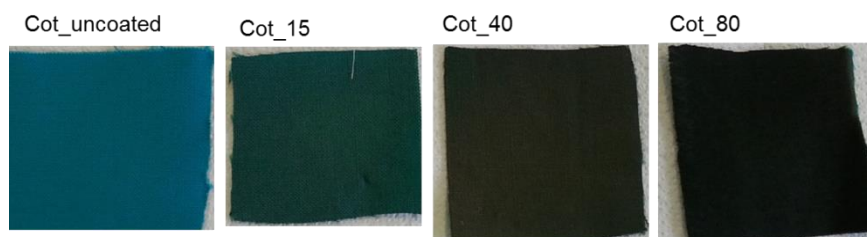
Figure 12: Images of the cotton fabric showing change in color with deposition time

Detailed compositional analysis of the cotton fabric surface before and after coating was performed through XPS. Figure 13 shows XPS survey spectra of uncoated (Cot_uncoated) and coated (Cot_40 and Cot_80) cotton fabric. In agreement with EDS spectra, the spectrum of uncoated cotton (Cot_uncoated) is mainly composed of oxygen (O-1s) and carbon (C-1s) peaks [149] whereas peaks related to silver and silicon are present in the spectra of coated cotton fabric (Cot_40, Cot_80).
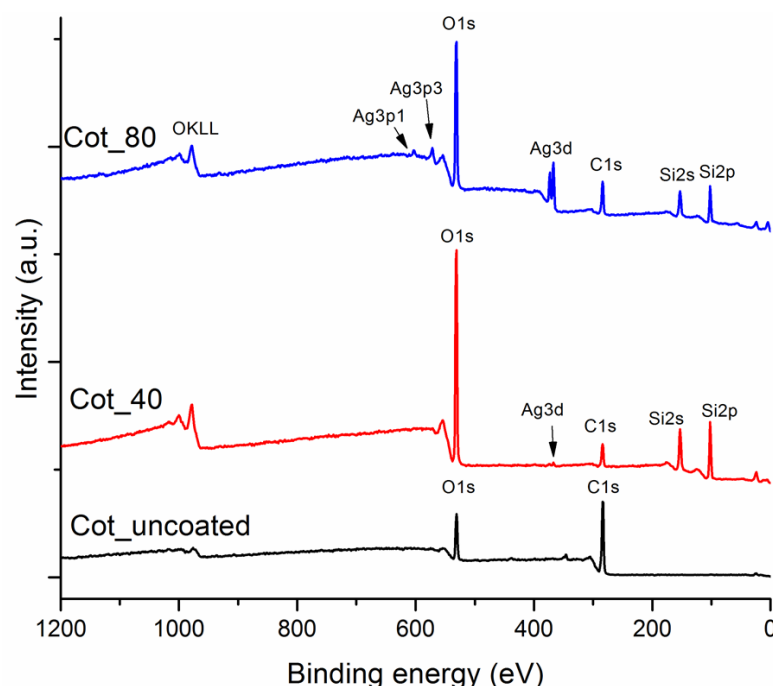
Figure 13: XPS survey spectra of uncoated (Cot_uncoated) and coated (Cot_40 and Cot_80) cotton fabric

To further analyze the bonding states of the elements detected in XPS survey spectra, high resolution scans were obtained in the C-1s, O-1s, Ag-3d and Si-2p core regions and are shown in Figure 14. Binding energies of different peaks and their relevant bond associations have been summarized in Table 2 and discussed as follows. C-1s peak of the uncoated cotton (Cot_uncoated) can be deconvoluted into sub peaks to identify three different bonds of carbon. The peak at 284.8 eV is attributed to C-C/C-H bonding, the sub peak at 286.2 eV is assigned to C-O and C-O-C bonds whereas the third sub peak at 287.9 eV is due to C=O and O-C-O bonds [150]. Theoretically, C–O, O–C–O and C–O–C peaks originate from pure cellulose structure whereas C-C and C-H peaks are usually detected in the cotton fibers due to impurities (natural waxes) or applied finishes comprised of hydrocarbons [150]. It is also commonly known that carbon can be adsorbed on polymeric and metallic surfaces when exposed to the environment. Therefore, C-1s peaks present in the spectra of coated cotton (Cot_40 and Cot_80) could be due to the carbon adsorbed on the fabric surface known as adventitious carbon [150] or it can also be partly from the substrate.
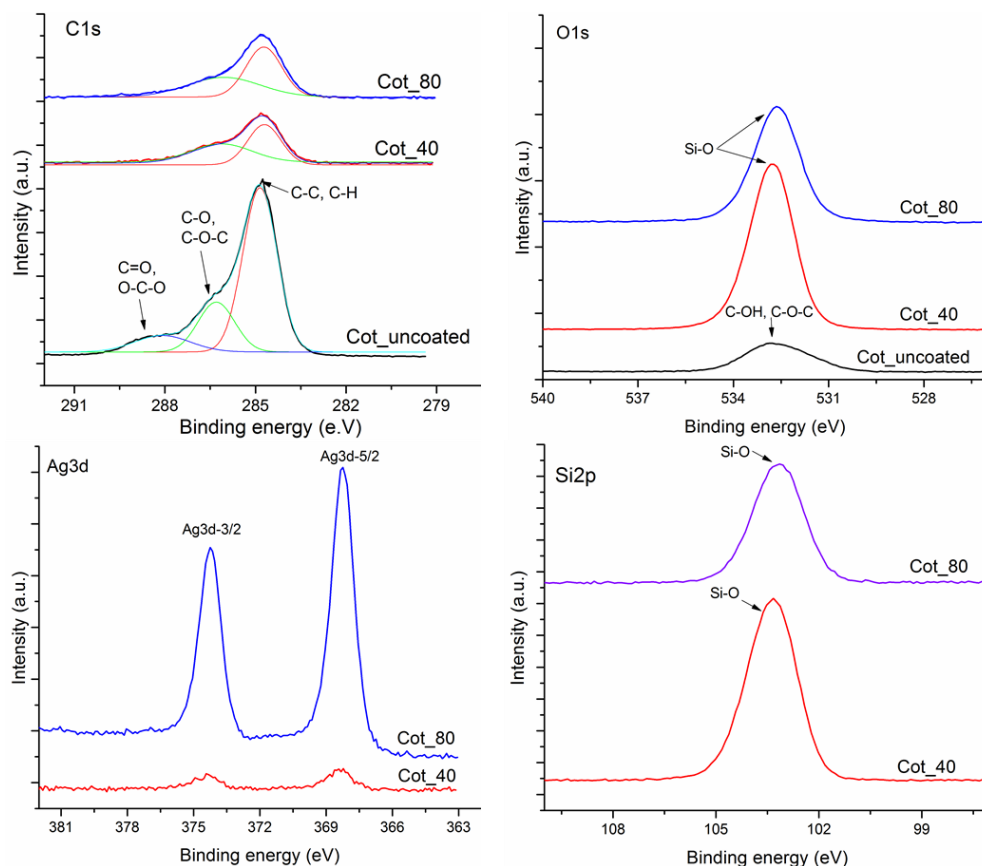
Figure 14: XPS high resolution spectra of C1s, O1s, Ag3d and Si2p peaks of uncoated (Cot_uncoated) and coated (Cot_40 and Cot_80) cotton fabric

The O-1s peak for uncoated cotton (Cot_uncoated) in Figure 14 appeared at 532.7 eV and is representative of C-O and C-O-C bonds [151]. While O-1s peak at 532.7 (or 532.6) eV on coated cotton surface (Cot_40 and Cot_80) can be attributed to the oxygen bonded with silicon atoms due to silica present in the silver nanoclusters/silica composite coating with Si-2p peak at 103.3 eV (or 103.1 eV) [152] [153]. The Ag-3d core level peaks in Figure 14 confirm the presence of metallic silver in the composite coating (Cot_40 and Cot_80). The two sharp peaks at binding energies of 374.2 eV and 368.2 eV are assigned to Ag-3d$_{3/2}$ and Ag-3d$_{5/2}$ signals respectively representing silver in Ag^0 state [79] [154].

Surface composition w.r.t atomic percent (at %) derived from XPS survey spectra is given in Table 3. Carbon at.% decreases whereas oxygen at.% increases after coating. Carbon at. % on coated cotton surface (Cot_40 and Cot_80) is considerably less than that of on uncoated cotton surface and could be mainly due to adsorption from environment or a contribution from the substrate also. The ratio O/Si for coated cotton surface is slightly greater than 2 (the stoichiometric ratio between O and Si in SiO$_2$) indicating that almost all the oxygen detected was due to silica. Oxygen present in slightly excess concentration than that of

stoichiometric concentration in silica could also be due to the oxygen adsorbed from the environment.

Table 2: Table summarizing different peaks, their binding energies and corresponding bonds in XPS spectrum of uncoated (Cot_uncoated) and coated (Cot_40 and Cot_80) cotton fabric

Peak	Bonding	Binding energy BE (eV)		
		Cot_uncoated	Cot_40	Cot_80
C-1s	C-C/C-H	284.8	284.7	284.7
	C-OH/C-O-C	286.2	286.2	285.8
	O-C-O/C=O	287.9	-	-
O-1s	C-OH/C-O-C	532.7	-	-
	Si-O	-	532.7	532.6
Si-2p	Si-O	-	103.3	103.1
Ag-3d$_{3/2}$	Ag^0	-	374.2	374.2
Ag-3d$_{5/2}$	Ag^0	-	368.3	368.2

Table 3: Composition (w.r.t atomic %) of the uncoated (Cot_uncoated) and coated (Cot_40 and Cot_80) cotton surface derived from XPS survey spectra

	Atomic %				
	C-1s	O-1s	Si-2p	Ag-3d	O/Si
Cot_uncoated	78.7	20.2	-	-	-
Cot_40	17.1	57.4	25.4	0.1	2.3
Cot_80	27	51.2	19.4	2.4	2.6

4.1.2 Total silver content and silver ions release in water

The total silver concentration in the silver nanoclusters/silica composite coating was determined through ICP-MS. ICP-MS was performed for the samples deposited for 40 minutes only (Cot_40) and silver amount was found to be 253 ± 38 ppm (253 mg per Kg of the fabric). Since deposition parameters were same and only deposition time was varied for the three coating thicknesses (Cot_15, Cot_40 and Cot_80), therefore, the total silver amount on Cot_80 is expected to be approximately double and for Cot_15 a little less than half of what were obtained for Cot_40.

Upon exposure to the wet environment, silver nano clusters get oxidized and release silver ions in the media as will be discussed later in detail in the following "Discussion" section. Silver ions are also considered to be responsible for antibacterial action, therefore, silver ion release behavior from the composite coating was analyzed through silver release test by immersing a 1x1 cm^2 sample in water and results are shown in Figure 15. The graph shows that silver release was dependent on the total silver content in the coating as well as on immersion duration. The silver ions release values were in the range 0-6.37 $\mu g/cm^2$ during 3 days of continuous sample immersion in water. The total silver ions released from Cot_40 after 3, 24 and 72 hours was 0.21, 1.8 and 3.84 $\mu g/cm^2$ which correspond to approximately 4, 35 and 74% of total silver (253ppm) deposited on Cot_40. The same percentage of silver release can be expected for Cot_15 and Cot_80 as they show silver release trend over time similar to that of Cot_40. The graphs in Figure 15 show a gradual and progressive ionic silver release behavior from the composite coating which can be attributed to the embedment of silver nanoclusters in the silica matrix which provides a degree of control to release of silver ions. Gradual release of ionic silver from the coating could be a beneficial aspect from the point of view of prolonged antibacterial activity.

EDS analysis was performed on Cot_40 samples to detect relative atomic % of Si and Ag after 3, 24 and 72 hours of silver release test in water and results are shown in Figure 16. The bars in Figure 16 show that the residual Ag at. % on Cot_40 samples gradually decreased with increasing duration of immersion in silver release test thus complementing the results shown in Figure 15. A partial dissolution of silica matrix of the composite coating is also evident. Compared with as deposited samples (0 h), Si atomic % decreased after silver release test.
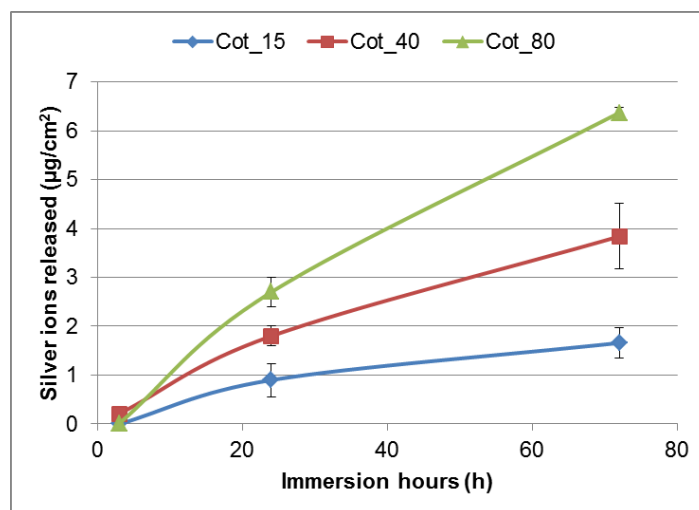
Figure 15: The amount of silver ions leached from coated cotton fabric in water during silver release test
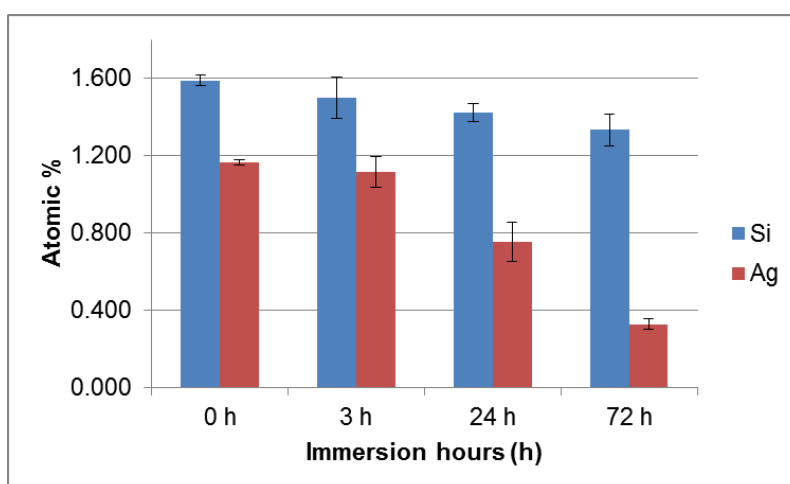
Figure 16: Relative atomic % of Si and Ag on Cot_40 after silver release test of 3, 24 and 72 hours in water

It is interesting to note that percent reduction in the silver at. % on Cot_40 is 4, 35 and 71 % after silver release test of 3, 24 and 72 hours respectively. This is in good agreement with percentage of ionic silver released from Cot_40 in water (4, 35 and 74%) and calculated with respect to total silver content on Cot_40 as measured by ICP-MS. This further complements that all the silver released from the composite coating was in ionic form rather than in particulate form.

4.1.3 Silver release in artificial sweat

Since human sweat is a body fluid that may come in direct contact with wearable antibacterial textiles (for example surgical gowns and other topical use textile products), therefore, the release behavior of silver from the silver nanoclusters/silica composite coating was also assessed in artificial sweat. The comparison of silver released in water and in artificial sweat from Cot_40 is shown in Figure 17. The figure shows that the amount of silver released in artificial sweat is higher than that released in water during the same time interval. It can be seen that the final amount of silver released in both the fluids was approximately the same. However, in artificial sweat, a plateau was reached after 24 hours due to accelerated release of silver ions.

The EDS of the samples after silver release test in water and in artificial sweat, shown in Figure 18 (a), shows that relatively lower silver atomic % was detected on samples after release test in artificial sweat (72_h_sw) than that was detected on samples with release test in water (72_h_w). The pH of the artificial sweat formulation used in this study was 3 and acidic pH favors silver release [104]. Moreover, the presence of Cl^{-1} in artificial sweat may lead to accelerated release of Ag^{+1} to form AgCl as confirmed by the presence of Cl in the EDS spectrum of Cot_40, after release test in artificial sweat (Cot_40_72 h sw), in Figure 18 (b). Therefore, higher amount of silver is expected to be released in artificial sweat compared with that of in water having approximately neutral pH and no Cl^{-1}.
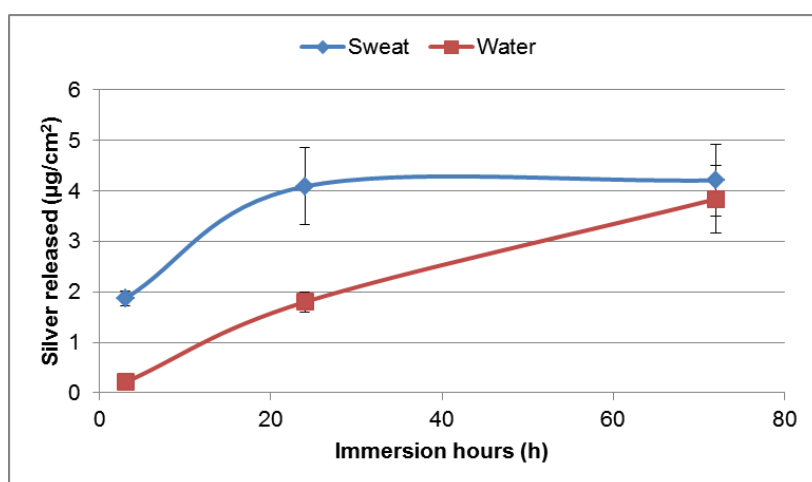
Figure 17: Comparison of silver released from Cot_40 in water and in artificial sweat
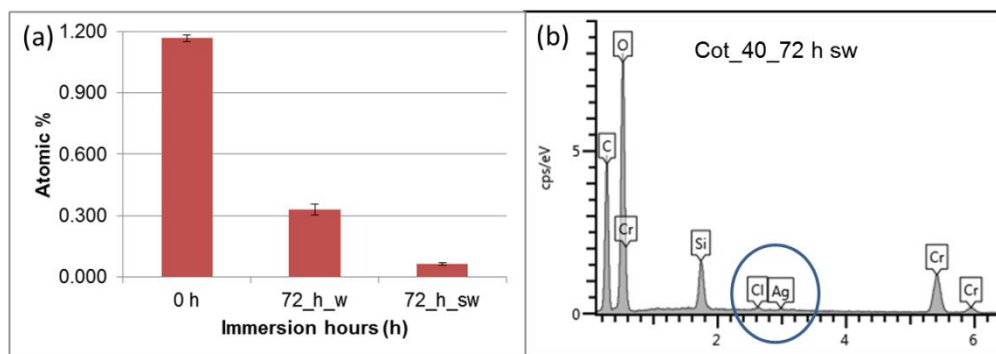
Figure 18: (a): Relative Ag atomic % on Cot_40: as deposited (0 h) and after 72 hours of silver release test in water (72_h_w) and in artificial sweat (72_h_sw), (b): EDS spectrum of Cot_40 after 72 h release test in artificial sweat

4.1.4 Antimicrobial test

Antimicrobial properties of the cotton fabric coated with silver nanoclusters/silica composite coating were verified through antimicrobial inhibition halo test. The inhibition halo test was performed against two bacterial and one fungal strain. The two bacterial strains include *staphylococcus aureus* (Gram positive bacterium) and *Escherichia coli* (Gram negative bacterium) whereas *Candida albicans* was used as fungal strain. The results of inhibition halo test are shown in Figure 19. In case of *S. aureus*, a well-defined inhibition halo of up to 3 mm in size was formed around all the coated cotton samples (Cot_15, Cot_40 and Cot_80) whereas no halo was formed around uncoated cotton (Cot_uncoated). The size of inhibition halo was approximately the same for the three depositions (15, 40 and 80 min.) showing that the thinner coating (≈60 nm after 15 min. deposition) was as effective against *S. aureus* as relatively thick coating (≈300 nm after 80 min. deposition).

Due to similar antibacterial effect of the three depositions against *S. aureus*, cotton fabric deposited for 40 minutes only (Cot_40) was tested against *E. coli* and *C. albicans*. An inhibition halo against *E. coli* can be observed around Cot_40 samples compared with that of Cot_unocated. However, the inhibition zone against *E. coli* is not as clear as it was against *S. aureus*. Some bacterial colonies of *E. coli* grew within the inhibition zone around the coated samples making the halo less transparent. This shows relatively higher resistance of *E. coli* against the antibacterial composite coating compared with *S. aureus*. A small inhibition halo of approximately 1 mm in size was also present around Cot_40 against *C. albicans*. The overall growth density of colonies of *C. albicans* on the agar surface was much less than that of *S. aureus* and *E. coli* due to which the formed halo is not prominent.
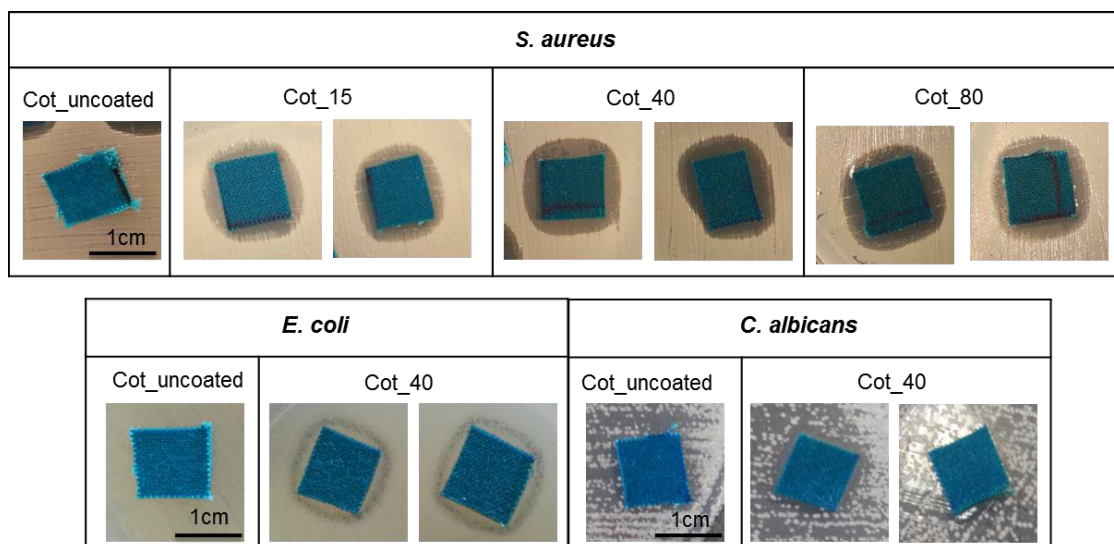
Figure 19: Inhibition halo test for uncoated and coated cotton fabric against *S. aureus*, *E. coli* and *C. albicans*

Inhibition halo test on Cot_40 samples was also performed after silver release test of 24 (Cot_40_24h) and 72 hours (Cot_40_72h) and results are shown in Figure 20. The formation of a good inhibition halo shows that the coated samples were able to retain antibacterial activity after 24 and 72 hours of continuous immersion in water.
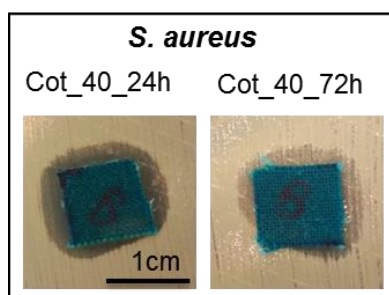
Figure 20: Inhibition halo test for Cot_40 after silver release test of 24 and 72 hours

4.1.5 Water wettability and air permeability

The effect of the silver nanoclusters/silica composite coating on water wettability of the cotton fabric was analyzed through three different tests namely: water contact angle test, water sorption test and moisture management testing. These tests were performed only on Cot_40. The contact angle of water on uncoated fabric was $124° \pm 6°$ whereas after coating it reduced to $36° \pm 7°$. The image of

the water droplet after 10 s of being introduced on the fabric surface is shown in Figure 21.
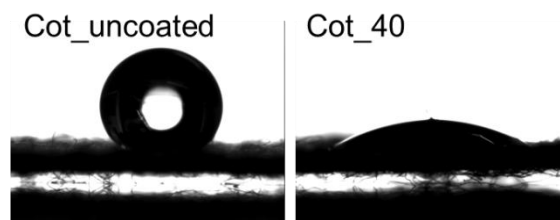
Figure 21: Image of water droplets on uncoated (Cot_uncoated) and coated (Cot_40) cotton fabric surface in contact angle test

The effect of the coating on water absorbing behavior of the cotton fabric was assessed by water sorption test on tensiometer and results are shown in Figure 22. Total water uptake by the uncoated and coated cotton fabric during water sorption test is shown in Figure 22 (a) whereas water uptake trend over time is shown in Figure 22 (b). Water uptake by cotton fabric was higher after coating showing an increase in hydrophilicity of the coated cotton in agreement with water contact angle test. Capillary constant of a solid material (fabric) is related to the structure and porosity of the textile substrate and can be used to estimate the wettability of the substrate. The higher the value of the capillary constant, the high will be the wettability and porosity of the substrate [155]. Capillary constant can also be determined on tensiometer using a nonpolar solvent. Hexane was used in this study to determine the capillary constants of uncoated and coated cotton (Cot_40) which were 1.0384×10^{-8} and 1.6718×10^{-8} respectively. Although the capillary constant values of the uncoated and coated cotton are of same order of magnitude, the capillary constant of the coated cotton was slightly higher than that of uncoated cotton. The applied coating was extremely thin and highly conformal, therefore, it was not expected to induce any changes in the structure and porosity of textile substrates at macro scale. Rather the coating introduced nano scale porosity on the fiber surface which may cause this small increase in the capillary constant leading to higher water pick up by the coated cotton fabric. Nevertheless, both water contact angle and water sorption tests show an increase in hydrophilicity of cotton fabric after coating.
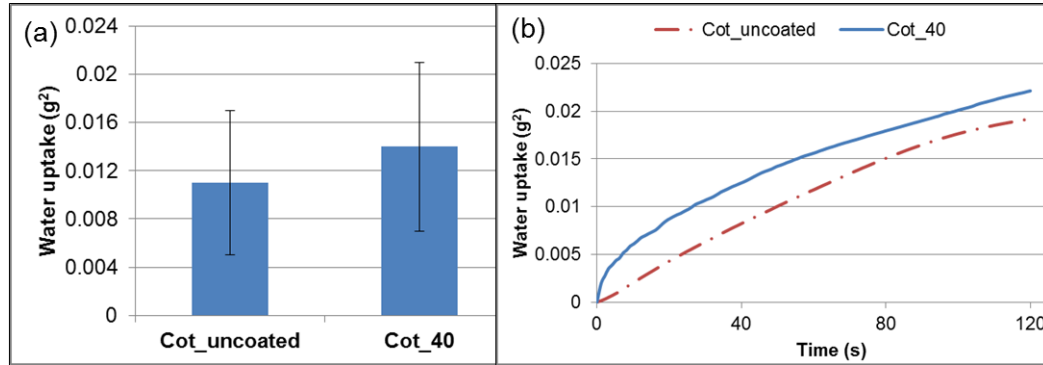
Figure 22: Water sorption test on tensiometer: (a) total water uptake by uncoated (Cot_uncoated) and coated (Cot_40) cotton fabric during water sorption test, (b) kinetics of water sorption over 120 s.

Moisture management properties (three dimensional moisture transport in the fabric) of the cotton fabric before and after coating were evaluated through moisture management tester (MMT) and results are shown in Figure 23. When water comes in contact with a fabric surface, it gets transferred in three dimensions of the fabric. This includes water transfer on top and bottom surface and through the thickness of the fabric. These properties are known as dynamic moisture management properties and are listed on right hand side of Figure 23.
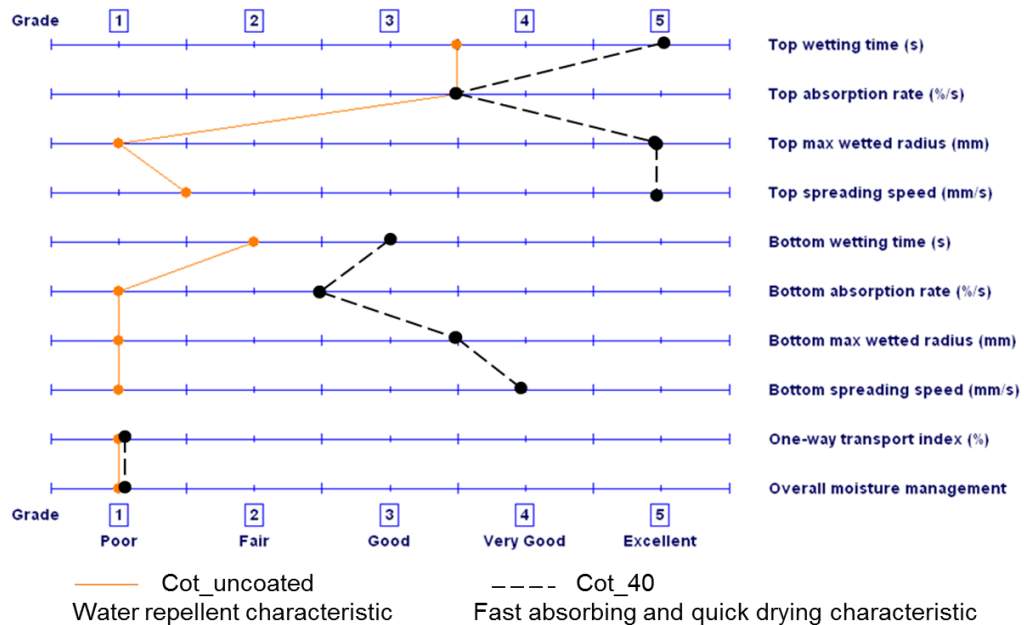
Figure 23: Moisture management properties of the cotton fabric before (Cot_uncoated) and after coating (Cot_40) as determined through moisture management tester

The software of the instrument evaluates the properties listed in Figure 23 on a scale of 1 (poor) to 5 (excellent). Based on the evaluation of these properties,

MMT can distinguish seven main categories of fabrics. These fabric categories are listed in Table 4.

Table 4: Different fabric evaluation categories by moisture management tester as described in the manual of the moisture management tester (MMT)

1. Water proof fabric if
    - Absorption is very slow
    - Spreading is slow
    - No penetration and no one way transport
2. Water repellent fabric if
    - No wetting
    - No absorption
    - No spreading
    - Poor one way transport
3. Slow absorbing and slow drying fabric if
    - Slow absorption
    - Slow spreading
    - Poor one way transport
4. Fast absorbing and slow drying fabric if
    - Medium to fast wetting
    - Medium to fast absorption
    - Small spreading area
    - Slow spreading
    - Poor one way transport
5. Fast absorbing and quick drying fabric if
    - Medium to fast wetting
    - Medium to fast absorption
    - Large spreading area
    - Fast spreading
    - Poor one-way transport
6. Water penetration fabric if
    - Small spreading area
    - Excellent one-way transport
7. Moisture management fabric if
    - Medium to fast wetting
    - Medium to fats absorption
    - Large spreading area at bottom surface
    - Fats spreading at bottom surface
    - Good to excellent one way transport

Figure 23 shows that wetting time, absorption rate, maximum wetting radius and wetting speed of the cotton fabric increased after coating. These properties show that uncoated cotton had water repellent characteristic whereas after coating, fast absorbing and quick drying characteristics were rendered to the fabric. It should be noted that cotton fabrics naturally have hydrophilic character. Water repellent nature of the uncoated cotton fabric in this study is possibly due to dense weaving pattern that may create a microstructure on the fabric surface to help repel water. Since surface per unit area of fabrics play an important role in creating water repellent applications [155], dense weaving may result in increased surface area due to surface patterning. Nonetheless, increase in maximum wetted radius of the coated cotton fabric after moisture management test is shown in Figure 24. Summarizing the results of water contact angle, water sorption and

moisture management tests, it can be concluded that silver nanoclusters/silica composite coating increased water wettability and imparted fast absorbing and quick drying properties to the cotton fabric.
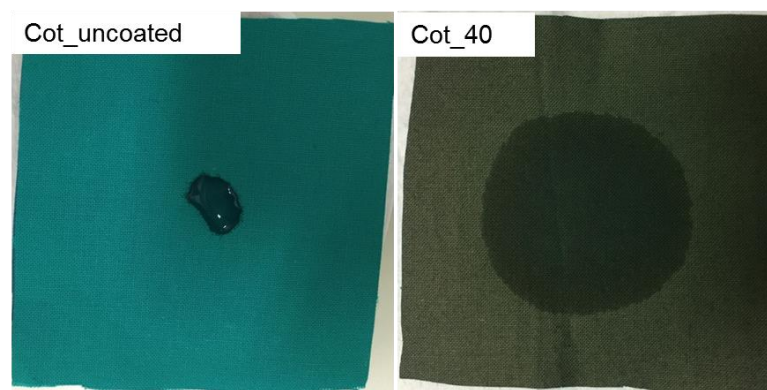
Figure 24: Maximum wetted radius on cotton fabric surface after moisture management test

Air permeability of the cotton fabric was evaluated using Branca Idealair™. Air permeability, in terms of air velocity through the fabric thickness, of uncoated and coated cotton fabric (Cot_40) was 69.32 ± 4.50 mm/s and 70.73 ± 4.60 mm/s respectively. This shows that coating deposition did not altered the air permeability of the cotton fabric. Air permeability of the fabric can be blocked if the applied coating is thick enough to cover completely the interstices among the fibers in the fabric. However, this study shows that highly conformal coatings can be deposited via sputtering on fabrics preserving their breathability.

4.1.6 Washing stability of coating

The washing stability of the composite coating was assessed after 1, 5 and 10 washing cycles. The washing was carried on samples deposited for 40 minutes (Cot_40) and was done with two soap solutions: one was commercial Castile soap and the other one was AATCC Standard Reference detergent without optical brightener (WOB). EDS spectra as well as photographs of samples washed with Castile soap are shown in Figure 25. EDS spectra of washed samples show that the coating dissolved with increasing number of washing cycles. After one washing (Cot_40_1wash), EDS spectrum appears comparable to that of unwashed sample (Cot_40_0wash). After 5 washing cycles (CO_40_5washes) the intensity of both Ag and Si peaks decreased significantly. Within 10 washing cycles (Cot_40_10washes), complete coating removal can be observed as no peak related to Si and Ag was detected in EDS spectrum. Coating dissolution is also evident from the sample photographs showing fading of the color that was imparted due to coating.
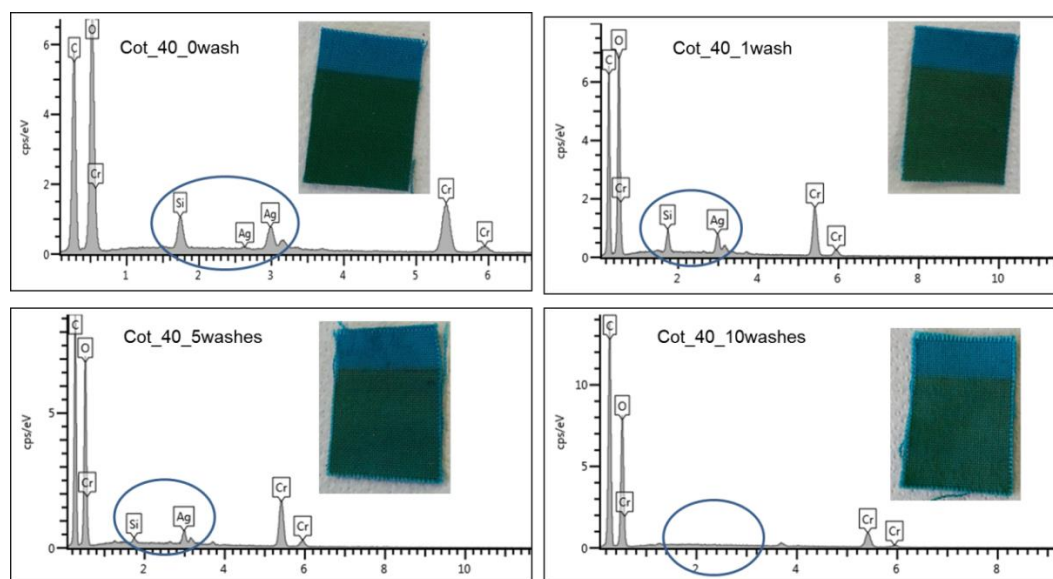
Figure 25: EDS spectra of Cot_40 after 1, 5 and 10 washing cycles with commercial Castile soap
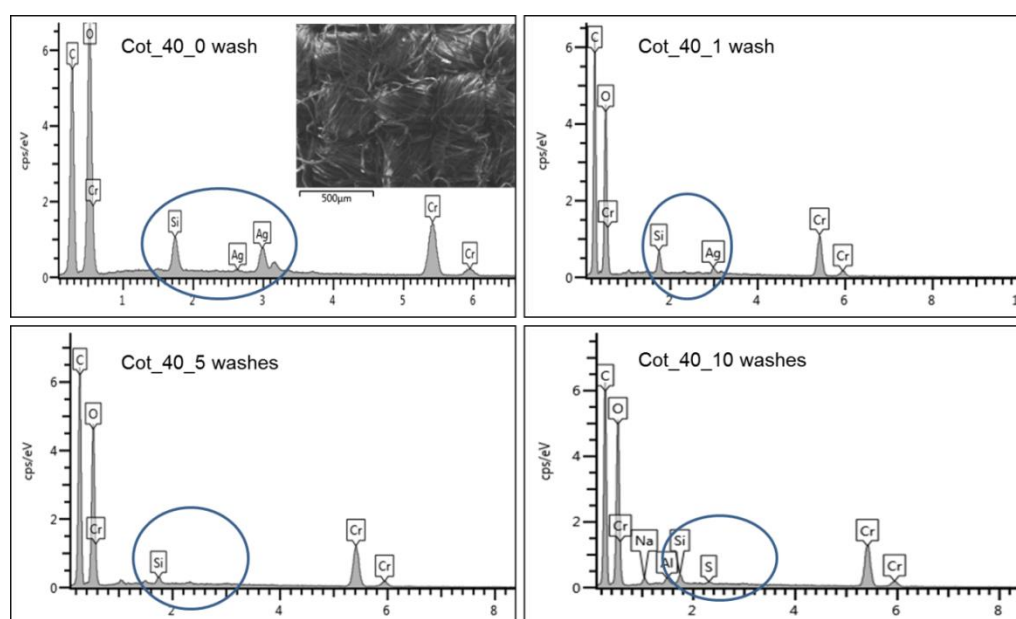
Figure 26: EDS spectrum of Cot_40 after 1, 5 and 10 washing cycles with AATCC standard detergent

EDS spectrum of the samples washed with AATCC detergent are shown in Figure 26. The figure shows that, contrary to Castile soap, AATCC detergent caused more dissolution of the silver as no Ag peak was detected after 5 washing cycles whereas Si peak was still present after 10 washing cycles. These results indicate that the two soaps had different impact on silver dissolution from the

coating and that the coating was not able to withstand significant number of washing cycles.

4.2 Kevlar[®]

4.2.1 Coating morphology and composition (FESEM, EDS, XPS)

Figure 27 shows the FESEM micrographs of the uncoated (Kev_uncoated) and silver nanoclusters/silica coated (Kev_15, Kev_40 and Kev_80) Kevlar[®] fabric. High magnification FESEM image reveals the smooth surface of the uncoated Kevlar[®] fibers [23]. The coating is extremely thin after 15 minute deposition (Kev_15) and its presence is not prominently evident on the surface. However, the presence of silver nanoclusters as bright dots on the fiber surface and corresponding EDS spectrum in Figure 28 indicates its existence. The texture of the surface changed after 40 minute deposition (Kev_40) resulting in relatively rougher surface but surface features of the uncoated fibers are still visible. Typical granular morphology of the coating deposited by sputtering is obtained after 80 minutes sputter deposition (Kev_80).

EDS spectra of the uncoated and coated Kevlar[®] fabric are given in Figure 28. The spectrum of the uncoated Kevlar[®] has peaks of carbon (C), nitrogen (N), oxygen (O), sodium (Na) and sulphur (S). C, N and O are present in the molecular structure of the fiber whereas Na and S may be left over impurities from fiber spinning process and has also been reported in literature [24]. Kevlar[®] is produced by solution spinning in sulphuric acid, sulphide can be a residue of this, whereas, after coagulation, the fiber is neutralized in sodium hydroxide which could be possibly the reason for the presence of sodium. Silver (Ag) and silicon (Si) peaks appear in the spectra of the Kevlar[®] fabric after coating which grow in intensity with the deposition time. From the EDS elemental composition with respect to atomic %, the ratio Ag/Si was calculated and reported on the corresponding spectrum in Figure 28. Approximately same ratio indicates uniformity in relative concentration of silver and silica in the composite coating for the three depositions.

Similar to cotton fabric substrate, the color of the uncoated Kevlar[®] fabric changed after coating as shown in Figure 29. The yellow color of uncoated Kevlar[®] fabric changed from light to dark brown depending upon the deposition time (and silver concentration) due to well know phenomenon of localized Surface Plasmon Resonance (L-SPR) of silver nanoclusters.
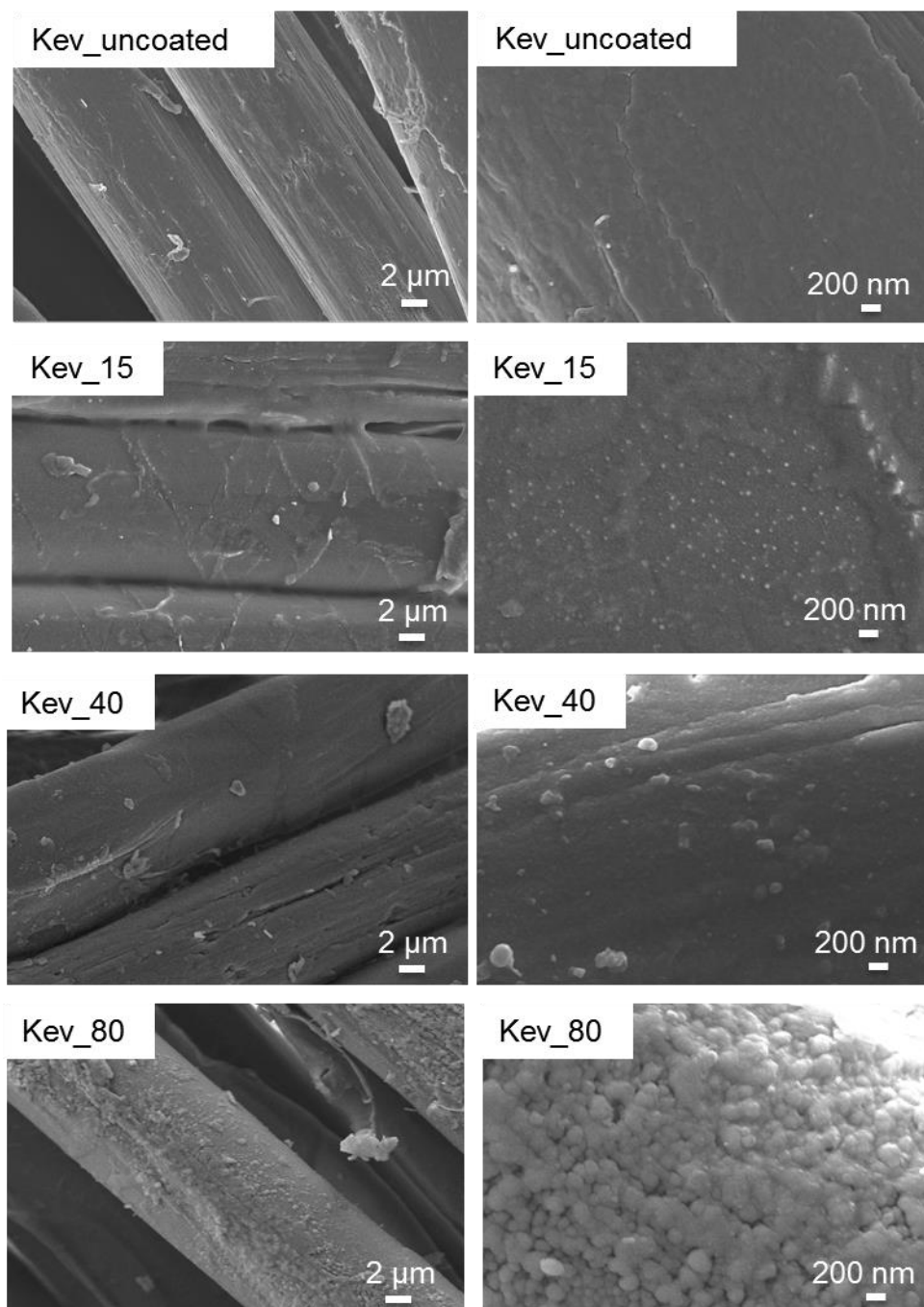
Figure 27: FESEM surface morphology of uncoated (Kev_uncoated) and coated (Kev_15, Kev_40 and Kev_80) Kevlar® fabric at low and high magnification
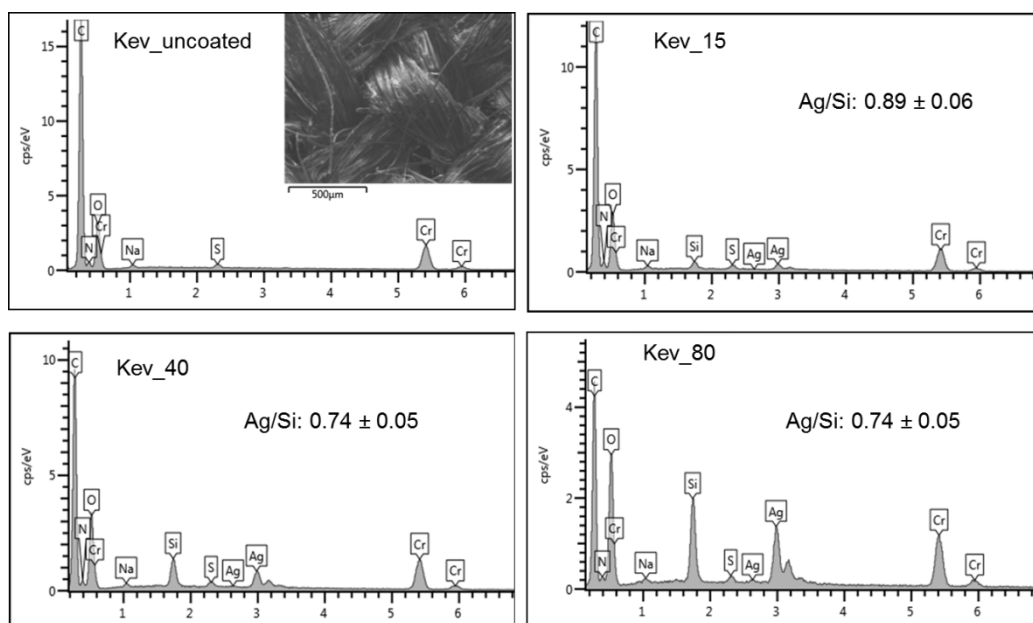
Figure 28: EDS spectra of the uncoated (Kev_uncoated) and coated (Kev_15, Kev_40 and Kev_80) Kevlar® fabric and corresponding Ag/Si (at. %) ratio
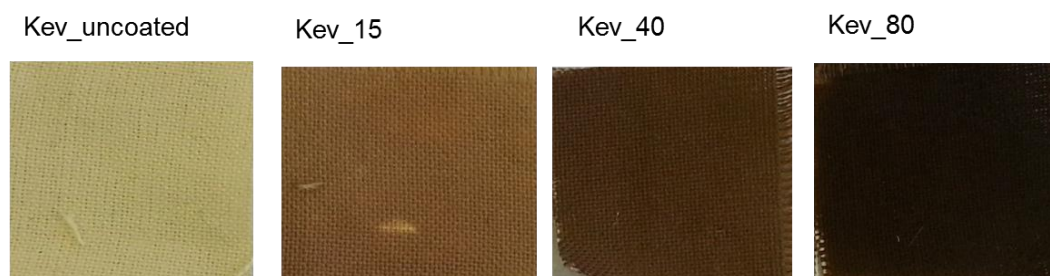
Figure 29: Images of the Kevlar® fabric showing change in color with deposition time

XPS is highly surface sensitive analytical technique and is limited to the few nano meters on the surface, therefore, provides detailed analysis of the elements, present on the surface, and their bonding states. Survey spectra of the uncoated (Kev_uncoated) and coated Kevlar® fabric (Kev_40 and Kev_80) is shown in Figure 30. Since carbon, oxygen and nitrogen are the main constituents of the molecular structure of the Kevlar® as shown in molecular structure of Kevlar in Figure 2, the survey spectrum of the uncoated Kevlar® fabric (Kev_uncoated) has distinct peaks of C-1s, O-1s and N-1s. The presence of other elements like Na, S and P in the spectrum of Kev_uncoated can be regarded as impurities as discussed earlier. Na and S were also present in the EDS spectrum due to their presence in relatively higher concentration. The spectra of the Kevlar® samples deposited with silver nanoclusters/silica composite coating (Kev_40 and Kev_80) contain peaks

related to Si and Ag along with carbon and oxygen, however, low intensity peaks of other elements including nitrogen are absent from these spectra. This is due to surface sensitivity of the XPS which is limited to the top most few nano meters of the fiber surface.
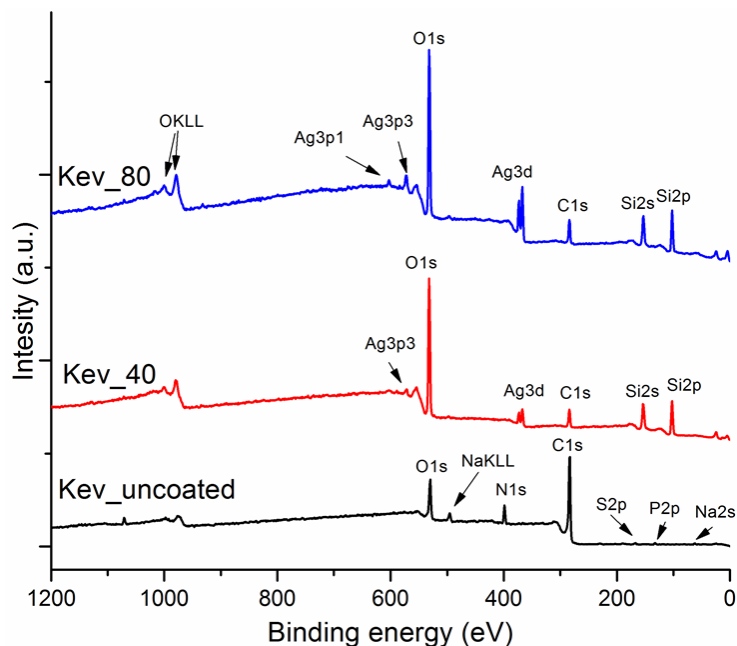
Figure 30: XPS survey spectra of uncoated (Kev_uncoated) and coated (Kev_40 and Kev_80) Kevlar® fabric

The oxidation states of the elements present on the surface of uncoated and coated Kevlar® fibers were analyzed by obtaining high resolution scans in the C-1s, O-1s, Si-2p and Ag-3d core regions and spectra are shown in Figure 31. The binding energies of these peaks and their corresponding bonds have been summarized in Table 5 and discussed as follows. C-1s peak of the uncoated Kevlar® can be deconvoluted into three sub peaks to identify three types of carbon bonds in the structure. The peak at binding energy (BE) 284.6 eV is representative of C-C bonds present in the structure of the benzene ring [23] [156]. The peak at BE 285.5 eV is from C-N bond whereas the peak at 287.8 eV can be attributed to the carbon atoms in the amide group (CONH) and C=O [157] [158]. The carbon peaks detected on coated Kevlar® (Kev_40 and Kev_80) are due to adventitious carbon [150] adsorbed on the surface or a contribution from the substrate. Oxygen peak O-1s from the spectrum of uncoated Kevlar® (Kev_uncoated) can also be deconvoluted into 2 peaks. The peak at BE 531.3 eV is attributed to CONH and the peak at 532.4 eV can be attributed to C=O bonding [159].

After silver nano clusters/silica coating, the O-1s peaks of Kev_40 and Kev_80 at binding energies of 532.7 eV and 532.9 eV respectively represent

oxygen of the silica [152]. Similarly, Si-2p peaks at 103.2 (103.5) eV is assigned to the Si of the silica [152] [153]. Ag-3d doublet known as Ag-3d$_{3/2}$ and Ag-3d$_{5/2}$ at binding energies 368(368.2) and 374 (374.2) are attributed to the silver in zero oxidation state and represent silver in metallic state.

The quantities of the elements, w.r.t atomic % obtained from XPS survey spectra, on the surface of the uncoated and coated Kevlar® are given in Table 6. The O/Si ratio on coated Kevlar® surface is slightly higher than 2 (the stoichiometric ratio between O and Si) which indicates that the oxygen present of the surface of coated Kevlar® was mainly due to silica. It can be inferred from the XPS results that the composite coating consists of silver nano clusters embedded in the silica matrix of the composite coating.
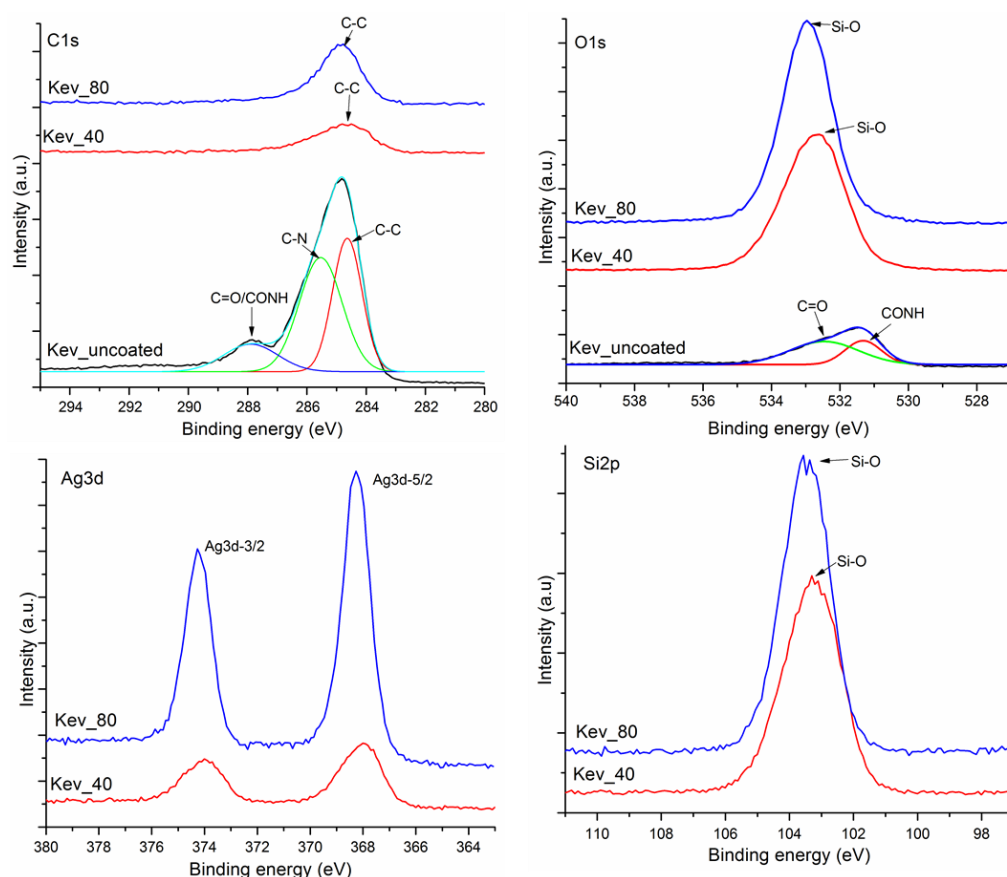
Figure 31: XPS high resolution spectra of C1s, O1s, Ag3d and Si2p peaks of uncoated (Kev_uncoated) and coated (Kev_40 and Kev_80) Kevlar® fabric

Table 5: Table summarizing different peaks, their binding energies and corresponding bonds in XPS spectrum of uncoated (Kev_uncoated) and coated (Kev_40 and Kev_80) Kevlar® fabric

Peak	Bonding	Binding energy BE (eV)		
		Kev_uncoated	Kev_40	Kev_80
C-1s	C-C	284.6	284.6	284.8
	C-N	285.5	-	-
	CONH/C=O	287.8	-	-
O-1s	CONH	531.3	-	-
	C=O	532.4	-	-
	Si-O	-	532.7	532.9
Si-2p	Si-O	-	103.2	103.5
Ag-3d$_{3/2}$	Ag^0	-	374.0	374.2
Ag-3d$_{5/2}$	Ag^0	-	368	368.2

Table 6: Composition (w.r.t atomic %) of the uncoated (Kev_uncoated) and coated (Kev_40 and Kev_80) Kevlar® surface derived from XPS survey spectra

	Atomic %								
	C	O	N	Si	Ag-3d	O/Si	Na	P	S
Kev_uncoated	74.9	13.9	8.6	-	-	-	1.4	0.7	0.5
Kev_40	17.2	55.8	-	25.9	1.1	2.15	-	-	-
Kev_80	18.7	55.5	-	22.9	2.2	2.42	-	-	-

4.2.2 Total silver content and silver ion release in Water

The amount of silver in silver nanoclusters/silica composite coating deposited on Kevlar® fabric was determined through ICP-MS. Samples deposited for 40 (Kev_40) and 80 (Kev_80) minutes were tested and the amount of silver was found to be 255 and 632 ppm (mg of silver/kg of fabric) respectively. Figure 32 shows the silver ion release profile from the coated Kevlar® fabric (Kev_15, Kev_40 and Kev_80) over a period of 3, 24 and 72 hours. Silver ions released from Kev_40 after 3, 24 and 72 hours of immersion in water was 2.4 %, 2.4 % and 6.8 % respectively of total silver on Kev_40 (255 ppm) whereas the same values from Kev_80 were 2.0 %, 1.9 % and 2.8 % with total silver content of 632 ppm on Kev_80. Silver ions were released in the range 0 - 0.45 µg/cm^2 from all the samples. In case of Kevlar® fabric, the ionic silver release is comparatively much less than that of released from cotton fabric (0 - 6.37 µg/cm^2) with similar coating thickness where silver ions of up to 74 % of total deposited silver were released.
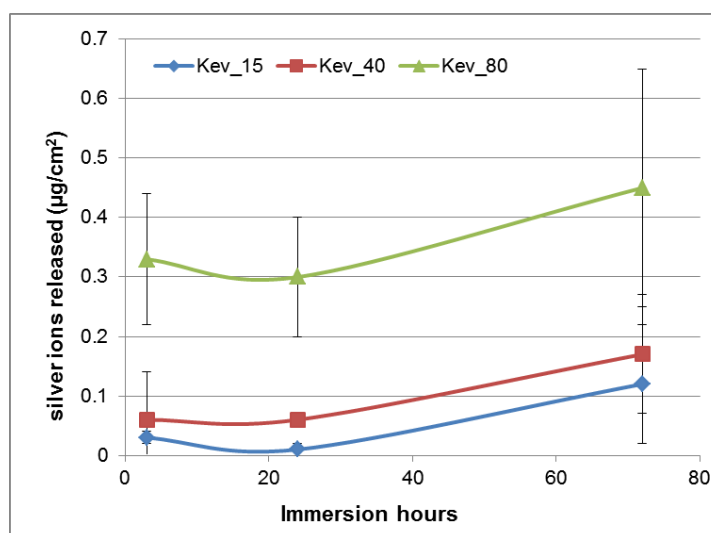
Figure 32: The amount of silver ions leached from coated Kevlar® fabric in water during silver release test

Theoretically, the same profile of silver ion release is expected from coated Kevlar® fabric as was obtained in case of cotton fabric. In fact, the EDS analysis of Kev_40 samples after silver release test shows the reduction trend in silver atomic % similar to what was observed for cotton fabric. The relative atomic % of Si and Ag, obtained from EDS elemental analysis, on Kev_40 as deposited and after 3, 24 and 72 hour silver release test is shown in Figure 33. Compared with as

deposited sample (0 hr), the reduction in silver atomic % after release test of 3, 24 and 72 hour was estimated to be 0, 38 and 76 % respectively which is similar to that of from cotton (Cot_40). This means that the amount of silver released from the coated Kevlar[®] was equivalent to what was released from coated cotton. However, in case of Kevlar[®], contrary to the cotton where all the silver was released and detected in ionic form, very little amount of silver ions were present in water and hence detected by silver photo meter which detects silver ions only. This could be due to some impurity released from Kevlar[®] during release test that reacts with silver ions and precipitates decreasing the amount of silver ions to be detected by silver photo meter. Possibly, this impurity could be sulphur ions (S) as S was detected in the EDS spectrum of uncoated Kevlar[®] fabric as shown in Figure 28. Silver ions show high reactivity towards sulphur ions to form silver sulfide which has very low solubility in water and precipitates quickly. The antibacterial action of silver is also attributed to the binding of silver ions with sulphur of the sulphur containing proteins in bacterial cells leading to their inactivation [74]. The reaction of silver ions with sulphur released from the Kevlar[®] itself to form precipitates of silver sulfide may also decrease bioavailability of the silver for antimicrobial action [160]. The presence of sulphur was also confirmed from ICP-MS which was calibrated to detect a maximum 2 ppm (mg/l) of S in the solution. The amount of S present in the solution was higher than this value (and therefore not reported) which complements the hypothesis that silver ions may form silver sulfide that gets precipitated. This reduced the amount of ionic silver for antimicrobial action as will be evident from inhibition halo test, and will be discussed in the following section, where coated Kevlar[®] samples formed comparatively smaller inhibition halo than that was obtained in case of coated cotton.
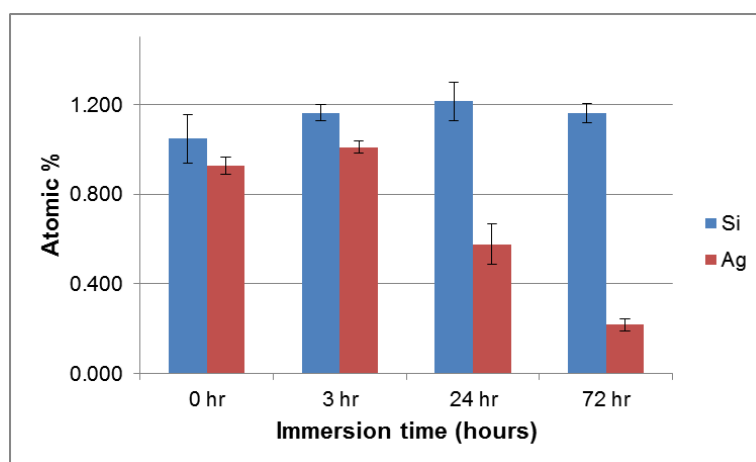
Figure 33: Relative atomic % of Si and Ag on Kev_40 after silver release test of 3, 24 and 72 hours in water

4.2.3 Silver release in artificial sweat

The release of silver in artificial sweat was also analyzed from Kev_40 over a period of 3, 24 and 72 hours of immersion of kev_40 samples in artificial sweat formulation. The comparison of the silver release profiles in water and in artificial sweat is shown in Figure 34. The quantity of silver released in artificial sweat ranged between 2.1–4.9 $\mu g/cm^2$ which is considerably higher than what was detected in water. As has already been discussed, this difference could be due to the presence of sulphur as residual impurity from fiber spinning process which may lead to precipitation of silver sulfide. This leads to no detection of silver ions in water although they were released from the sample.

However, situation could be different in artificial sweat formulation containing significant concentration of chloride ions. It has been reported that in the presence of high concentration of chloride ions, the formation of $AgCl_{(s)}$ or soluble chloride complexes are favored thermodynamically rather than Ag_2S [160]. Possibly due to this reason the silver dissolved in artificial sweat was not influenced by the precipitation of Ag_2S and was detected in the solution. The values of silver released in artificial sweat from Kev_40 are comparable to those that were obtained for cotton with an equivalent coating (Cot_40). In any case, despite no detection of ionic silver in water, a gradual time dependent release of silver in artificial sweat is evident from the graph. Analyzing abrupt or gradual release of silver was the basic objective of the silver release test in both the fluids.
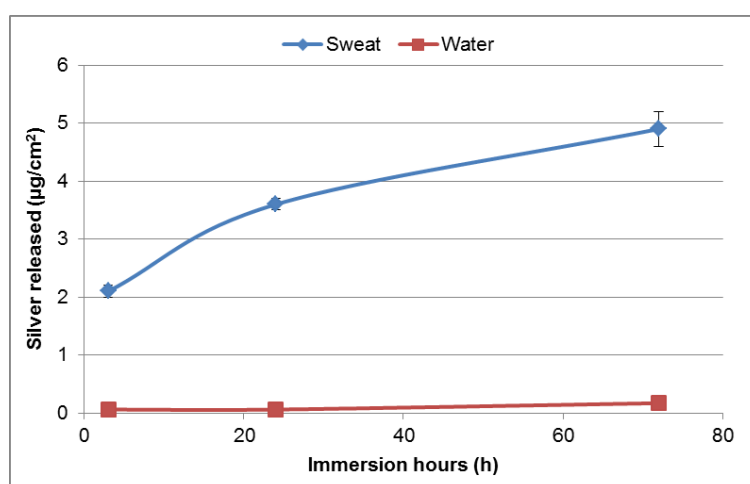
Figure 34: Comparison of silver released from Kev_40 in water and in artificial sweat

4.2.4 Antimicrobial test

Antimicrobial performance of Kevlar® fabric deposited with silver nanoclusters/silica composite coating was evaluated through inhibition halo test. The results of the inhibition halo test performed against three microbial strains

namely *S. aureus* (Gram positive bacterium), *E. coli* (Gram negative bacterium) and *C. albicans* (fungas) are shown in Figure 35. All the deposited samples (Kev_15, Kev_40 and Kev_80) were evaluated against *S. aureus* whereas only Kev_40 was tested against *E. coli* and *C. albicans*. Figure 35 shows both front and back side of the agar surface to have complete over view of the inhibitory effect of the coating on bacterial growth on the agar surface. About 1 mm non uniform inhibition zone can be seen around Kev_40 and Kev_80 samples against *S. aureus* with the exception of some edges that were not adherent to the agar surface and thus allowed bacterial growth underneath those edges. Whereas relatively less significant effect was observed for Kev_15 having thinnest coating and lower concentration of silver. The formation of inhibition halo is not prominent around Kev_40 samples against *E. coli* and *C. albicans* but inhibitory effect can be seen around the samples. However, in both the cases the back side images of the agar surface show that the surface of the coated samples appear completely antimicrobial as it did not allow growth of any colonies of *E. coli* or *C. albicans* underneath the sample surface. On the contrary, bacteria grew under the surface of the uncoated samples.
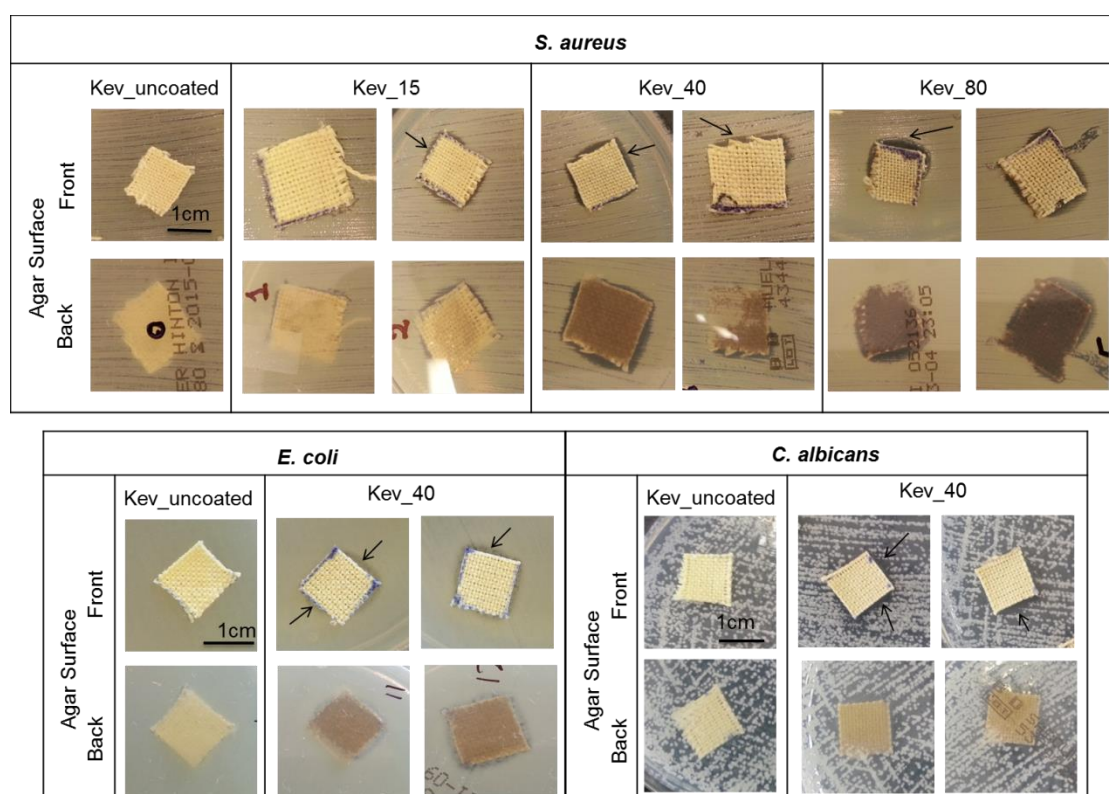
Figure 35: Inhibition halo test for uncoated and coated Kevlar® fabric against *S. aureus*, *E. coli* and *C. Albicans*

Antimicrobial activity of the silver nano clusters/silica composite coating on Kevlar® fabric is not as intense as was obtained for cotton fabric reported in the

previous section. The difference in the intensity of antimicrobial action of the coating on the two substrates can be linked to their silver ion release profiles. Silver ions are considered to be responsible for antimicrobial action (as will be discussed in detail in "Discussion" section). The negligible amount of silver ions released from coated Kevlar® fabric compared with that released from coated cotton fabric is responsible for this difference. Because of the presence of sulphur (S) in the Kevlar® fibers, it is hypothesized that in wet environment both sulphur and silver are released/activated from the Kevlar® fabric. Sulphur has high reactivity with silver and therefore, consumes majority of the silver ions released from the coating to form silver sulfide. The reactivity of the silver with sulphur of the sulphur containing proteins in the bacterial cells is also considered to be important mechanism of antibacterial action of silver nano particles [112]. Therefore, the consumption of silver ions by sulphur before being leached in the surrounding environment on the agar surface reduces the bioavailability of the silver and affects antimicrobial performance of the coated Kevlar® fabric. It is reported that after being sulfidized (Ag_2S formation), the bio availability and toxicity of silver nanoparticles is reduced [161]. Most of the silver nano particles released into the environment from silver nano particle containing products are converted into silver sulfides in the soil. This is also considered to reduce the environmental risk that could be associated with the release of nano metric silver particles from silver containing textiles or products [161].

Inhibition halo test against *S. aureus* was also performed on Kev_40 and Kev_80 samples used for silver release test of 24 and 72 hours and results are shown in Figure 36. The results show that the size of inhibition halo around the samples after silver release test was comparatively much higher than that of around as deposited samples in Figure 35. This variation can also be linked to the silver ion release mechanism. The silver ion release profiles in Figure 32 show that the amount of silver ions was negligible during first 24 hours of sample immersion in water. Whereas an increase in the amount of silver ions is evident from 24 to 72 hours. This means that after initial consumption of silver ions by sulphur that was readily available within 24 hours because of being near to the surface, relatively less sulphur was released from the bulk of the Kevlar® fibers later and thus making relatively higher amount of silver ions available for antibacterial action. Consequently, the size of the inhibition halo is comparable to the one obtained for cotton samples after silver release test in Figure 20. This again supports the assumption that it is the presence of sulphur in the Kevlar® fibers that affects the performance of the antimicrobial coating on Kevlar® fabric.

S. aureus

Kev_40_24h   Kev_40_72h   Kev_80_72h
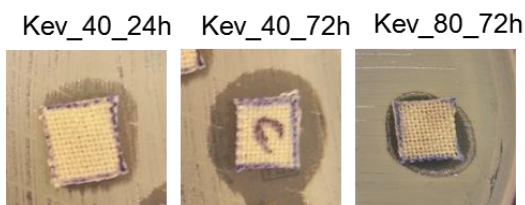
Figure 36: Inhibition halo test for Kev_40 after silver release test of 24 and 72 hours

Since antimicrobial performance of the silver nano clusters/silica composite coating on Kevlar® fabric was not as pronounced in inhibition halo test as was in case of cotton fabric, therefore, it was further investigated quantitatively through colonies forming unit (CFU) method using broth dilution test. Broth dilution test was performed on Kev_40 and can be used to evaluate the antimicrobial performance in terms of microbial adhesion on the sample surface as well as microbial proliferation in the broth. After incubation of the uncoated and coated samples in the broth tubes containing physiological solution as described in detail in "Experimental" chapter, the McFarland index of the broth suspensions was measured. McFarland index is a measure of the turbidity of the liquid media, the solution containing more bacterial suspensions will have greater turbidity index. Therefore, the difference in the McFarland index of the broth solutions containing uncoated and coated samples can be regarded as semi quantitative measure of the antimicrobial activity of the coated samples in terms of bacterial proliferation in the solution. The McFarland index of the broth solution containing uncoated Kevlar® samples (Kev_uncoated) was measured to be 1.80 ± 0.05 whereas that of coated Kevlar® samples (Kev_40) was 1.42 ± 0.47. This suggests a small decrease in the bacterial proliferation in the broths containing coated Kevlar® samples. However, this decrease is not significant as can be seen from the results of broth proliferation test in Figure 37.

Figure 37 shows that the number of colonies forming units (CFU) of bacteria, grown on the surface of the blood agar plates when spread with an aliquot from the broth solution incubated with coated Kevlar® (Kev_40) samples, is almost equivalent to the CFU grown when broth solution of uncoated Kevlar® (Kev_uncoated) was used. This indicates that the composite coating had less significant effect on proliferation of bacteria in the broth. Since bacterial proliferation can be supressed by release of silver ions, therefore, low silver ion release profiles may be responsible for poor proliferation control of bacteria in the broths.
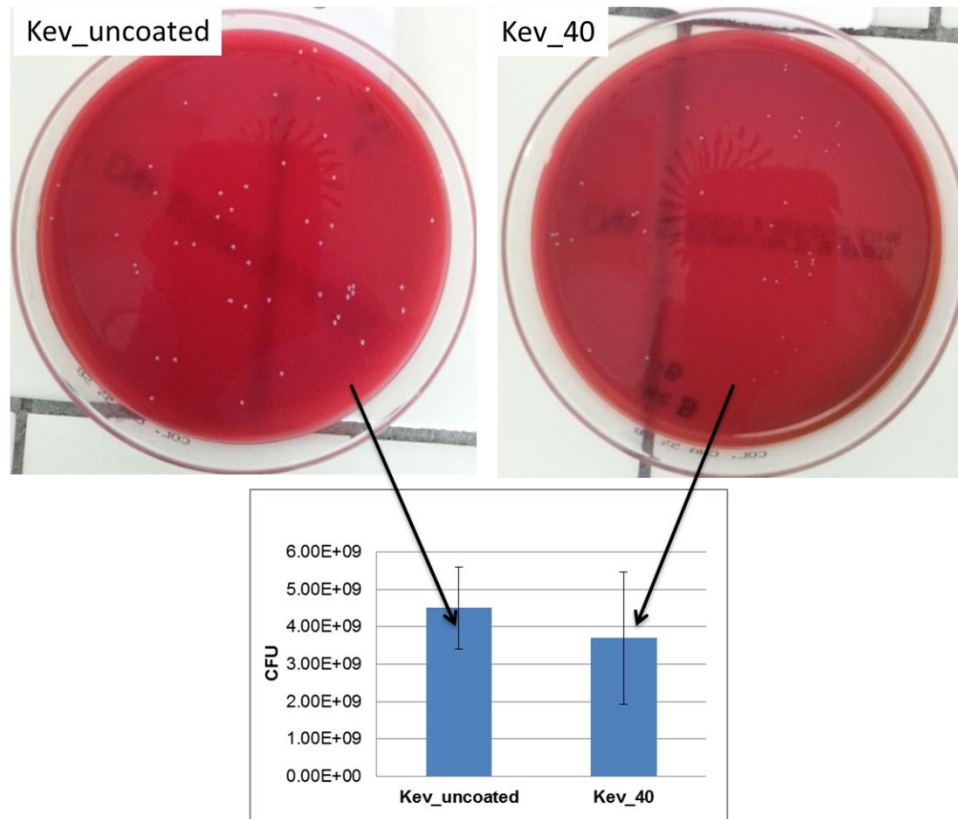
Figure 37: Broth dilution test showing bacterial proliferation in the broths containing uncoated (Kev_uncoated) and coated (kev_40) Kevlar® samples

Although no significant effect was observed on bacterial proliferation, the results of bacterial adhesion in Figure 38 show that the number of CFU on the surface of the coated samples (Kev_40) was one order of magnitude less than that of on uncoated samples (Kev_uncoated). This indicates that less number of bacteria adhered to the surface of coated Kevlar® samples due to antibacterial effect of the composite coating. This is in agreement with the results of inhibition halo test where surface of the samples remained antibacterial even in the absence of significant inhibition halo. Again in the broth dilution test, the role of sulphur to capture silver ions on the fiber surface and hence to interfere with antimicrobial activity appears to be dominating as discussed in inhibition halo test.
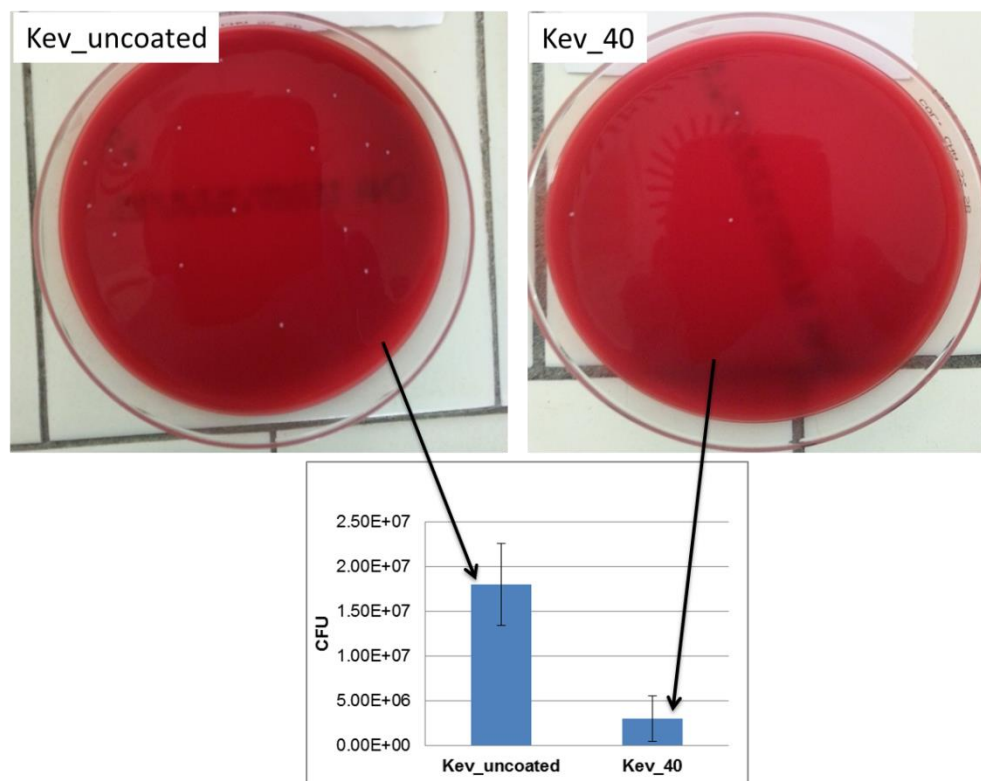
Figure 38: Broth dilution test showing bacterial adhesion on the surface of the uncoated (Kev_uncoated) and coated (kev_40) Kevlar® samples

4.2.5 Water sorption test

The effect of the coating on water wettability of the Kevlar® fabric was determined through water sorption test on tensiometer. Kevlar® fabric used in this study was not adequate for water contact angle test because of loose weave structure of the fabric that caused immediate absorption of the water droplet introduced on the fabric surface. Therefore, water wettability was analyzed only through water sorption test and results are shown in Figure 39. Figure 39 (a) shows total water uptake and Figure 39 (b) shows kinetics of water uptake during water sorption test. The results show that water uptake by the Kevlar® fabric increased a little bit after coating indicating an increase in water wettability of the fabric surface after coating. Kevlar® fibers have low moisture uptake and can be regarded hydrophobic, therefore, this property could be useful for the applications requiring strength of a high performance fiber like Kevlar® along with certain degree of hydrophilicity.
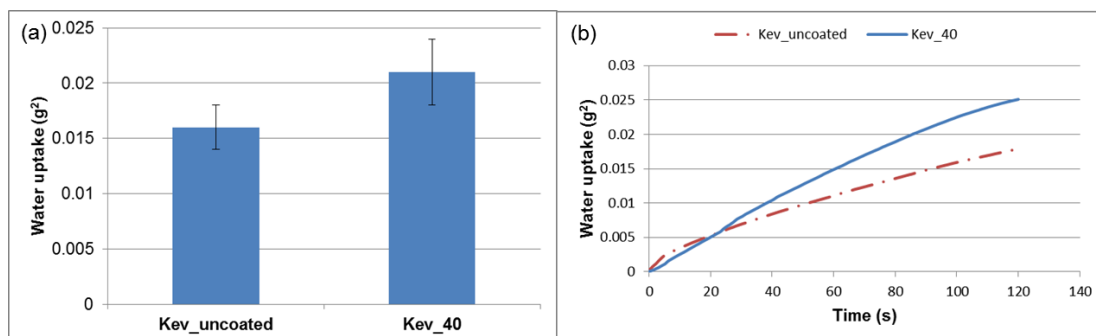
Figure 39: Water sorption test on tensiometer: (a) total water uptake by uncoated (Kev_uncoated) and coated (Kev_40) Kevlar® fabric during water sorption test, (b) kinetics of water sorption over 120 s.

4.2.6 Washing stability of coating

The resistance of silver nanoclusters/silica composite coating to washing was evaluated by subjecting Kev_40 samples to multiple washing cycles. The washing was carried with two different soap solutions: one was commercial Castile soap and the other one was AATCC standard detergent without optical brightener (WOB). After washing, the samples were analyzed through FESEM and EDS.

EDS spectra of Kev_40 samples after 0, 1, 5 and 10 washing cycles with Castile soap is shown in Figure 40. The EDS spectra show that the coating was almost intact after first washing cycle whereas it dissolved significantly with increasing number of washing cycles. After 10 washing cycles, no Si peak was detected whereas Ag peak was present. However, some patches of the coating containing both silica and silver were noticed on some areas of the fiber surface as shown in FESEM surface image in Figure 41.

FESEM analysis after 10 washing cycles (Kev_40_10washes) in Figure 41 showed that the coating was removed from fiber surface (Figure 41 a). However, some patches of the coating were found on some areas of the fiber surface that consisted of mostly silver detectable in the form of bright particles (Figure 41 b).
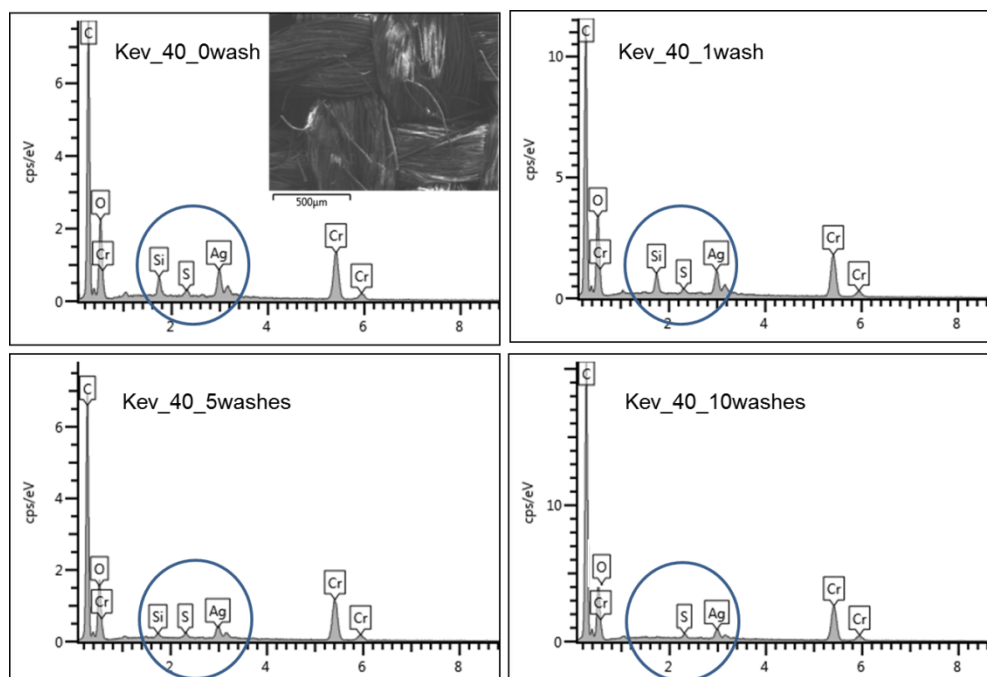
Figure 40: EDS spectra of Kev_40 after 1, 5 and 10 washing cycles with commercial Castile soap
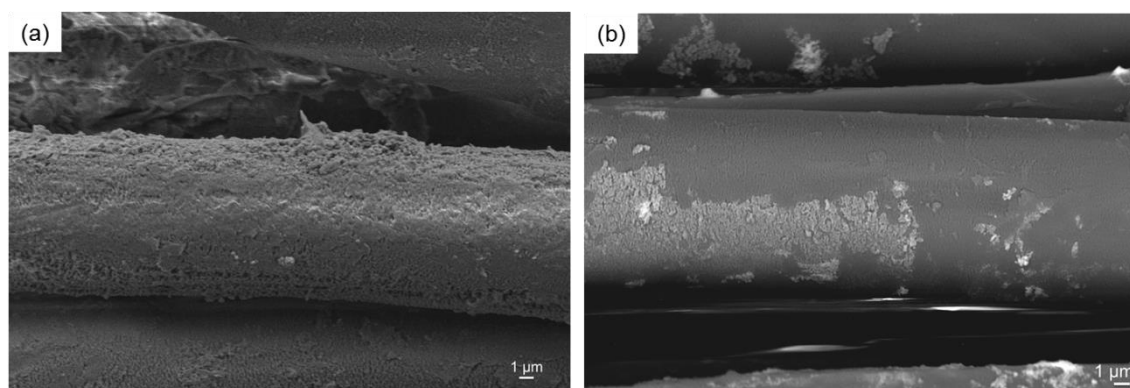
Figure 41: FESEM micrographs of Kev_40 subjected to 10 washing cycles: (a) complete removal of the coating, (b) patches of the coating present on some areas of the fibers with silver as bright particles

EDS spectra of Kev_40 washed with AATCC standard detergent is shown in Figure 42. Similar to the results reported previously for cotton substrate, the EDS spectra indicate that AATCC detergent caused more dissolution of Ag as Ag peak is hardly detectable after 10 washing cycles (Kev_40_10washes) in Figure 42. Similar results have been reported in the previous section for cotton fabric. In both the cases, significant dissolution of the coating occurred within 10 washing cycles suggesting poor resistance of the coating towards repeated washing cycles.
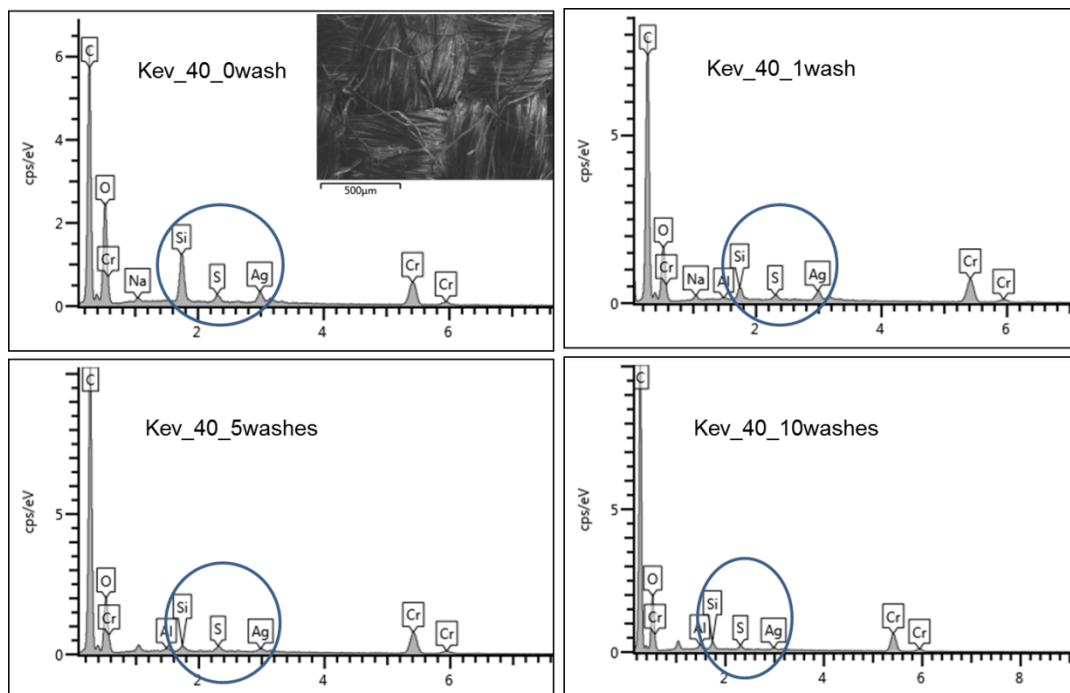
Figure 42: EDS spectra of Kev_40 after 1, 5 and 10 washing cycles with AATCC detergent

4.3 Vectran®

4.3.1 Coating morphology and composition (FESEM, EDS, XPS)

Morphology of the uncoated and Vectran® fabric deposited with silver nanoclusters/silica composite coating is shown in Figure 43. The growth of the coating with increased deposition time can be seen on the fiber surface at high magnification. However, contrary to cotton and Kevlar® where a typical granular morphology of sputter coating was observed after 80 min. deposition, a relatively smooth surface can be observed in case of Vectran® (Vec_80). Possibly because of relatively smoother surface, silver nanoclusters are more visible on Vec_80 in Figure 43 contrary to what was observed previously on Cot_80 and Kev_80 in Figure 10 and Figure 27 respectively. The nature of the underlying fiber surface may influence the nucleation and growth of the granular coating morphology and finally coalescence of the grains to give relative rougher or smoother surface.
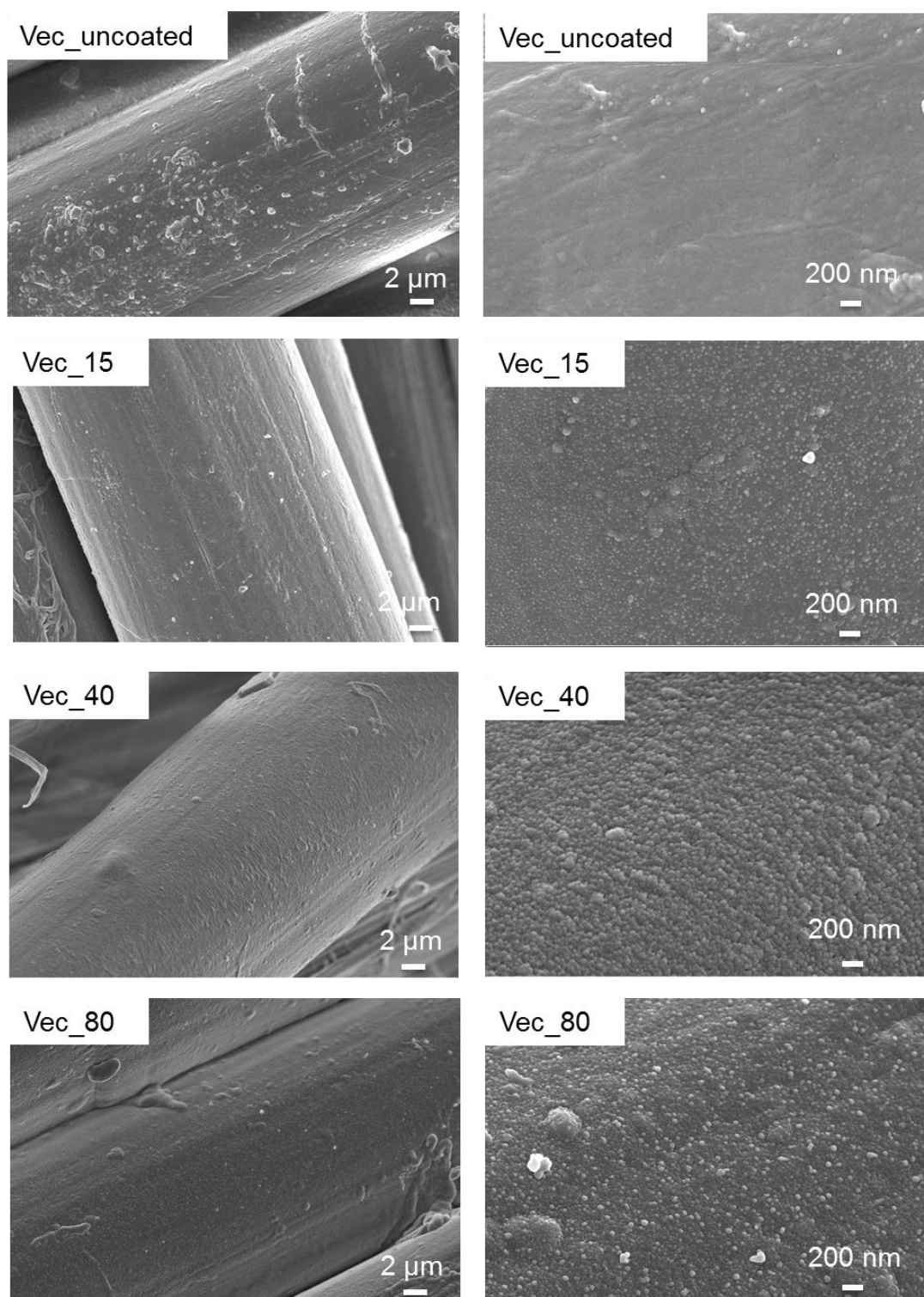
Figure 43: FESEM surface morphology of uncoated (Vec_uncoated) and coated (Vec_15, Vec_40 and Vec_80) Vectran® fabric at low and high magnification

EDS spectrum of uncoated (Vec_uncoated) and coated (Vec_15, Vec_40 and Vec_80) Vectran® fabric is shown in Figure 44. From the elemental composition obtained through EDS, the ratio Ag/Si was calculated and reported in the respective EDS spectrum in Figure 44. The ratio was fairly the same for the three depositions similar to what was obtained for cotton and Kevlar®. The golden color of the uncoated Vectran® fabric changed from light to dark brown depending upon deposition time and hence nano silver concentration in the composite coating.
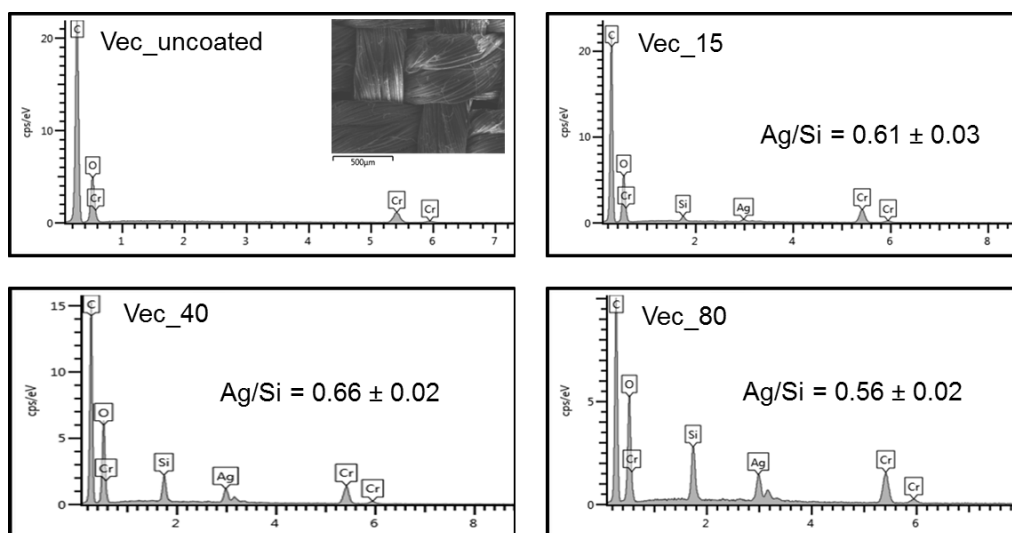
Figure 44: EDS spectra of the uncoated (Vec_uncoated) and coated (Vec_15, Vec_40 and Vec_80) Vectran® fabric and corresponding Ag/Si (at. %) ratio

XPS survey spectra of uncoated (Vec_uncoated) and coated (Vec_40 and Vec_80) Vectran® fabric is shown in Figure 45. Vectran® fibers are composed of carbon and oxygen, therefore, XPS survey spectrum of uncoated Vectran® fiber surface consists of C-1s and O-1s peaks. Silver and silicon peaks are present in the survey spectra of Vectran® fabric deposited with silver nanoclusters/silica composite coating. The analysis about chemical states of elements detected on uncoated and coated Vectran® surface was accomplished by obtaining high resolution spectra of these elements and given in Figure 46. The binding energies (BE) of the C-1s, O-1s, Ag-3d and Si-2p peaks and corresponding bond associations have been identified and listed in Table 7.

Three types of carbon bond associations can be identified by deconvoluting C-1s spectrum of the uncoated Vectran® (Vec_uncoated) fiber surface into three sub peaks. The sub peak at BE 284.4 eV represent C-C bonds, the sub peak at 286.2 eV is attributed to C-O whereas the sub peak at 288.9 eV is due to -COO- functional group [137]. The C-1s peaks on coated samples (Vec_40 and Vec_80) can be due to advantageous carbon adsorbed from the environment or a

contribution from the fabric substrate. The O-1s peak at 532.7 eV and Si-2p peak at 103.4 eV (103.5 eV) on coated Vectran[®] surface (Vec_40 and Vect_80) are representative of silica [152] whereas Ag-3d$3_{3/2}$ and Ag-3d$_{5/2}$ at binding energies of 368.0 eV and 374.1 eV represent metallic silver [162] as has also been discussed in detail in case of cotton and Kevlar[®] fabrics in previous sections.

Changes in the surface composition with respect to elemental at. % before and after coating are reported in Table 8. The ratio between oxygen and silicon on coated fiber surface is a little higher than 2, as was also observed in case of Kevlar[®] and Cotton, suggesting that majority of the oxygen detected was from silica. The amount of oxygen higher than stoichiometric oxygen of silica could be adsorbed from the environment or contribution from the fabric substrate. Silver is present almost entirely in metallic state as has been discussed above.
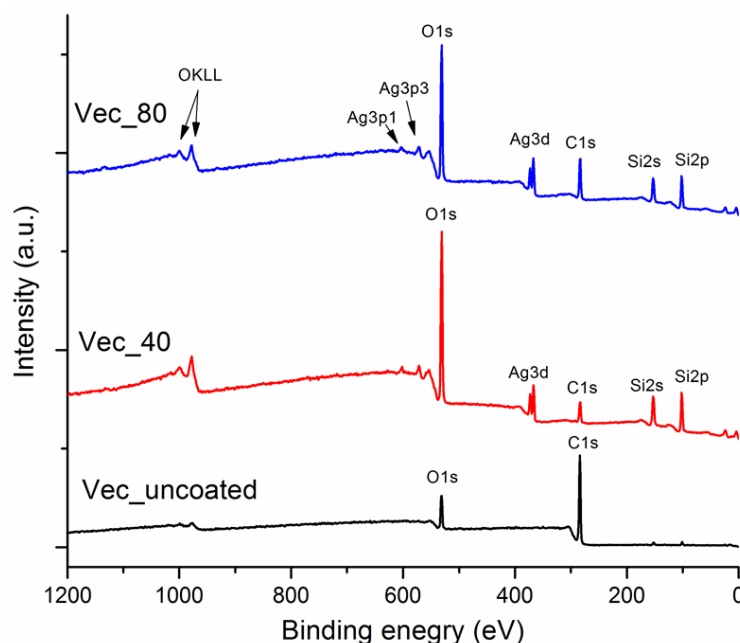
Figure 45: XPS survey spectra of uncoated (Vec_uncoated) and coated (Vec_40 and Vec_80) Vectran[®] fabric
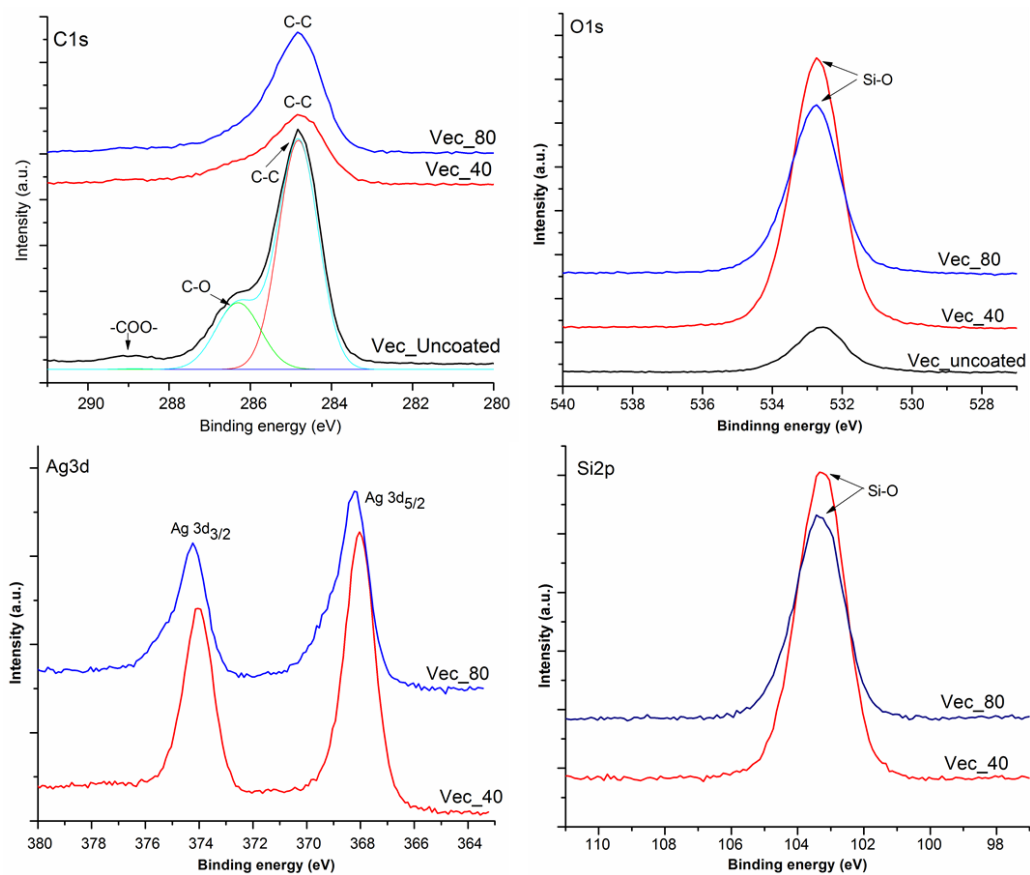
Figure 46: XPS high resolution spectra of C1s, O1s, Ag3d and Si2p peaks of uncoated (Vec_uncoated) and coated (Vec_40 and Vec_80) Vectran® fabric

Table 7: Table summarizing different peaks, their binding energies and corresponding bonds in XPS spectrum of uncoated (Vec_uncoated) and coated (Vec_40 and Vec_80) Vectran® fabric

Peak	Bonding	Binding energy BE (eV)		
		Vec_uncoated	Vec_40	Vec_80
C-1s	C-C	284.8	284.8	284.8
	C-O	286.2	-	-
	-COO-	288.9	-	-

O-1s	C-O-C	532.5	-	-
	Si-O	-	532.7	532.7
Si-2p	Si-O	-	103.3	103.4
Ag-3d$_{3/2}$	Ag^0	-	374.1	374.2
Ag-3d$_{5/2}$	Ag^0	-	368.0	368.2

Table 8: Composition (w.r.t atomic %) of the uncoated (Vec_uncoated) and coated (Vec_40 and Vec_80) Vecran$^®$ surface derived from XPS survey spectra

	Atomic %				
	C-1s	O-1s	Si-2p	Ag-3d	O/Si
Vec_uncoated	82.3	15.6	2.1	-	-
Vec_40	18.6	57.1	22.4	1.9	2.5
Vec_80	33.9	45.2	18.9	1.9	2.4

4.3.2 Total silver content and silver ion release in water

The amount of silver deposited on Vectran$^®$ fabric surface under three deposition conditions (Vec_15, Vec_40 and Vec_80) was determined through ICP-MS. The amount of silver deposited after 15 (Vec_15), 40 (Vec_40) and 80 (Vec_80) min. of sputter deposition was found to be 166, 308 and 574 ppm (mg per kg on fabric weight) respectively. Ionic silver release profiles from the Vectran$^®$ fabric with three depositions, obtained through silver release test in water over a duration of 3, 24 and 72 hours, are shown in Figure 47. Unlike Kevlar$^®$ the graph shows ionic silver release behavior from coated Vectran$^®$ fabric similar to what was observed in case of cotton fabric, as described in previous sections. A gradual silver ion release is evident from the graph which is dependent on the coating thickness (consequently the amount of silver deposited) as well as duration of sample immersion in water.

The amount of ionic silver released from Vec_15, Vec_40 and Vec_80 in water within 72 hours of silver release test was 1.39, 3.84 and 4.3 μg/cm^2 respectively which correspond to 33, 50 and 30 % of the total silver deposited under three conditions.
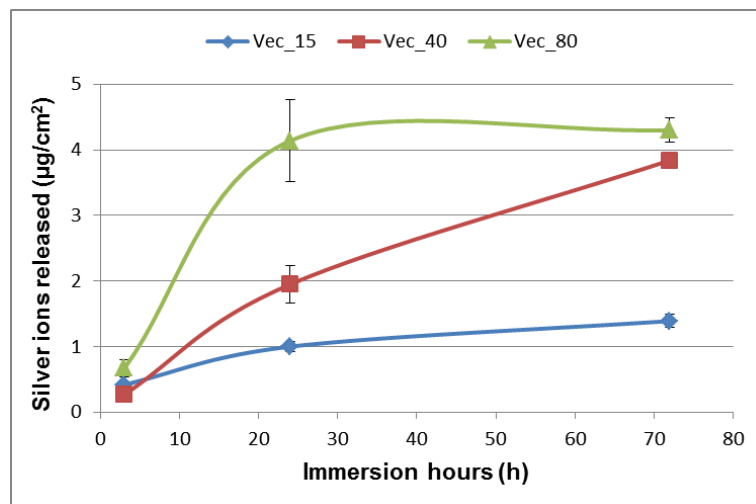
Figure 47: The amount of silver ions leached from coated Vectran® fabric in water during silver release test

EDS analysis was performed on Vec_40 after silver release test and residual atomic % of Si and Ag compared with as deposited Vec_40 is shown in Figure 48. The reduction percentage in silver atomic % was 6, 33 and 58 % , after silver release test of 3, 24 and 72 hours respectively. Whereas the same reduction percentage on Vec_40, as calculated from total silver concentration determined through ICP-MS and ionic silver release determined through silver photometer reported above, was 4, 25 and 50% which is comparable to the values obtained through EDS. This confirms that almost all the silver leached in water from coated Vectran® was in ionic form rather than particle form.
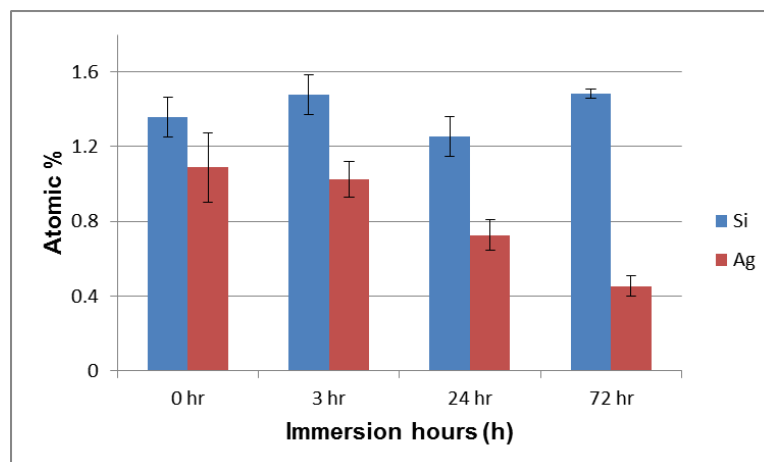
Figure 48: Relative atomic % of Si and Ag on Vec_40 after silver release test of 3, 24 and 72 hours in water

The amount of silver deposited on Vectran[®] fabric under three deposition durations (Vec_15, Vec_40 and Vec_80) and percentage of the deposited silver released during silver release test is summarized in Table 9. In case of Vec_40, approximately 50 % of the deposited silver was released after 72 hours which is comparatively less than that was released in case of cotton fabric (74%) with an equivalent coating thickness (Cot_40). The data in Table 9 suggests that regarding Vec_15 and Vec_80, approximately 33 % and 30 % of the deposited silver was released after 72 hours of immersion in water which is almost equivalent to the release values after 24 hours from these samples. One possible explanation of relatively lower ionic silver from Vectran[®] compared with other substrates could be the higher adhesion of the coating with the Vectran[®] fiber surface due to which lower silver was released from the coating layer next to the fiber surface. The nature of the fabric substrate can possibly influence the adhesion of the coating with the substrate surface. The results of the washing stability tests for the coated textile fabric substrates support this assumption. It was shown that in case of cotton and Kevlar[®], almost all the coating was removed within 10 washing cycles. Whereas relatively higher silver concentration was confirmed on Vectran[®] fabric surface after 10 washing cycles as confirmed by EDS spectrum as well as FESEM images presented in the relevant washing sections. This could be due to higher adhesion of the coating with Vectran[®] fabric surface compared with that of cotton and Kevlar[®].

Table 9: The amount of silver deposited on Vectran® fabric under three deposition conditions and its percentage released within 3, 24 and 72 hours of silver release test

Sample	Deposited silver (ppm)	Silver released (% of deposited silver)		
		3 hr	24 hr	72 hr
Vec_15	166	10	25	33
Vec_40	308	4	25	50
Vec_80	576	5	29	30

4.3.3 Silver release in artificial sweat

The analysis of silver release in artificial sweat from Vec_40 within 3, 24 and 74 hours was performed and its comparison with silver release in water is shown in Figure 49. The amount of silver released in artificial sweat was higher (2.21 – 5.04 $\mu g/cm^2$) than that was released in water (0.23 – 3.84 $\mu g/cm^2$) due to low pH of artificial sweat. However, a gradual release behavior can be observed rather than abrupt or simultaneous release of all the silver. Despite variations in ionic silver release profiles in water, similar release behavior in artificial sweat has also been discussed in previous sections in case of cotton (1.87 – 4.21 $\mu g/cm^2$) and Kevlar® (2.1 – 4.9 $\mu g/cm^2$) substrates.
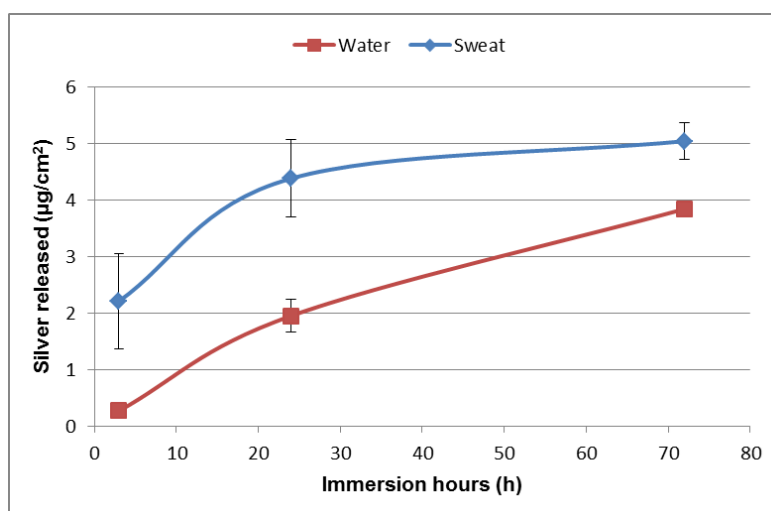
Figure 49: Comparison of silver released from Vec_40 in water and in artificial sweat

4.3.3 Antimicrobial test

Antimicrobial inhibition halo test for uncoated and coated Vectran® fabric was performed against *S. aureus* and *E. coli* and results are shown in Figure 50. Samples deposited under three conditions (Vec_15, Vec_40 and Vec_80) were tested against *S. aueus* whereas Vec_40 was tested against *E. coli*. An inhibition halo of about 1, 2 and 3 mm can be observed around Vec_15, Vec_40 and Vec_80 respectively. Whereas in case of *E. coli,* similar to the results obtained for cotton substrate, the inhibition halo formed around Vec_40 samples was not as transparent as was obtained against *S. aureus*. This was due to the growth of some of the *E. coli* colonies in the inhibition zone. However, in all the cases no bacterial colony was observed underneath the surface of the coated samples compared with control (Vec_uncoated).
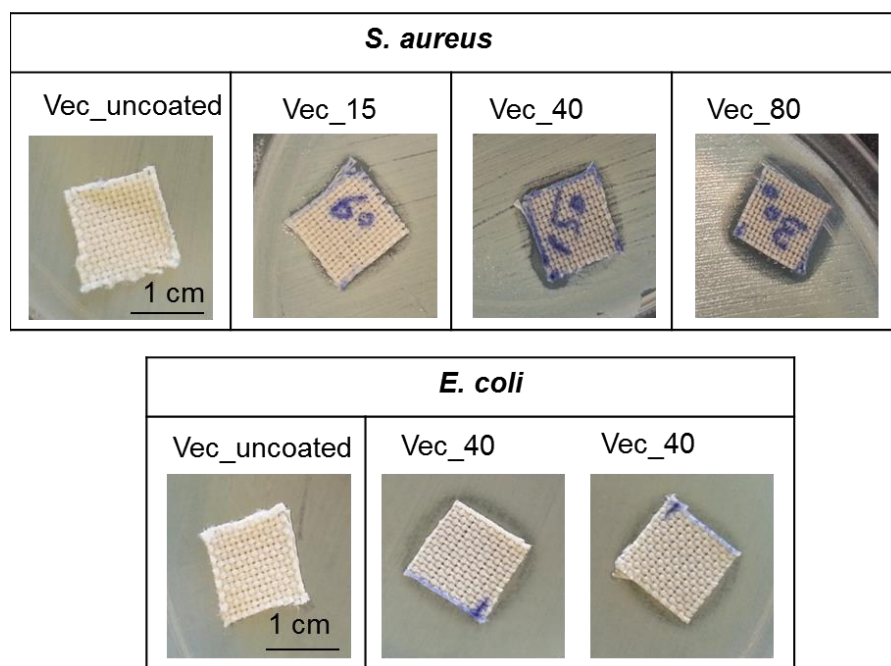
Figure 50: Inhibition halo test for uncoated and coated Vectran® fabric against *S. Aureus* and *E. Coli*

4.3.4 Washing stability of coating

Washing stability of the coating on Vectran® fabric was assessed on samples deposited for 40 minutes (Vec_40) after 1, 5 and 10 washing cycles with two soap solutions: commercial Castile soap and AATCC detergent without optical brightener (WOB). FESEM and EDS analysis was performed on the samples after washing. EDS spectra of the samples washed with commercial Castile soap is given in Figure 51. The spectrum indicates the presence of the coating even after 10 washing cycles (Vec_40_10washes). These results are comparatively different

than those of obtained for cotton and Kevlar® substrates where almost all the coating (and particularly silica) was removed within 10 washing cycles with Castile soap. This is in agreement with the results of silver release test where it was suggested that relatively lower silver was released from the coating layer immediately next to the fiber surface. This supports the assumption that the adhesion of the coating with the Vectran® fiber surface was better than that of with cotton and Kevlar® fiber surfaces. FESEM micrograph of Vec_40_10washes in Figure 52 supports this argument as presence of the silver nano clusters is clearly evident on the fiber surface after 10 washing cycles. This implies that the nature of the substrate, which has been suggested to influence the nucleation and growth of the coating (and hence coating morphology) on the surface by sputtering [111], may influence the adhesion of the coating with the surface as well.

EDS spectra of Vec_40 after washing with AATCC detergent is shown in Figure 53. Contrary to the washing with Castile soap, AATCC detergent proved corrosive and caused more dissolution of the Ag as is evident from the intensity of the Ag peaks in Figure 51 and Figure 53. Washing with AATCC detergent resulted in dissolution of almost all the coating (particularly silver) from the fabric surface. Similar results, of different dissolution of silver with the two washing liquids, have also been reported previously for cotton and Kevlar® substrates. The presence of other elements in the EDS spectrum of washed samples could be due to the residuals from washing solution that escaped rinsing.
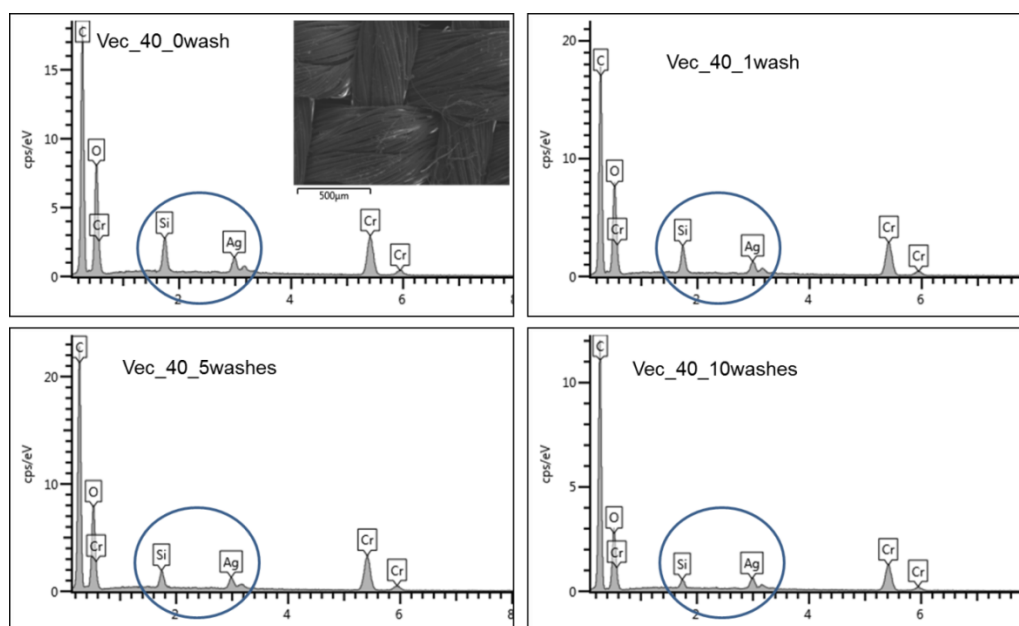
Figure 51: EDS spectra of Vec_40 after 1, 5 and 10 washing cycles with commercial Castile soap
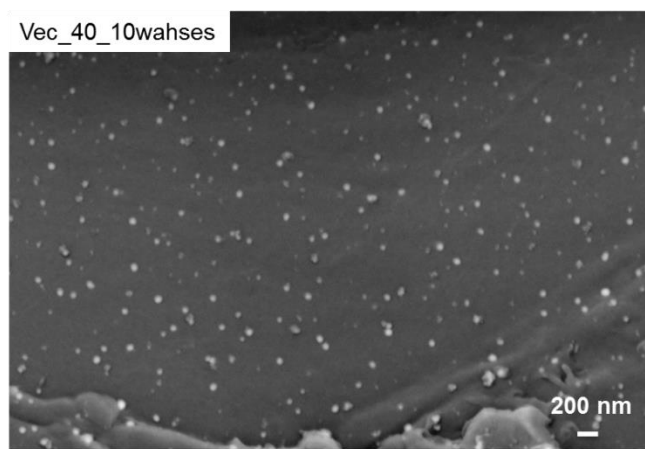
Figure 52: FESEM micrograph (in backscattered mode) showing presence of silver nanoclusters on the surface of Vec_40 after 10 washing cycles with Castile soap
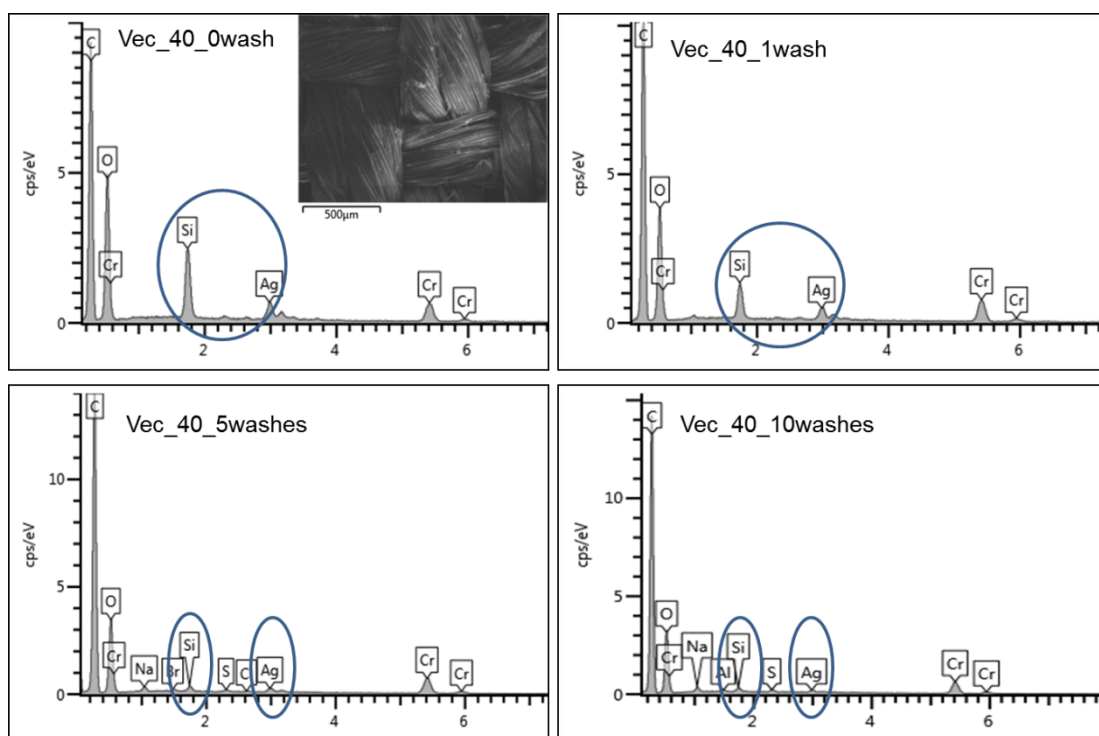
Figure 53: EDS spectra of Vec_40 after 1, 5 and 10 washing cycles with AATCC detergent

4.4 Activated Carbon Fabric (ACF)

4.4.1 Coating morphology and composition (FESEM, EDS, XPS)

Activated carbon fabric (ACF) used in this study was intended for air filtration applications. The surface morphology of the uncoated and coated ACF fabric is shown in Figure 54. The surface of the uncoated ACF fabric is porous as can be seen from FESEM micrograph at high magnification (ACF_uncoated). The porosity on the surface of the ACF fabric is to enhance the specific surface area of the fabric for maximum adsorption of the contaminants from the air. The specific surface area of uncoated ACF fabric was 1300 m^2/g as reported by the manufacturer. After sputter deposition of the silver nanoclusters/silica composite coating, the surface porosity of the ACF was reduced. Surface porosity was preserved to some extent at reduced deposition time that result in relatively thinner coating (ACF_15). Whereas, complete surface coverage of the fiber was observed for longer depositions (ACF_40 and ACF_80). Due to porosity on the surface, the morphology of the coating observed on ACF was different from that of observed on other textile substrates used in this study as reported previously.

EDS spectra of coated and uncoated ACF fabric are shown in Figure 55. The spectrum of the uncoated ACF (ACF_uncoated) consists mainly of C with small percentage of O. Ag and Si peaks were detected on ACF fabric coated with silver nanoclusters/silica composite coating. Ag/Si ratio with respect to atomic %, as calculated from the elemental composition obtained through EDS and reported in respective spectrum in Figure 55, was approximately same for the three deposition times and at the same level similar to other textile substrates reported previously. The color change of the ACF substrate, due to Localized Surface Plasmon Resonance (LSPR) of silver nanoclusters, was not noticeable due to black color of the ACF fabric itself.

Further analysis was performed through XPS to investigate the chemistry of the deposited coating and to have an insight into any possible interaction between silver nano clusters and ACF substrate. XPS survey spectra, shown in Figure 56, indicates surface composition of uncoated (ACF_uncoated) and coated (ACF_40 and ACF_80) ACF fabric. Survey spectra of uncoated ACF consists of a prominent C-1s peak along with a tiny O-1s peak. This shows that the surface of the uncoated ACF is mainly composed of carbon with a small amount (2.7% only) of oxygen. After sputter deposition of silver nano clusters/silica composite coating, peaks related to Ag and Si appear along with an increase in intensity of oxygen peak due to oxygen in silica and decrease in intensity of carbon peak.
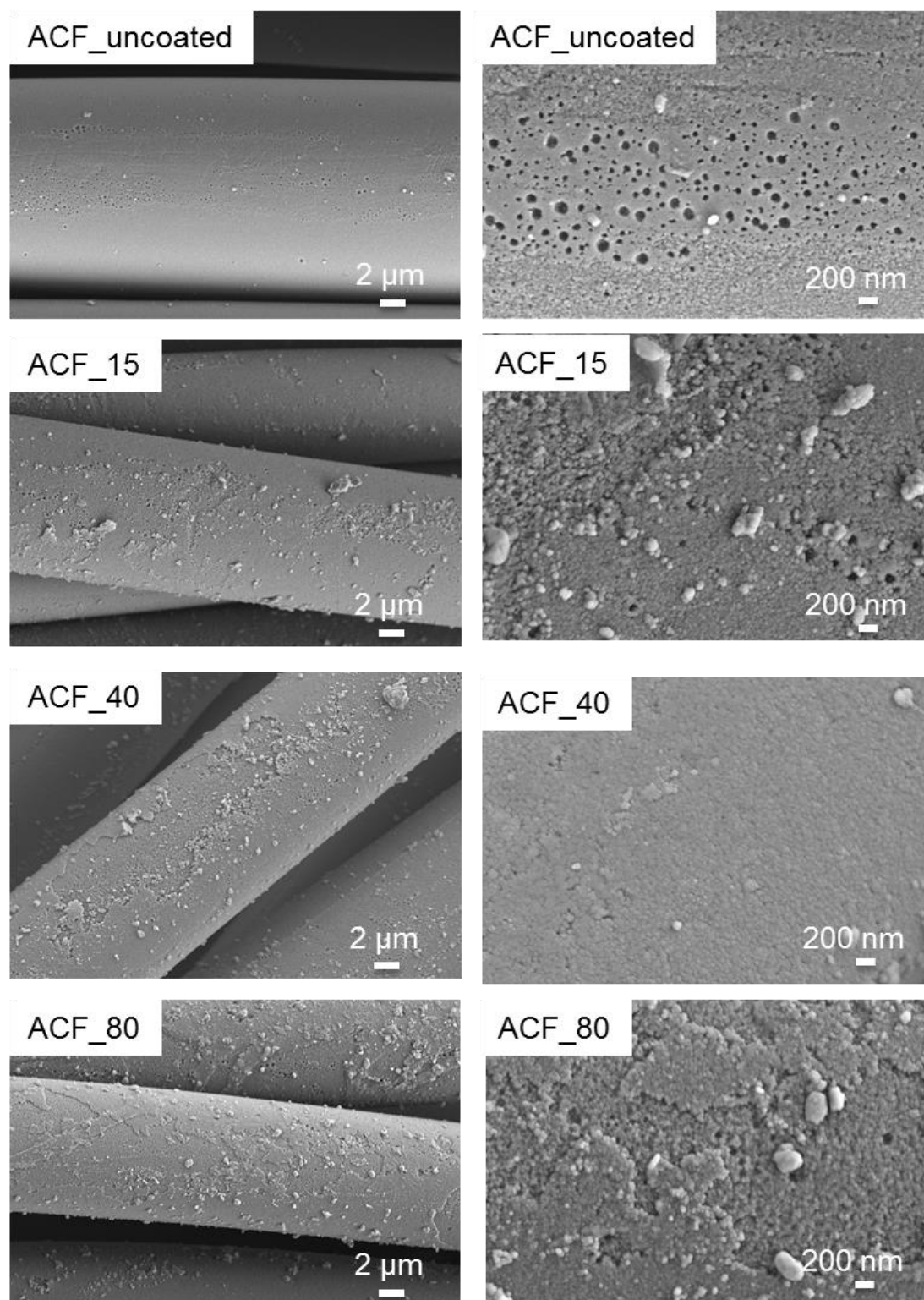
Figure 54: FESEM surface morphology of uncoated (ACF_uncoated) and coated (ACF_15, ACF_40 and ACF_80) ACF fabric at low and high magnification
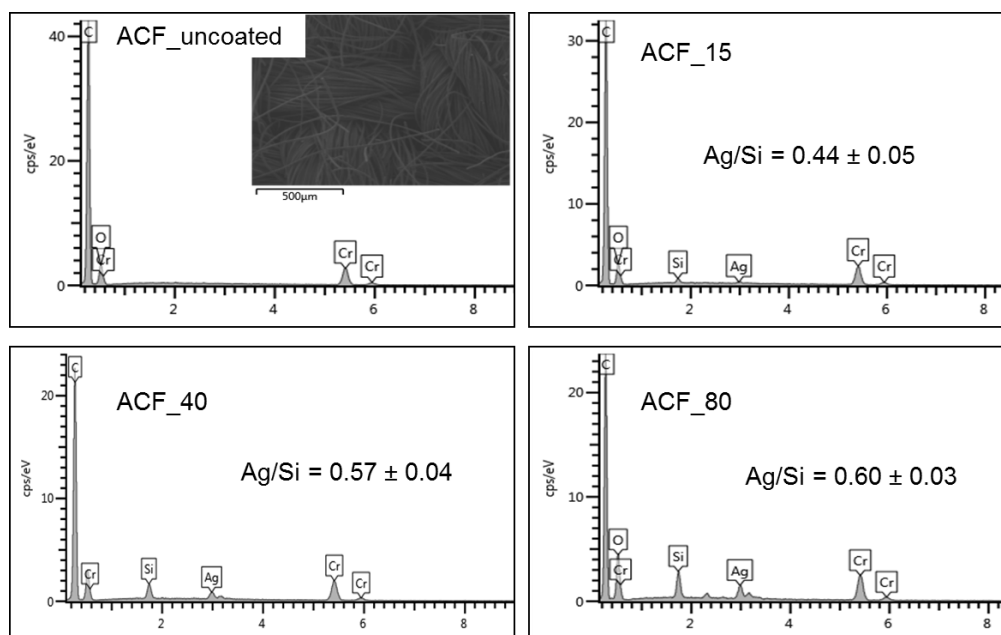
Figure 55: EDS spectra of the uncoated (ACF_uncoated) and coated (ACF_15, ACF_40 and ACF_80) ACF fabric and corresponding Ag/Si (at. %) ratio
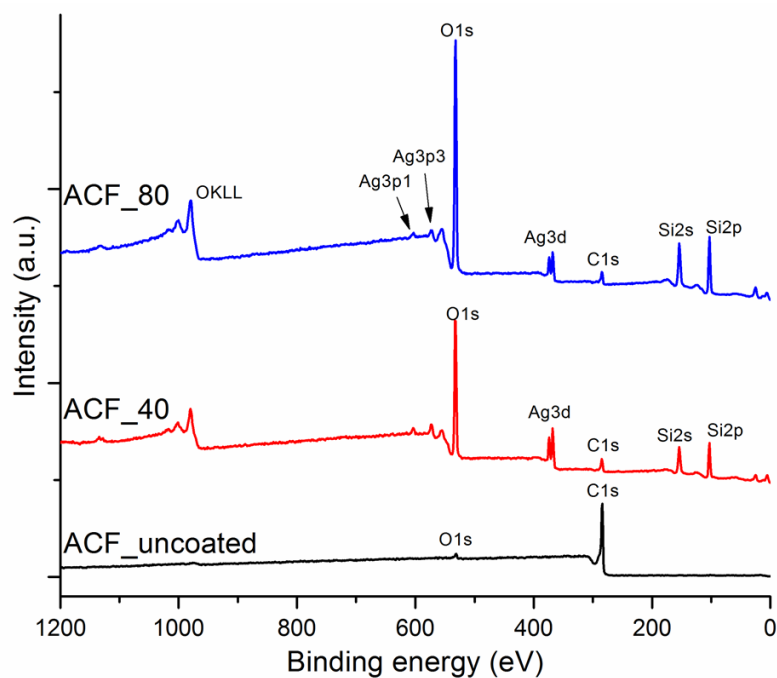
Figure 56: XPS survey spectra of uncoated (ACF_uncoated) and coated (ACF_40 and ACF_80) ACF fabric

To further analyze the bonding states of the elements detected in the survey spectra, high resolution scans of C-1s, O-1s, Ag-3d and Si-2p were obtained and results are shown in Figure 57. The binding energies (BE) of the C-1s, O-1s, Ag-3d and Si-2p peaks and their bond associations have been summarized in Table 10 and discussed as follows. The C-1s peak of ACF_uncoated at binding energy (BE) 284.7 eV represents graphitic carbon in ACF and the tiny peak at about 290.5 eV could be representative of carboxylic groups possibly due to the presence of small amount of oxygen detected on uncoated ACF surface [16]. Whereas the C-1s peaks detected on coated ACF (ACF_40 and ACF_80) are due to advantageous carbon or a contribution from the fabric substrate. The O-1s peak of ACF_uncoated seems to be flat due to small amount of oxygen but is centered at 532.2 eV that can be associated to carboxylic groups [163]. On the other hand, the O-1s peaks in the spectra of coated ACF (ACF_40 and ACF_80) are present at BE 532.7 eV which are due to the oxygen present in silica as O-1s peak at BE 532.7 eV and Si-2p peak at BE 103.2 eV are attributed to silica [152]. These peaks are similar to the O-1s peaks reported previously for other coated textiles substrates and are at the same BE. This confirms that the O-1s peaks found on all the coated textile substrates in this study were due to silica only eliminating any contribution from the formation of silver oxides. The stoichiometric ratio between O and Si in silica is 2 and that of calculated from O/Si presented in Table 11 is 2.4 which further confirms that the detected oxygen peaks were mainly from silica

The Ag-3d$_{3/2}$ and Ag-3d$_{5/2}$ peaks on coated ACF (ACF_40 and ACF_80) located at BE 374.3 eV and 368.3 eV respectively are representative of metallic Ag [16]. However, on ACF_40 a shoulder peak can be seen at lower BE on both Ag-3d$_{3/2}$ and Ag-3d$_{5/2}$ at BE 373.7 eV and 367.7 eV respectively which was not detected on ACF_80 and on other substrates reported in previous sections. In literature, Ag-3d doublet at these BE is assigned to Ag^{1+} species that are generally associated with Ag$_2$O formation [163]. However, the formation of silver oxide is less likely in this case as the corresponding oxygen peak associated with silver oxide, which is reported to be at 530.75 eV [109], cannot be observed in Figure 57. One of the possible reasons for these shoulder peaks could be due to the possible interaction of the silver nano clusters, present in the coating layers next to the fabric surface, with the ACF support [16].

Activated carbon fibers have been reported to possess electron acceptor properties and, therefore, are used as redox mediators [164]. On the other hand silver nanoparticles/clusters can get readily oxidized in moist conditions or by absorbing moisture at ambient conditions. This can establish electron donor-acceptor interaction between ACF fabric and silver nano clusters resulting in partial oxidation of silver nano clusters in contact with ACF support. This

interaction of silver nanoclusters with ACF substrate vanished with the increment in coating thickness and hence it did not influenced the Ag-3d peaks on ACF_80. Therefore, the silver particle adjacent to the ACF surface may be linked to the ACF either through Ag-O-C [163] or Ag-C covalent bond due to electron transfer from Ag to carbon in ACF [165]. Keeping in view the quantitative information as well as oxygen peek position, the Ag-C bond is more likely than Ag-O-C bonding. This covalent linkage of silver present in silver nano clusters immediately next to the ACF surface could be of interest to produce longer lasting antibacterial air filters and can help retain silver during washing as well as to control its leaching in wet environments. Possibly it was the influence of this interaction that can be seen in the results of silver release test as well as washing stability test in the following sections. Silver release test showed that very low quantities of silver ions, compared with cotton and vectran® fabrics with similar coatings, were released from coated ACF. Similarly, silver particles remained attached to the ACF surface even when matrix of the coating was removed during repeated washing cycles.
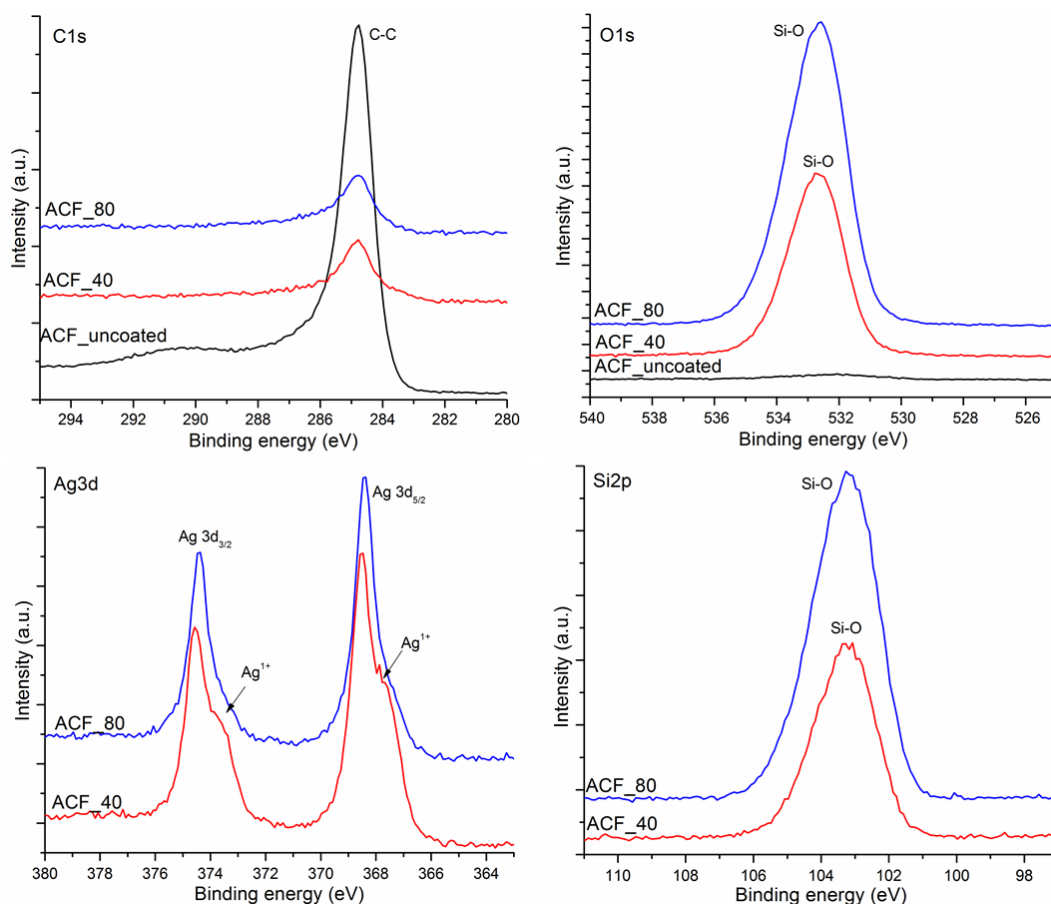
Figure 57: XPS high resolution spectra of C1s, O1s, Ag3d and Si2p peaks of uncoated (ACF_uncoated) and coated (ACF_40 and ACF_80) ACF fabric

Table 10: Table summarizing different peaks, their binding energies and corresponding bonds in XPS spectrum of uncoated (ACF_uncoated) and coated (ACF_40 and ACF_80) ACF fabric

Peak	Bonding	Binding energy BE (eV)		
		ACF_uncoated	ACF_40	ACF_80
C-1s	C-C	284.7	284.7	284.7
C-1s	-O-C=O	290.5	-	-
O-1s	-O-C=O	532.2	-	-
O-1s	Si-O	-	532.5	532.7
Si-2p	Si-O	-	103.1	103.3
Ag-3d$_{3/2}$	Ag^0	-	374.6	374.4
	Ag-C	-	373.6	-
Ag-3d$_{5/2}$	Ag^0	-	368.6	368.4
	Ag-C	-	367.6	-

Table 11: Composition (w.r.t atomic %) of the uncoated (ACF_uncoated) and coated (ACF_40 and ACF_80) ACF fabric surface derived from XPS survey spectra

	Atomic %					
	C	O	Si	Ag	S	O/Si
ACF_uncoated	97	2.7	0.3	-	0.1	-
ACF_40	13.6	59.5	24.2	2.6	-	2.4
ACF_80	8.1	64.3	26.3	1.3	-	2.4

4.4.2 Silver ions release in water

Silver ion release profiles in water from ACF fabric with three coating thicknesses (ACF_15, ACF_40 and ACF_80) are given in Figure 58. The graph shows that, compared with thinner coatings (ACF_15 and ACF_40), more silver ions were released from thick coating (ACF_80) with maximum release of 1.65 µg/cm^2 within 72 hours of release test. However, these silver ion release values are far less than those were obtained from equivalent coating thickness on cotton (6.37 µg/cm^2) and Vectran$^®$ (4.3 µg/cm^2) substrates.

EDS analysis of ACF_40 after release test of 3, 24 and 72 hours, shown in Figure 59, also indicate that lower amount of silver was released with reference to total deposited one. It was due to this ionic silver release behavior that, despite the surface of the sample being antibacterial, the formation of inhibition halo around coated ACF samples was not observed as will be shown later in inhibition zone antibacterial test. The possible electron donor-acceptor interaction between ACF and silver nano particles/clusters, as discussed in detail in XPS results, could be the possible reason resulting in relatively lower ionic silver release from coated ACF. This could be possibly due to redox adsorption mechanism of silver with ACF in aqueous environment. Activated carbon nano spheres have been reported to remove even trace amount of Ag(I) from water dominantly by redox adsorption mechanism [166]. Possibly, the same redox adsorption comes into play that slows the release of silver ions from coated ACF fabric. The flattening of the release curves after 24 hours shows that possibly an equilibrium may be established between silver ion formation and their readsorption by ACF.
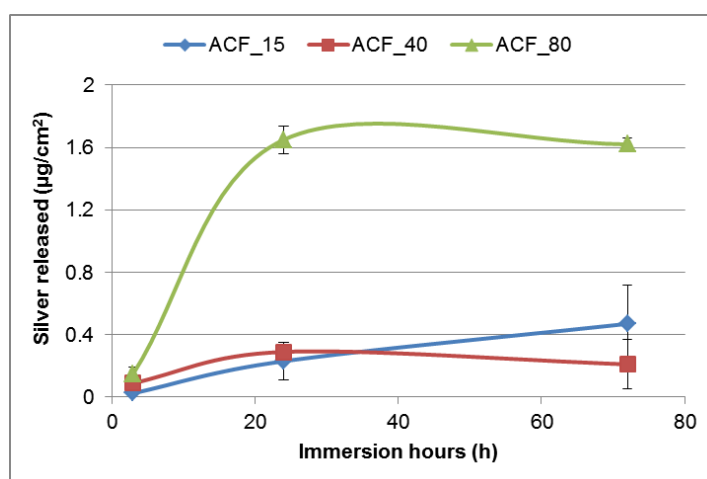
Figure 58: The amount of silver ions leached from coated ACF fabric in water during silver release test
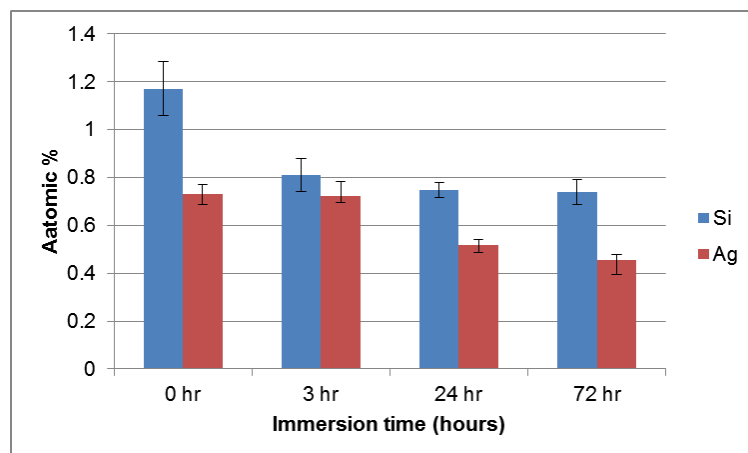
Figure 59: Relative atomic % of Si and Ag on ACF_40 after silver release test of 3, 24 and 72 hours in water

4.4.3 Antibacterial test

Antibacterial performance of the silver nanoclusters/silica composite coating on ACF was evaluated in inhibition halo test against *S. Epidermidis* and *E. coli* and results are shown in Figure 60. In case of *S. epidermidis*, no inhibition zone can be observed around uncoated (ACF_uncoated) and coated (ACF_40) ACF samples. However, no bacterial growth was observed under the surface of the coated ACF (ACF_40) whereas bacterial growth is clearly evident on the surface of uncoated ACF (ACF_uncoated) as is evident from the back agar surface image in Figure 60.

Whereas, an inhibition zone can be seen around some edges of the samples against *E. coli*. Again, despite non uniform inhibition zone against *E. coli*, no bacterial growth can be seen under the sample surfaces compared with that of control (ACF_uncoated). This indicates that the surface of the coated ACF was completely antibacterial even if no inhibition halo was formed around the samples. In fact the formation of inhibition halo is a result of silver ion leaching from the coating around the sample on the agar surface [64]. It has been shown earlier that negligible amount of silver ions were released from the coated ACF, therefore, no (or incomplete) inhibition halo was formed around coated ACF. However, the presence of silver on ACF surface rendered antibacterial activity to the ACF surface. This leads to the antibacterial effect only on the surface of the ACF fabric rather than formation of inhibition zone around the samples.
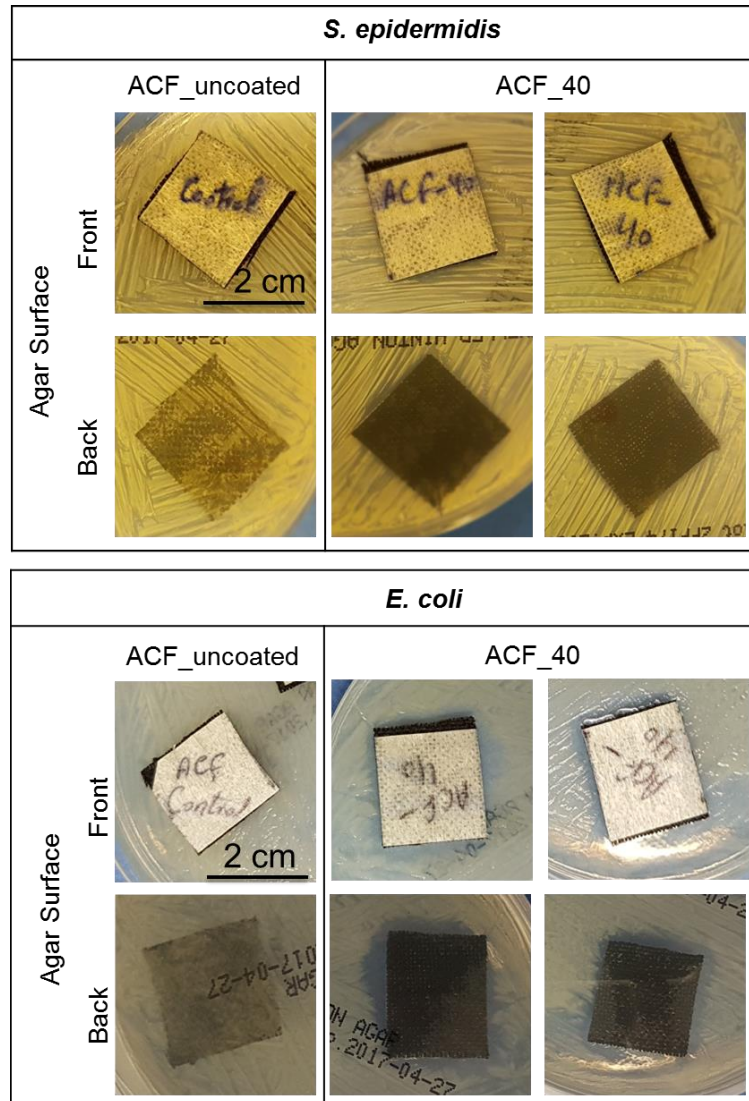
Figure 60: Inhibition halo test for uncoated and coated ACF fabric (ACF_40 only) against *S. epidermidis* and *E. coli*

Similar results have been reported in [64] where glass fabrics were deposited with copper, silver, gold, platinum and platinum/rhodium using magnetron sputtering and their antimicrobial properties were studied against two bacterial strains: *S. aureus* and *K. pneumonia* and three fungal strains: *Aspergillus niger, Chaetomium globosum and Penicillium funiculosum*. Silver and copper formed well defined inhibition zone in antibacterial test whereas other fabrics deposited with gold, platinum and platinum/rhodium layers did not formed any inhibition zone. But their surfaces were still antibacterial because no growth of bacteria under the sample surfaces was observed compared with that of controls. The authors attributed this difference to no release of corresponding metal ions in the surrounding environment to form the inhibition halo due to high reduction potential of these metals. Metal ions are considered to be responsible for

bactericidal action. Therefore, even if no inhibition halo was formed around ACF, the surface of the samples showed antibacterial effect by not letting the bacteria to grow under it. This ability of ACF, to retain silver in wet conditions, is different than other substrates used in this study and is a promising property of ACF to produce antimicrobial filters with longer life spans and possibility of regeneration.

4.4.4 Washing stability of coating

The washing stability of the silver nano clusters/silica composite coating on ACF was evaluated by subjecting ACF_40 samples to 1 and 5 washing cycles with commercial Castile soap. The washed samples were analyzed through FESEM and EDS. The EDS spectrum of ACF_40 after 0, 1 and 5 washing cycles is given in Figure 61. The effect of the washing is evident as the intensity of the Si and Ag peaks reduced significantly even after 1st washing cycle (ACF_40_1wash). No Si peak was detected after 5th washing cycle suggesting that the coating was removed within 5 washing cycles. In comparison to other textile substrates used in this study where coating was almost intact after 1st washing cycle, the coating on ACF appears to have minimum washing stability. The poor washing stability of the coating on ACF compared with other substrates, could be attributed to the high surface porosity on ACF meant for filtration purposes. Highly porous nature of the ACF fibers may result in relatively poor adhesion of the coating with the fiber surface as well as porous coating and hence the coating was easily removed during 1st washing cycle as is also shown in FESEM images in Figure 62. However, in agreement with EDS spectrum in Figure 61, the presence of silver nanoparticles can be seen in FESEM micrograph in backscattered mode after 5 washing cycles (ACF_40_5washes) in Figure 62. This again points to a possible interaction of nano silver with the ACF substrate suggesting that even after complete removal of the coating matrix, silver particles were attached to ACF.
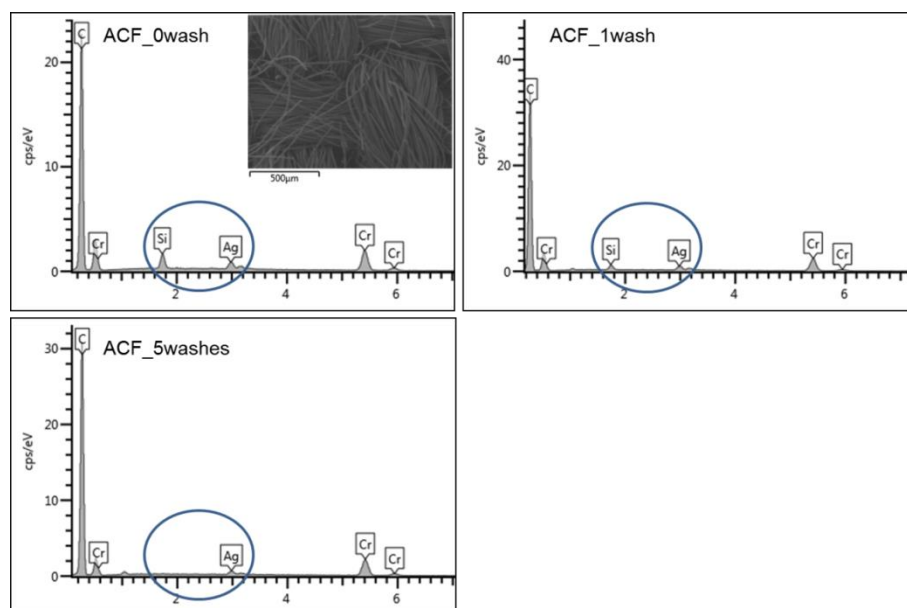
Figure 61: EDS spectra of ACF_40 after 1 and 5 washing cycles with commercial Castile soap
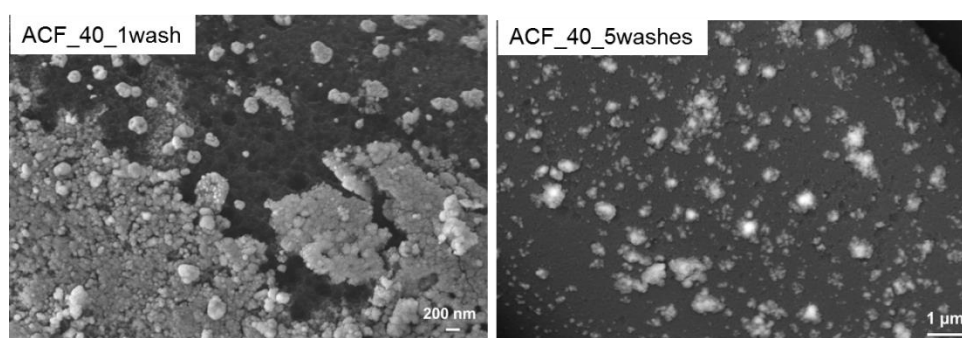
Figure 62: FESEM micrograph of ACF_40 after 1 and 5 (back scattered mode) washing cycles showing significant coating removal after 1 washing (ACF_40_1wash) and presence of silver particles attached to the fiber surface even after 5 washing cycles (ACF_40_5washes)

4.4.5 Air permeability

Air filtration was the intended application of the ACF fabric used in this study. Therefore, it was of relevant importance to evaluate the effect of the coating on the air permeability of ACF. The air permeability of ACF deposited for 40 minutes (ACF_40) was evaluated and compared with that of uncoated ACF. The air permeability, measured in terms of air speed (mm/s) through the fabric, of uncoated ACF was 744 ± 31 mm/s whereas that of coated ACF (ACF_40) was found to be 791 ± 24 mm/s. This shows a small increase in the air permeability of

ACF after coating which could be due to highly delicate nature of ACF fabric that can cause a little bit loosening of the fabric structure during cutting, deposition and handling. Nevertheless, it shows that the deposition process did not cause any decrease in the air permeability of the ACF fabric.

Discussion

Silver nanoclusters/silica composite coating has been deposited, via co-sputtering technique, on four different textile fabrics composed of natural as well as high performance synthetic fibers. Three depositions, for 15, 40 and 80 minutes, were carried on all the four substrates to yield approximately 60, 150 and 300 nm thick coating respectively. The sputtering process parameters were used to control the flux of the extracted atoms, both from silica and silver targets, so that the silica is deposited as matrix of the composite coating while silver is deposited in the form of nano clusters embedded in the silica matrix. The presence of the silver nano clusters on the surface of the fibers can be observed at lower deposition time.

At lower deposition time (15 and/or 40 min.), the coating is too thin to cover all the surface features of the respective fibers. The coating thickness increased with the increase in deposition time (80 min.) resulting in a clear granular morphology typical of sputter coatings. Since the nature of the substrate may influence the nucleation and growth of these grains [111], the growth kinetics of these grains and their coalescing could be different on different fiber surfaces that could affect the final morphology of the coating. Possibly due to this reason, differences in coating morphology were observed on different fabric substrates as was evident from the FESEM images of the four textiles. More importantly, despite morphological differences, silver nano clusters of 25-50 nm in size, were uniformly distributed and embedded in the silica matrix independent of the nature of the substrate. This is one of the biggest advantage of the co-sputtering technique in comparison to other conventional methods of loading silver nano particles on the fabric surface. Conventional approaches may result in silver nano particle agglomeration in colloid or on the fabric surface and hence particular efforts are required to stabilize them in the colloid and/or to uniformly distribute them on the fabric surface [16]. To increase the uniformity of their distribution, silver NPs can be loaded in different matrices, usually silica obtained through organic-inorganic hybrid silica precursor via sol-gel method. However, this is usually a multistep process where creation of the silica matrix and loading and synthesis of silver NPs is done separately. In addition, creation of silica matrix via sol-gel involves additional steps of drying and curing at high temperatures [167].

EDS spectrum of all the coated and uncoated samples was obtained at lower magnification (250X) to incorporate information from broader surface area to estimate homogeneity of the coating. The relative concentration of the elements present in the coating can be estimated using EDS analysis [25] [51] [167]. EDS spectrum was obtained from three different surface areas of the samples. From the elemental composition obtained through EDS, Ag/Si ratio (at.%) was calculated and average was reported. The ratio was fairly same and varied within narrow range (approximately about 0.60 ± 0.10) for the three depositions on the four substrates indicating reproducibility and uniformity in composition of the coating. This shows that the deposition duration changed only the coating thickness while maintaining relative atomic % of Ag and Si in the coating. This estimation was helpful for attaining uniform distribution and embedment of approximately same sized silver nano clusters in the silica matrix for all the textile substrates.

The change in color of the textile substrates was observed after deposition of silver nanoclusters/silica composite coating due to Localized Surface Plasmon Resonance (LSPR) of silver nano clusters. Noble metal (Ag, Au etc) nano particles or clusters absorb in the visible region of light (silver nano particles usually in 420-450 nm) and impart color to the textile substrate to which they are applied [83] [79] [63]. The absorption results in collective oscillation of the surface electrons of metal nano particles/clusters and is known as LSPR [79]. The intensity of the surface plasmon absorption band may increase/decrease with increase/decrease in concentration of silver nano particles/clusters giving darkening effect to the imparted color [63]. Therefore, light to dark brown color was imparted to the textile substrates depending upon the deposition time and hence concentration of the silver nano clusters on the fabric surface.

XPS is a surface sensitive technique with depth profiling of up to 10 nm on the surface and can provide more precise analysis of the thin surface coating composition [23]. XPS results on all the four substrates demonstrate that the deposited coating contains elemental silver in zero oxidation state. In this study, the coating was deposited in a co-sputtering scheme from two independent sputtering targets (silica and silver) resulting in silver nanoclusters/silica composite coating. In case the deposited silver is oxidized (for example Ag_2O is formed), the O-1s peak is reported to be shifted to lower binding energy as reported by *Mejía et al* [109]. *Mejía et al* deposited silver coating on cotton fabric using single target magnetron sputtering and reported that the O-1s peak was shifted from 532.6 eV for uncoated cotton to 530.75 eV on silver sputtered cotton which was attributed to formation of Ag_2O. The O-1s peak for uncoated cotton in this study (532.7 eV) is fairly in good agreement with that of reported by *Mejía et al* (532.6 eV) but contrary to their finding, the O-1s peak increased in intensity

after coating deposition (due to silica) and was not shifted to lower BE. In their study, the O-1s peak at 532.6 eV decreased drastically and a new peak emerged at 530.75 eV (indicating Ag_2O) that increased in intensity with silver deposition time. The amount of oxidized silver for depositions higher than 60s was reported to be same though the total amount of deposited silver varied significantly at increased deposition times. The authors concluded that the oxidized silver was mainly present at the interface of silver layer. It was not, however, reported whether the formation of Ag_2O occurred during the deposition or upon aging during exposure to the environment. On the other hand the results of this study show that O-1s peak, for all the textile substrates, was not shifted to lower binding energy after the deposition of the coating. In fact, no peak was observed below 531 eV for all the substrates suggesting the absence of oxygen associated with silver.

Furthermore, the atomic ratio between O and Si, as determined from XPS survey spectra, was found to be a little higher than 2 (the stoichiometric ratio between O and Si in SiO_2) in all the cases. Therefore, it can be concluded that the oxygen peaks on coated textiles substrates are mainly due to the oxygen of the silica. In addition, the position and sharpness of the Ag-3d peaks suggest that no oxidized silver species are present even on the interface. The only exception was the ACF substrate where peak assigned to Ag^{1+} species was observed in relatively thin coating (ACF_40) possibly due to Ag-C bonding on ACF as has been discussed in detail in the relevant sections previously. Silica is stable against light, heat and chemical attacks [97] and can provide protection to the embedded silver nano clusters against environment contrary to the case where silver is sputtered alone. Nonetheless, this is one of the key advantages of the adopted co-sputtering technique which results in fabrication of silver nanoclusters embedded in the silica matrix on the substrate surface. Summarizing the results of FESEM, EDX and XPS, it can be concluded that silver nanoclusters/silica composite coating, with silver nanoclusters uniformly distributed on the surface and embedded in the silica matrix, was successfully deposited on all the textile substrates irrespective of the presence or absence of any functional groups on the fiber surfaces.

The total silver concentration in the composite coating was found to be in the range 166-632 ppm under three deposition conditions as determined through ICP_MS. Since no oxidized silver was detected through XPS on any substrate (except Ag^{1+} species on ACF due to redox interaction between Ag and ACF), all silver is supposed to be present in metallic form. This suggests that silver amount can be controlled easily by varying the deposition time that varies the coating thickness as well as the amount of deposited silver. Good antibacterial performance was detected even at lower silver concentration (15 minute

deposition) which could be a beneficial aspect from cytotoxic point of view where the coated surface is expected to come in direct contact with human skin. Silver is considered to be non/less toxic for humans at lower concentration levels [168]. In addition, despite lower silver content, embedding silver nano clusters in the silica matrix may reduce direct exposure of the nano silver to the skin and thus further reducing the risk of cytotoxicity. Porous and hydrophilic nature of the applied coating may facilitate diffusion of the silver ions in the humid surrounding leading to effective antibacterial action. This helps avoiding bacterial contamination even in conditions suitable for bacterial growth. Coatings obtained through wet processing routes may contain high silver concentrations to obtain a good level of antibacterial action due to less availability of applied silver for biocidal action. Commercially available silver containing textiles were reported to have silver concentration up to 2925 ppm and those with lower silver content were found to exhibit no antibacterial action [87].

Although all the silver deposited on textile substrates is believed to be in metallic form, silver nano particle/clusters react with moisture, present on skin, wound or in any other humid media and get ionized and ionized silver is highly reactive [112]. Silver nano clusters/particles have high surface area compared with other forms of silver and thus show higher sensitivity to moisture and oxygen and hence get oxidized in humid environment [99]. The potential of silver leaching increases as the size of the silver particles decreases to nano scale [99]. The oxidation of silver nanoclusters/nanoparticles to release silver ions is known to be strongly dependent on dissolved oxygen and presence of protons (pH) in the water. The role of dissolved oxygen in water is more important because silver ions release was found to be inhibited even at the lowest pH in deoxygenated water. Therefore, silver ion release is a cooperative oxidation process where oxygen has important role to initiate the oxidation of silver. From thermodynamic point of view, under common conditions of dissolved oxygen and relevant environmental pH of simple aqueous media, Ag^0 does not persist, rather Ag^+ is the equilibrium product. The oxidation of Ag^0, which is a simple redox reaction, to release Ag^+ follows the following reaction stoichiometry with peroxide intermediates [71]

$$2Ag_{(s)} + \frac{1}{2}O_{2(aq)} + 2H^+_{(aq)} \leftrightarrow 2Ag^+_{(aq)} + H_2O_{(l)}$$
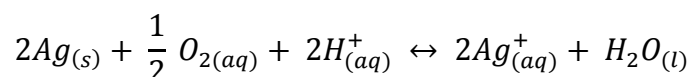
Silver treated textile products are found to release highest amount of ionic silver compared to other products containing silver. Silver ions (and reactive oxygen species produced as a result of silver oxidation) released from the coated textiles are considered to be responsible for antimicrobial action [99], therefore, the release behavior of ionic silver from silver nanoclusters/silica composite coating was assessed. For all the substrates, a gradual time dependent release of

ionic silver was observed. No abrupt release was observed in any case. This can ensure antibacterial performance over an extended period of time that may not be possible in case of abrupt silver release. According to the thermodynamics of the silver oxidation, the amount of dissolved silver is directly proportional to the amount of dissolved oxygen and inversly proportional to the pH. Consequently, acidic pH increases silver release while basic pH decreases the silver release [104]. Therefore, an increased amount of silver release was found in this study in artificial sweat compared with silver release in water. Similar results have also been reported by other researchers in literature [90] [92]. It is important to note that no abrupt release of silver in artificial sweat was observed in any case even the test was carried under harsh conditions (highly acidic sweat formulation: pH=3 and continuous immersion for three days) which reduces the risk of exposure to high concentration of silver under practical conditions. The available literature on release of silver in different fluids from silver coated textiles have been reviewed in detail in Chapter 2.

After being immobilized and removed from the coating, either by water, sweat or any other liquid, silver nanoparticles may have potential to penetrate the human skin. Although silver nanoparticles are considered to be less toxic to humans at relatively lower concentrations, however, they may have potential to penetrate human skin and cause inflammation or irritation. Silver nano particles are the most commonly used nano materials applied not only to textiles but found also in many other consumer products, but still there is lack of data on percutaneous penetration of silver from silver nano particle containing products [68]. The potential of dermal penetration of silver released from silver nanoclusters/silica composite coating deposited on different substrates in this study was assessed by other partners in the frame work of the same project at Universita` di Torino, Italy and findings were published jointly [147]. The dermal penetration was analyzed through Franz static diffusion cell method using cryopreserved skin. The total amount of silver permeated through the skin within 24 hours of test and found in the receptor compartment of the "Franz diffusion cell" was 3.21 ± 0.63 ng/cm^2. The amount of silver absorbed within the skin was measured by splitting the skin in epidermis and dermis. The amount of silver absorbed in epidermis was 29 ± 1 ng/cm^2 whereas that of in dermis was 17 ± 5 ng/cm^2. These results indicate that higher amount of silver was retained in epidermis than in dermis and that silver released from silver coated textiles (in ionic form) has the potential to permeate through human skin. Several experimental variables can affect silver absorption through the skin [169]. These may include total amount of silver deposited on the textiles, the amount of silver released, exposed skin area compared with total body area, duration of exposure etc. This may lead to under/over estimation of real absorption potential.

Furthermore, there is lack of any reference limits for exposure to silver nanoparticles/clusters [170] as well as toxicity of silver nano particles against human cells is not yet fully understood [74] which makes it difficult to assess health risks that could result due to silver absorption from silver coated textiles. It should be noted that this penetration of silver is expected to be in ionic form which later can result in their accumulation (or transformation) in the skin depending upon biological environment [169].

The antimicrobial efficacy of the silver nanoclusters/silica composite coating was verified against bacterial and fungal strains. *S. aureus,* and *E. coli* were selected as representative Gram positive and Gram negative bacterial strains respectively whereas *C. albicans* was selected as representative fungal strain. In case of ACF, *S. epidermidis* was used which is a Gram positive bacterium. The antimicrobial properties were mainly evaluated through inhibition halo test for all the substrates. The inhibition halo test was performed by spreading the bacterial strain over an agar culture medium and putting the coated samples over the agar surface. The agar plates are then incubated to grow the bacteria. Agar culture is a transparent media and if bacterial growth is inhibited, an inhibition zone in the form of clear halo, where bacteria did not grow during incubation, can be observed around the samples.

The silver nanoclusters/silica composite coating showed effective antimicrobial effect against the tested microbes. However, the intensity of antimicrobial effect was different against different microbes with maximum intensity against *S. aureus*. These differences, at a given concentration of silver nano particles/clusters, against different bacterial species has also been reported in literature [83] [171] [172]. Different sensitivity level of Gram positive and Gram negative bacteria is also demonstrated towards other antibacterial agents like quaternary ammonium compounds [46] and triclosan [54]. This could be attributed to the biological differences among different microbial species. Gram negative bacteria have an extra outer lipid membrane which is not present in Gram positive bacteria and thus offer an extra barrier layer for antimicrobial agent to pass through [46] [65].

Generally, antibacterial effect of metal nano particles is attributed to their gradual release from the coated textiles to the surroundings [99]. However, the exact mechanism of antimicrobial action of silver nano particles is not agreed upon and is still debated in literature. The detailed discussion has been done in Chapter 2. Briefly, different studies suggest that both silver nano particles as well as silver ions can cause antimicrobial action. Silver nano particles can penetrate through the bacterial cell wall and disrupt the cell functions. Silver ions, on the

other hand, are highly reactive and can bind to the sulphur containing proteins of bacterial cell structure leading to the cell death [112] [74]. It was shown in this study, that silver was released almost entirely in the form of silver ions from silver nanoclusters/silica composite coating. Therefore, the finding of this study support the hypothesis that silver nanoparticles/clusters can be considered as a source of silver ions which are mainly responsible for the bactericidal action. Moreover, silver nanoparticles are considered to undergo a slow reactive dissolution to convert into silver ions. This allows for a controlled release of silver ions compared with other forms of silver (silver salts) applied to textiles. This makes silver nanoparticles more effective antimicrobial agent compared with silver salts at same concentration level [72]. In addition, embedding silver nano particles/clusters in a matrix can provide another degree of control to the release of silver ions that can be helpful in retaining antibacterial activity in the long run. This is also evident from the antibacterial test on samples that were subjected to silver release test for 24 or 72 hours where a good inhibition halo was formed around the samples.

The effect of the silver nanoclusters silica composite coating on wettability of the textile substrates was also evaluated through water contact angle, water sorption and moisture management tests. The loose weave structure of Kevlar® and Vectran® fabrics used in this study was not helpful for water contact angle and moisture management tests, therefore, these tests were performed only on cotton fabric and sorption test was performed both on cotton and Kevlar® fabrics. It can be concluded from the results of these tests that silver nanoclusters/silica composite coating improves water wettability and increases hydrophilicity of the textiles to which it is applied. This is possibly due to the amorphous silica as well as due to porous nature of the composite coating. Generally, hydrophobicity is considered to be helpful in imparting antibacterial properties to textiles as it can prevent moisture penetration/absorption by the textiles to avoid developing favorable conditions for microbial growth [29]. Textile structures (woven, knitted, non-woven etc) themselves are well known to retain enough moisture to facilitate microbial growth. To avoid moisture absorption by the textile, silica based hydrophobic coatings can be obtained through sol-gel process using tetraethoxysilane (TEOS) as a silica precursor [29]. However, it was shown in this study that after coating, the cotton fabric turned into fast absorbing and quick drying fabric. This could be interesting for various applications requiring fast absorption of liquids along with antimicrobial characteristics, for example, wound dressings. The basic purpose of a wound dressing is to protect from infection, absorb blood and other exudate, promote healing and/or apply medicine. To perform these functions, a wound dressing is usually made of three parts: (1) a wound contact layer (2) an absorbent layer and (3) a flexible base material to

provide support [5]. In wound dressing applications, silver nanoclusters/silica composite coating can potentially improve the performance of wound contact layer. The fast absorbing feature of the contact layer due to the composite coating can promote absorption of blood and other liquids to be stored in absorbent layer as well as providing protection against infections due to antimicrobial effect. Another potential application could be outdoor garments or extreme environment clothing where different moisture management properties on inner and outer surface of the garment may be desired. In outdoor garments an inner hydrophilic surface is preferred to absorb sweat from the skin for pleasant feeling whereas a hydrophobic outer surface can give water proof effect to protect from rain [155]. Since co-sputtering of silver nanoclusters/silica coating is carried on one side of the fabric, the hydrophilic properties can be introduced only on the inner side of the fabric along with antibacterial protection guaranteed by silver nanoclusters. In such types of clothing, the color change of the substrate due to coating may become irrelevant because the aesthetic look of the fabric being preserved on outer fabric surface.

Maintaining air permeability of fabrics is important for preserving thermo physiological comfort properties of textiles [155]. Functional finishes applied through traditional wet processes usually decrease air breathability of textiles [99]. A suitable combination of moisture and air permeability of textile products may also be required for various medical and surgical applications [5]. It was shown in this study that silver nanoclusters/silica composite coating applied via co-sputtering technique maintained original air permeability level of the textile substrates. This is an important advantage that plasma based finishing techniques offer compared with wet finishing processes.

Air filtration was another intended application of one of the fabric substrates (ACF) used in this study for which maintaining air permeability was important. The porous as well as conformal nature of the deposited silver nano clusters/silica composite coating may help in maintaining the original air breathability of the fabric substrates. This is highly desirable characteristic required for ACF to maintain its air filtration properties along with being antimicrobial. However, other than evaluating the effect on air permeability, the effect of the coating on surface porosity of ACF would also be helpful to establish how much the filtration capacity of ACF is influenced by the coating. Silver nano particles loading has been reported to slightly decrease the specific surface area of ACF [16]. Specific surface area can be analyzed by Brunauer–Emmett–Teller (BET) method, therefore, it would be helpful further to perform BET analysis which was not performed in this study.

The washing stability of the composite coating on textile substrates was analyzed using two different soap solutions. One was commercial Castile soap and the other one AATCC standard detergent without optical brightener. AATCC detergent caused more dissolution of silver than Castile soap. This could be most probably due to different compositions of the two soap solutions but it implies that silver dissolution may be controlled to some extent by proper soap selection keeping in view the nature of the applied coating. Different behavior of textile coatings towards different detergents has also been reported in literature [41] where varying levels of antimicrobial activities were observed when cotton fabric coated with chitosan was washed with ECE and Tween 20 detergents. Antibacterial activity of coated cotton fabric reduced to half after 5 washing cycles with ECE detergent whereas only a slight reduction in the antimicrobial activity occurred after 5 washing cycles with Tween 20 detergent. The authors attributed this effect to the different interaction of chitosan with two detergents. Chitosan, because of positive charge due to protonated amino groups, can develop strong interactions with anionic detergent like ECE that can result in its removal from the cotton fabric. Whereas washing with nonionic detergent like Tween 20 can result in less removal of chitosan due to lack of any strong interaction between the two and hence antibacterial activity of chitosan was maintained after 5 washes [41]. Therefore, it can be suggested that an appropriate soap selection may possibly result in minimum silver leaching and thus help in prolonging the life of antibacterial coatings.

Sputtering is a physical vapor deposition technique and therefore, applied coating may not develop chemical bonding with the textile substrate. This may results in poor washing stability of the coatings applied to textiles. The washing stability of the coatings deposited on textiles by means of sputtering has been found not to be satisfactory in another study also [113]. *Wang et al* deposited conductive silver coating on nylon fabric to be used as an electrode and tested its performance in an electrocardiograph. Although electrocardiograph signal measured by as deposited textile electrode was equivalent to that of commercial electrode, electrical conductivity of the silver coated nylon fabric decreased greatly even after one washing cycle [113].

Although silver nanoclusters/silica composite coating was not able to withstand significant number of washing cycles, it can be attractive for many applications which do not require washing. Aerospace applications represent one such category where washing of the surfaces made of high performance textiles, for example surfaces of inflatable habitat module, is not performed in space. On the other hand, providing safe and hygienic environment to the astronauts is of utmost importance, especially during prolonged space missions. Kevlar® and

Vectran® fabrics used in this study were intended to be used in inflatable habitat module for space stations. Disposable medical and surgical textile products is another category where washing stability of antibacterial coating is not required. Majority of the textile related health care products are of disposable nature [5].

For aerospace applications, ensuring the mechanical integrity of the structures made of high performance textiles, for example inflatable habitat module, is more important than the ability of any functional coating to withstand repeated washing cycles. Therefore, it is important to ensure that the surface modification/functionalization process does not deteriorate the mechanical properties of the textiles made of high performance fibers like Kevlar® and Vectran®. In this context, the effect of the sputtering process on the mechanical properties of Kevlar® fabric was studied in detail by other project partners and results were published jointly [148]. The tensile and tear strength of the fabric after sputter deposition, both in warp and weft direction of the fabric, were found to be equivalent to the uncoated fabric. A small decrease in the puncture resistance of the fabric was observed after coating whereas abrasion resistance of the fabric increased after sputter coating. The increase in abrasion resistance could be possibly due to increased fiber to fiber friction after coating due to increased roughness introduced on the fiber surface due to coating. These results indicate that the sputtering process did not deteriorate the mechanical properties of the fabric. Rather it enhanced the functional surface properties only which is probably the most desirable characteristic of any surface modification process.

Another important feature of the silver nanoclusters/silica composite is its high thermal stability. It has been demonstrated previously that the coating sputtered on silica and steel substrates was able to retain its antimicrobial properties after heat treatments till 450 °C [173] [174]. High thermal stability of the coating can be highly useful to design fiber based filters that can be thermally regenerated. In this scenario, ACF seems an attractive substrate which was found to have redox adsorption capability for silver nano particles/clusters that can be helpful for producing long lasting antibacterial air filters with thermal regeneration possibilities.

Conclusion

Conclusions and future insights

An antimicrobial silver nanoclusters/silica composite coating was applied on four different textile substrates via an ecofriendly radio frequency (RF) co-sputtering technique. The substrates include cotton fabric to be used in medical textiles, high performance Kevlar® and Vectran® fabrics intended to be used in inflatable habitat module for space applications and activated carbon fabric (ACF) for air filtration. The coating was applied under three conditions by varying the deposition time for 15, 40 and 80 minutes resulting in coating of approximately 60, 150 and 300 nm in thickness on each substrate. The coating was characterized in detail for its morphological, compositional and functional properties.

Morphological analysis by FESEM showed that the coating had granular morphology typical of sputter coatings. The granular morphology was prominent for longer depositions (80 minutes). However, the nature of the underlying fibrous substrate was found to have an influence on coating growth that resulted in morphological differences on the four substrates. FESEM observations revealed that coating was highly conformal to the fiber shapes and silver nano clusters (25-50 nm in size) were uniformly distributed and firmly embedded in the silica matrix of the composite coating on the fiber surface. EDS measurements showed that the coating was mainly composed of silica hosting silver nano clusters. Chemical analysis by XPS confirmed the metallic nature of deposited silver contained in silica. It was concluded from FESEM, EDS and XPS results that the desired silver nano clusters/silica composite coating, where silver nano clusters were uniformly distributed on the fiber surface and embedded in the silica matrix, was successfully deposited on the four textile substrates. XPS investigations also pointed to a possible redox/covalent interaction of silver nano clusters with ACF fabric.

Silver release test, over a period of 3 days, showed a gradual and progressive release of silver ions in water depending upon coating thickness and immersion time in water. It was also found that any impurity present in the substrate that can possibly react with silver can consume silver ions and possibly influence antimicrobial performance of the coating. This was observed for Kevlar® fabric containing considerable amount of sulphur that has high reactivity with silver. In case of ACF, possible redox adsorption of silver on ACF was supposed to be responsible for lower ionic silver release in water. Relatively higher silver was released in artificial sweat than in water due to lower pH. Nevertheless, gradual silver release behavior of the coating may help retain antimicrobial properties for extended period of time as was confirmed by antimicrobial performance of samples subjected to 3 days silver release test. Silver skin permeation results from the other project partners showed that the silver, released from the coating, can permeate through human skin and was detected in the dermis and epidermis of human skin in in-vitro skin permeation test.

The coated textile substrates exhibited effective antimicrobial properties against the tested microbes: *S. aureus* and *S. epidermidis* (Gram positive bacteria), *E. coli* (Gram negative bacterium) and *C. albicans* (a fungus). The intensity of the antimicrobial effect varied depending upon silver ion release profiles from the corresponding substrates as well the nature of the microbes. These findings suggest that silver ions play a leading role in antimicrobial action as there is still discussion in literature about whether these are silver ions or silver particles responsible for antimicrobial mechanism. The findings of this study support the concept that silver nano particles or clusters are actually source of silver ions that are then responsible for biocidal action.

The water contact angle and sorption tests showed that coating imparts hydrophilic properties to the surface due to amorphous silica and porous nature of the coating. Dynamic moisture management properties analysis further confirm that coating renders the fabric surface with fast absorbing and quick drying characteristic which could be desirable for outdoor clothing as well as wound dressings. The air breath ability of the fabric was preserved after coating which is one of the advantages of the adopted technique compared with traditional textile finishing techniques that may results in considerable reduction in air permeability of the fabric due to reduced porosity. This is an attractive feature to maintain thermo physiological comfort of medical textiles as well as textiles used in air filtration, for example ACF. However, the coating showed poor washing stability as it was removed within 10 washing cycles. The two soap solutions, used in this study, were found to cause different dissolution of silver nanoclusters.

Good washing stability is an important feature of the applied coating however, it may not always be required depending upon the type of applications. In aerospace applications ensuring the mechanical strength of the parts made of high performance textiles is more important. The results from the other project partners showed the mechanical properties of the high performance fabrics like Kevlar$^{®}$ were not deteriorated during sputter deposition. This is another advantage compared with traditional textile finishing techniques.

It can be concluded from these results that sputtering, a relatively less explored technique for textiles, offers attractive advantages to functionalize textile surfaces while maintaining their bulk properties. Further research may be focused to introduce different functionalities on textile surfaces by combination of different sputtering materials. For example, silver can be replaced by relatively cheaper metals like copper and zinc and their antimicrobial potential can be explored. The matrix of the composite coating can be changed with some other materials to add another desired functionality depending upon requirements of particular application. Catalytic properties of silver nano clusters obtained by sputtering for dye degradation in textile waste water can be explored. To overcome the poor washing stability of the coating, the matrix of the coating may possibly be achieved by a novel combination of plasma polymerization, another ecofriendly technique, and sputtering. In that case the matrix can be plasma polymerized on the textile surface while metal nano clusters can be deposited by sputtering in a simultaneous single step process. Other than antimicrobial textiles, sputtering holds potential to produce smart textiles (to be used in flexible electronics, super capacitors, batteries etc). In fact initial work on some of the above mentioned future research prospects has already been started that will continue after this dissertation.

References

[1] E-R Kenawy, S.D Worley, and R Broughton, "The chemistry and applications of antimicrobial polymers: a state-of-the-art review," *Biomacromolecules*, vol. 8, pp. 1359-1384, 2007.

[2] Y Gao and R Cranston, "Recent Advances in Antimicrobial Treatments of Textiles," *Textile Research Journal*, vol. 78, pp. 60-72, 2008.

[3] C Brunon et al., "Characterization of plasma eehanced chemical vapor deposition–physical vapor deposition transparent deposits on textiles to trigger various antimicrobial properties to food industry textiles," *Thin Solid Films*, vol. 519, pp. 5838–5845, 2011.

[4] A.R Horrocks and S.C Anand, *Handbook of Technical Textiles*, 1st ed. Cambridge , England: Woodhead Publishing Limited, 2000.

[5] A.J Rigby, S.C Anand, and A.R Horrocks, "Textile materials for medical and healthcare applications," *The Journal of The Textile Institute*, vol. 88, pp. 83-89, 1997.

[6] I Perelshtein et al., "Making the hospital a safer place by sonochemical coating of all its textiles with antibacterial nanoparticles," *Ultrasonics Sonochemistry*, vol. 25, pp. 82-88, 2015.

[7] J Won, M.A Said, and A.M Seyam, "Development of UV protective sheath for high performance fibers for high altitude applications," *Fibers and Polymers*, vol. 14, pp. 647-652, 2013.

[8] [Online]. https://www.nasa.gov/press-release/nasa-to-attach-test-first-expandable-habitat-on-international-space-station

[9] [Online]. http://www.nss.org/adastra/volume25/beam.html

[10] [Online]. https://www.nasa.gov/feature/beam-facts-figures-faqs

[11] N Novikova et al., "Survey of environmental biocontamination on board the International Space Station," *Research in Microbiology*, vol. 157, pp. 5-12, 2006.

[12] L.A Mermel, "Infection prevention and control during prolonged human space travel," *Healthcare Epidemiolgy*, vol. 56, pp. 123-130, 2009.

[13] D.L Pierson, "Microbial contamination of spacecraft," *Gravitational and Space Biology Bulletin*, vol. 14, pp. 1-6, 2001.

[14] D.A Coil et al., "Growth of 48 built environment bacterial isolates on board the International Space Station (ISS)," *PeerJ*, 2016.

[15] J-D Gu, "Microbial colonization of polymeric materials for space applications and mechanisms of biodeterioration: A review," *International Biodeterioration & Biodegradation*, vol. 59, pp. 170–179, 2007.

[16] C Tang, W Sun, and W Yan, "Green and facile fabrication of silver nanoparticles loaded activated carbon fibers with long-lasting antibacterial activity," *RSC Advances*, vol. 4, pp. 523–530, 2014.

[17] P.C, Bianchi, R, Verstraete, W, Vandevivere, "Treatment and reuse of wastewater from the textile wet-processing industry: Review of emerging technologies," *Journal of Chemical Technology and Biotechnology*, vol. 72, pp. 289-302, 1998.

[18] E Bizani, K Fytianos, I Poulios, and V Tsiridis, "Photocatalytic decolorization and degradation of dye solutions and waste waters in the presence of titanium dioxide," *Journal of Hazardous Materials*, vol. 136, pp. 85–94, 2006.

[19] E Ozturk, U Yetis, F.B Dilek, and G.N Demirer, "A chemical substitution study for a wet processing textile mill in Turkey," *Journal of Cleaner Production*, vol. 17, pp. 239–247, 2009.

[20] [Online].   http://www.tevonews.com/features/210-efficient-technology-options-for-textile-dyers?showall=&start=1

[21] [Online].   https://textiles.ncsu.edu/news/2017/01/walmart-innovation-el-shafei/

[22] [Online]. http://www.kornit.com/rolltoroll/rtrprinter/#oht:lang=en-us

[23] M Widodo, A El-Shafei, and P.J Hauser, "Surface nanostructuring of Kevlar fibers by atmospheric pressure plasma-induced graft polymerization for multifunctional protective clothing," *Journal of Polymer Science Part B: Polymer Physics*, vol. 50, pp. 1165–1172, 2012.

[24] D Sun and X Chen, "Plasma modification of Kevlar fabrics for ballistic applications," *Textile eseach Journal*, vol. 82, pp. 1928–1934, 2012.

[25] H Wang et al., "Preparation and characterization of silver nanocomposite textile," *Journal of coating technology and research*, vol. 4, pp. 101-106, 2007.

[26] S Shahidi, M Ghoranneviss, B Moazzenchi, A Rashidi, and M Mirjalili, "Investigation of antibacterial activity on cotton fabrics with cold plasma in the presence of a magnetic field," *Plasma Processes and Polymers*, vol. 4, pp. S1098–S1103, 2007.

[27] I Perelshtein et al., "Sonochemical coating of silver nanoparticles on textile fabrics (nylon, polyester and cotton) and their antibacterial activity," *Nanotechnology*, vol. 19, pp. 1-6, 2008.

[28] A.L Mohamed, M.E El-Naggar, T Shaheen, and A.G Hassabo, "Novel nano polymeric system containing biosynthesized core shell silver/silica nanoparticles for functionalization of cellulosic based material," *Microsystem Technologies*, vol. 22, pp. 979-992, 2016.

[29] J Foksowicz-Flaczyk, J Walentowska, M Przybylak, and H Maciejewski, "Multifunctional durable properties of textile materials modified by biocidal agents in the sol-gel process," *Surface & Coatings Technology*, vol. 304, pp.

160–166, 2016.

[30] C.K Kang et al., "Antibacterial cotton fibers treated with silver nanoparticles andquaternary ammonium salts," *Carbohydrate Polymers*, vol. 151, pp. 1012–1018, 2016.

[31] B Simoncic and D Klemencic, "Preparation and performance of silver as an antimicrobial agent for textiles: A review," *Textile Research Journal*, vol. 86, pp. 210-223, 2015.

[32] J Bruenke, I Roschke, S Agarwal, T Riemann, and A Greiner, "Quantitative comparison of the antimicrobial efficiency of leaching versus nonleaching polymer materials.," *Macromolecular Bioscience*, vol. 16, pp. 647–654, 2016.

[33] G Xi, Y Xiu, L Wang, and X Liu, "Antimicrobial N-halamine coatings synthesized via vapor-phase assisted polymerization," *Journal of Applied Polymer Science*, vol. 132, pp. 1-7, 2015.

[34] K.M Babu and K.B Ravindra, "Bioactive antimicrobial agents for finishing of textiles for health care products," *The Journal of The Textile Institute*, vol. 106, pp. 706–717, 2015.

[35] Y Liu, J Li, X Cheng, X Ren, and T.S Huang, "Self-assembled antibacterial coating by N-halamine polyelectrolytes on a cellulose substrate," *Journal of Materials Chemistry B*, vol. 3, pp. 1446-1454, 2015.

[36] J Luo and Y Sun, "Acyclic N-Halamine Coated Kevlar Fabric Materials: Preparation and Biocidal Functions," *Industrial & Engineering Chemistry Research*, vol. 47, pp. 5291–5297, 2008.

[37] F Hui and C Debiemme-Chouvy, "Antimicrobial N-Halamine polymers and coatings: A review of their synthesis, characterization, and applications," *Biomacromolecules*, vol. 14, p. 585−601, 2013.

[38] X Cheng et al., "Preparation and characterization of antimicrobial cotton fabrics via N-halamine chitosan derivative/poly (2-acrylamide-2-

methylpropane sulfonic acid sodium salt) self-assembled composite films," *Journal of Industrial Textiles*, vol. 46, pp. 1039–1052, 2015.

[39] Y Liu, Y Liu, X Ren, and T.S Huang, "Antimicrobial cotton containing N-halamine and quaternary ammonium groups by grafting copolymerization," vol. 296, pp. 231–236, 2014.

[40] K Choi, M-J Nam, J.Y Kim, J Yoon, and J-C Lee, "Synthesis and characterization of biocidal poly(oxyethylene)s having N-Halamine side groups," *Macromolecular Research*, vol. 19, pp. 1227-1232, 2011.

[41] F Ferrero, M Periolatto, and S Ferrario, "Sustainable antimicrobial finishing of cotton fabrics by chitosan UV-grafting: from laboratory experiments to semi industrial scale-up," *Journal of Cleaner Production*, vol. 96, pp. 244-252, 2015.

[42] D.S Morais, R.M Guedes, and M.A Lopes, "Antimicrobial approaches for textiles: From research to market," *Materials*, vol. 9, pp. 1-21, 2016.

[43] D Stawski et al., "N,N,N-trimethyl chitosan as an efficient antibacterial agent for polypropylene and polylactide nonwovens," *The Journal of The Textile Institute*, vol. 108, pp. 1041-1049, 2016.

[44] A El-Shafei, M ElShemy, and A Abou-Okeil, "Eco-friendly finishing agent for cotton fabrics to improve flame retardant and antibacterial properties," *Carbohydrate Polymers*, vol. 118, pp. 83-90, 2015.

[45] M.M Hassan, "Binding of a quaternary ammonium polyme-grafted-chitosan onto a chemically modified wool fabric surface: assessment of mechanical, antibacterial and antifungal properties," *RSC Advances*, vol. 45, pp. 35497–35505, 2015.

[46] M Tischer, G Pradel, K Ohlsen, and U Holzgrabe, "Quaternary Ammonium Salts and Their Antimicrobial Potential: Targets or Nonspecific Interactions? ," *ChemMedChem*, vol. 7, pp. 22–31, 2012.

[47] M Messaoud, E Chadeau, P Chaudouët, N Oulahal, and M Langlet,

"Quaternary Ammonium-based Composite Particles for Antibacterial Finishing of Cotton-based Textiles," *Journal of Materials Science & Technology*, vol. 30, pp. 19-29, 2014.

[48] Y Liu et al., "Antibacterial efficacy of functionalized silk fabrics by radical copolymerization with quaternary ammonium salts," *Journal of Applied Polymer science*, vol. 133, pp. 1-6, 2016.

[49] D Gao, J Feng, J Maa, B Lüa, and X Jia, "Zinc oxide sol-containing diallylmethyl alkyl quaternary ammonium salt synthesized by sol–gel process: characterization and properties," *The Journal of The Textile Institute*, vol. 106, pp. 593–600, 2015.

[50] H.W Kim, B.R Kim, and Y.H Rhee, "Imparting durable antimicrobial properties to cotton fabrics using alginate–quaternary ammonium complex nanoparticles," *Carbohydrate Polymers*, vol. 79, pp. 1057–1062, 2010.

[51] G Bedoux, B Roig, O Thomas, V Dupont, and B Le Bot, "Occurrence and toxicity of antimicrobial triclosan and by-products in the environment," *Environ. Sci. Pollut. Res.*, vol. 19, pp. 1044–1065, 2012.

[52] R Peila, C Vineis, A Varesano, and A Ferri, "Different methods for b-cyclodextrin/triclosan complexation as antibacterial treatment of cellulose substrates," *Cellulose*, vol. 20, pp. 2115–2123, 2013.

[53] M Orhan, D Kut, and C Gunesoglu, "Improving the antibacterial property of polyethylene terephthalate by cold plasma treatment," *Plasma Chemistry and Plasma Processing*, vol. 32, pp. 293–304, 2012.

[54] M Orhan, D Kut, and C Gunesoglu, "Improving the antibacterial activity of cotton fabrics finished with triclosan by the use of 1,2,3,4-butanetetracarboxylic acid and citric acid," *Journal of Applied Polymer Science*, vol. 111, pp. 1344–1352, 2009.

[55] D Savoia, "Plant-derived antimicrobial compounds: alternatives to antibiotics," *Future Microbiology*, vol. 7, pp. 979–990, 2012.

[56] A Upadhyay, I Upadhyaya, A Kollanoor-Johny, and K Venkitanarayanan, "Combating pathogenic microorganisms using plant-derived antimicrobials: a mini review of the mechanistic basis," *BioMed Research International*, vol. 2014, pp. 1-18, 2014.

[57] S.W Ali, R Purwar, and M Joshi, "Antibacterial properties of Aloe vera gel-finished cotton fabric," *Cellulose*, vol. 21, pp. 2063–2072, 2014.

[58] P Pisitsak and U Ruktanonchai, "Preparation, characterization, and in vitro evaluation of antibacterial sol–gel coated cotton textiles with prolonged release of curcumin," *Textile Research Journal*, vol. 85, pp. 949–959, 2015.

[59] K.B Ravindra and K.M Babu, "Study of antimicrobial properties of fabrics treated with ocimum sanctum l (tulsi) extract as a natural active agent," *Journal of Natural Fibers*, vol. 13, pp. 619–627, 2016.

[60] R Singh, A Jain, S Panwar, D Gupta, and S.K Khare, "Antimicrobial activity of some natural dyes," *Dyes and Pigments*, vol. 66, pp. 99-102, 2005.

[61] M.B Kasiri and S Safapour, "Natural dyes and antimicrobials for green treatment of textiles," *Environmental Chemistry Letters*, vol. 12, pp. 1-13, 2014.

[62] S Islam and F Mohammad, "Natural colorants in the presence of anchors so-called mordants as promising coloring and antimicrobial agents for textile materials," *Sustainable Chemistry & Engineering*, vol. 3, p. 2361−2375, 2015.

[63] B Tang et al., "Functionalization of bamboo pulp fabrics with noble metal nanoparticles," *Dyes and Pigments*, vol. 13, pp. 289-298, 2015.

[64] J Scholz, G Nocke, F Hollstein, and A Weissbach, "Investigations on fabrics coated with precious metals using the magnetron sputter technique with regard to their anti-microbial properties," *Surface & Coatings Technology*, vol. 2005, pp. 252-256, 2005.

[65] I Perelshtein et al., "The sonochemical coating of cotton withstands 65 washing cycles at hospital washing standards and retains its antibacterial properties," *Cellulose*, vol. 20, pp. 1215–1221, 2013.

[66] A Khani and N Talebian, "In vitro bactericidal effect of ultrasonically sol–gel-coated novel CuO/TiO2/PEG/cotton nanocomposite for wound care," *Journal of Coatings Technology and Research*, vol. 14, pp. 651–663, 2017.

[67] I Perelshtein et al., "Ultrasound radiation as a "hrowing stones" technique for the production of antibacterial nanocomposite textiles," *Applied Materils and Interfaces*, vol. 2, pp. 1999-2004, 2010.

[68] C Bianco et al., "Pilot study on the identification of silver in skin layers and urine," *Talanta*, vol. 136, pp. 23-28, 2015.

[69] M.E Samberg, S.J Oldenburg, and N.A Monteiro-Riviere, "Evaluation of silver nanoparticle toxicity in skin in vivo and keratinocytes in vitro," *Environmental Health Perspectives*, vol. 18, pp. 407-413, 2010.

[70] M Ahamed, M.S AlSalhi, and M.K.J Siddiqui, "Silver nanoparticle applications and human health," *Clinica Chimica Acta*, vol. 411, pp. 1841–1848, 2010.

[71] J Liu and R.H Hurt, "Ion release kinetics and particle persistence in aqueous nano-silver colloids," *Environmental Science and Technology*, vol. 44, pp. 2169–2175, 2010.

[72] A Zille et al., "Size and aging effects on antimicrobial efficiency of silver nanoparticles coated on polyamide fabrics activated by atmospheric DBD plasma," *Applied Materials and Interfaces*, vol. 7, pp. 13731-13744, 2015.

[73] W He, Y-T Zhou, W.G Wamer, M.D Boudreau, and J-J Yin, "Mechanisms of the pH dependent generation of hydroxyl radicals and oxygen induced by Ag nanoparticles," *Biomaterials*, vol. 33, pp. 7547-7555, 2012.

[74] T Kruk, K Szczepanowicz, D Kregiel, L Szyk-Warszynska, and P Warszynski, "Nanostructured multilayer polyelectrolyte films with

silvernanoparticles as antibacterial coatings," *Colloids and Surfaces B: Biointerfaces*, vol. 137, pp. 158-166, 2016.

[75] J Fabrega, S Fawcett, J.C Renshaw, and J.R Lead, "Silver nanoparticle impact on bacterial growth: effect of pH, concentration, and organic matter," *Envorinmental science and Technology*, vol. 43, pp. 7285–7290, 2009.

[76] Z Lu, J Xiao, Y Wang, and M Meng, "In situ synthesis of silver nanoparticles uniformly distributed on polydopamine-coated silk fibers for antibacterial application," *Journal of Colloid and Interface Science*, vol. 452, pp. 8–14, 2015.

[77] R Masood, M Miraftab, T Hussain, and V Edward-Jones, "Development of slow release silver-containing biomaterial for wound care applications," *Journal of Industrial Textiles*, vol. 44, pp. 699–708, 2013.

[78] H.B Ahmed and H.E Emam, "Layer by Layer assembly of nanosilver for high performance cotton fabrics," *Fibers and Polymers*, vol. 17, pp. 418-426, 2016.

[79] M Rehan, Mowafi, S Hamada M. Mashaly, A Abou El-Kheir, and Emam H.E, "Multi-functional textile design using in-situ Ag NPs incorporation into natural fabric matrix.," *Dyes and pigments*, vol. 118, pp. 9-17, 2015.

[80] M.R Nateghi and M Shateri-Khalilabad, "Silver nanowire-functionalized cotton fabric," *Carbohydrate Polymers*, vol. 117, pp. 160-168, 2015.

[81] A Yildiz and M Degirmencioglu, "Synthesis of Silver Abietate as an Antibacterial Agent for Textile Applications," *Bioinorganic Chemistry and Applications*, vol. 2015, p. 5, 2015.

[82] F.F Larese et al., "Human skin penetration of silver nanoparticles through intact and damaged skin," *Toxicology*, vol. 255, pp. 33–37, 2009.

[83] S Davidovic et al., "Impregnation of cotton fabric with silver nanoparticles synthesized by dextran isolated from bacterial species Leuconostoc

mesenteroides T3," *Carbohydrate Polymers*, vol. 131, pp. 331-336, 2015.

[84] Z.A Raza et al., "Development of antibacterial cellulosic fabric via clean impregnation of silver nanoparticles," *Journal of Cleaner Production*, vol. 101, pp. 377-386, 2015.

[85] P Kumar, M Govindaraju, S Senthamilselvi, and K Premkumar, "Photocatalytic degradation of methyl orange dye using silver (Ag) nanoparticles synthesized from Ulva lactuca," *Colloids and Surfaces B: Biointerfaces*, vol. 103, pp. 658– 661, 2013.

[86] D.M Mitrano et al., "Presence of nanoparticles in wash water from conventional silver and nano-silver textiles," *Nano*, vol. 8, pp. 7208–7219, 2014.

[87] C Lorenz et al., "Characterization of silver release from commercially available functional (nano) textiles," *Chemosphere*, vol. 89, pp. 817-824, 2012.

[88] T.M Benn and A.P Westrehoff, "Nanoparticle silver released into water from commercially available sock fabrics," *Environmental Science and Technology*, vol. 42, pp. 4133–4139, 2008.

[89] M.E Quadros et al., "Release of silver from nanotechnology-based consumer products for children," *Environmental Science and Technology*, vol. 47, pp. 8894 - 8901, 2013.

[90] A.B Stefaniak et al., "Dermal exposure potential from textiles that contain silver nanoparticles," *International Journal of Occupational and Environmental Health*, vol. 20, pp. 221-234, 2014.

[91] N von Goetz et al., "Migration of Ag- and TiO2-(Nano)particles from textiles into artificial sweat under physical stress: experiments and exposure modeling," *Environmental Science & Technology*, vol. 47, p. 9979−9987, 2013.

[92] Y Yan, H Yang, J Li, X Lu, and C Wang, "Release behavior of nano-silver

textiles in simulated perspiration fluids," *Textile Research Journal*, vol. 82, pp. 1422-1429, 2012.

[93] S-j Yu, Y-g Yin, J-b Chao, M-h Shen, and J-f Liu, "Highly Dynamic PVP-Coated Silver Nanoparticles in Aquatic Environments: Chemical and Morphology Change Induced by Oxidation of Ag0 and Reduction of Ag+," *Environmental Science & Technology*, vol. 48, p. 403−411, 2014.

[94] I Perelshtein et al., "antibacterial properties of an in situ generated and simultaneously deposited nanocrystalline ZnO on fabrics," *Applied Materials and Interfaces*, vol. 1, pp. 361–366, 2009.

[95] P Petkova, A Francesko, I Perelshtein, A Gedanken, and T Tzanov, "Simultaneous sonochemical-enzymatic coating of medical textiles with antibacterial ZnO nanoparticles," *Ultrasonics Sonochemistry*, vol. 29, pp. 244-250, 2016.

[96] S Brzeziński, D Kowalczyk, B Borak, M Jasiorski, and A Tracz, "Nanocoat finishing of polyester/cotton fabrics by the sol-gel method to improve their wear resistance," *Fibers & Textiles in Eastern Europe*, vol. 6, pp. 83-88, 2011.

[97] B Mahltig, H Haufe, and H Bottcher, "Functionalisation of textiles by inorganic sol–gel coatings," *Journal of Material Chemistry*, vol. 15, pp. 4385–4398, 2005.

[98] B Mahltig, "Hydrophobic sol–gel-based coating agent for textiles: improvement by solvothermal treatment," *The Journal of The Textile Institute*, vol. 102, pp. 455–459, 2011.

[99] B Tomsic et al., "Sol–gel coating of cellulose fibres with antimicrobial and repellent properties," *J Sol-Gel Sci Technol*, vol. 47, pp. 44-57, 2008.

[100] A Sobczyk-Guzenda et al., "Morphology, photocleaning and water wetting properties of cotton fabrics, modified with titanium dioxide coatings synthesized with plasma enhanced chemical vapor deposition technique," *Surface & Coatings Technology*, vol. 217, pp. 51−57, 2013.

[101] M.L Gulrajania and D.D Gupta, "Emerging techniques for functional finishing of textiles," *Indian Journal of Fibre & Textile Research*, vol. 36, pp. 388-397, 2011.

[102] Y Chu, X Chen, D.W Sheel, and J.L Hodgkinson, "Surface modification of aramid fibers by atmospheric pressure plasma-enhanced vapor deposition," *Textile Research Journal*, vol. 84, pp. 1288-1297, 2014.

[103] M Karaman and T Ucar, "Enhanced mechanical properties of low-surface energy thin films by simultaneous plasma polymerization of fluorine and epoxy containing polymers," *Applied Surface Science*, vol. 362, pp. 210-216, 2016.

[104] J Gilabert-Porres et al., "Design of a nanostructured active surface against gram-positive and gram-negative bacteria through plasma activation and in situ silver reduction," *Applied Materials & Interfaces*, vol. 8, p. 64−73, 2015.

[105] JH Yim et al., "Development of antimicrobial coatings by atmospheric pressure plasma using a guanidine-based precursor," *ACS Applied Materials & Interfaces*, vol. 5, p. 11836−11843, 2013.

[106] M Drábik, J Pešička, H Biederman, and D Hegemann, "Long-term aging of Ag/a-C:H:O nanocomposite coatings in air and in aqueous environment," *Science and Technology of Advanced Materials*, vol. 16, pp. 1-17, 2015.

[107] A.Y Nikiforov et al., "Atmospheric pressure plasma deposition of antimicrobial coatings on non-woven textiles," *Eur. Phys. J. Appl. Phys.*, vol. 75, pp. 1-6, 2016.

[108] Q Wei, Y Xu, and Y Wang, "Textile surface functionalization by physical vapor deposition (PVD)," in *Surface Modification of Textiles*. United Kingdom: Woodhead Publishing Limited, 2009, pp. 58-90.

[109] M.I Mejía et al., "Magnetron-sputtered ag surfaces. New evidence for the nature of the ag ions intervening in bacterial inactivation," *Applied Materials and Interfaces*, vol. 2, pp. 230-235, 2010.

[110] J Yip, S Jiang, and C Wong, "Characterization of metallic textiles deposited by magnetron sputtering andtraditional metallic treatments.," *Surface & Coatings Technology*, vol. 204, pp. 380–385, 2009.

[111] Y Wu et al., "Surface functionalization of nanostructured LaB6-coated Poly Trilobalfabric by magnetron sputtering," *Applied Surface Science*, vol. 384, pp. 413–418, 2016.

[112] S.L Jiang, W.F Qin, R.H Guo, and L Zhang, "Surface functionalization of nanostructured silver-coated polyester fabric by magnetron sputtering," *Surface & Coating Technology*, vol. 204, pp. 3662–3667, 2010.

[113] R.X Wang, M Tao, Y Wang, G.F Wang, and S.M Shang, "Microstructures and electrical conductance of silver nanocrystalline thin films on flexible polymer substrates," *Surface & Coatings Technology*, vol. 204, pp. 1206–1210, 2010.

[114] Q.F Wei, F.L. Huang, D.Y. Hou, and Y.Y Wang, "Surface functionalisation of polymer nanofibres by sputter coating of titanium dioxide," *Applied Surface Science*, vol. 252, pp. 7874-7877, 2006.

[115] Q.F Wei, H Ye, D.Y Hou, H.B Wang, and W.D Gao, "Surface Functionalization of Polymer Nanofibers by Silver Sputter Coating," *Journal of Applied Polymer Science*, vol. 99, pp. 2384–2388, 2006.

[116] F Liu, S Shang, Y Duan, and L Li, "Electrical and optical properties of polymer-au nanocomposite films synthesized by magnetron cosputtering," *Journal of Applied Polymer Science*, vol. 123, pp. 2800-2804, 2012.

[117] Q Wei, Q Xu, Y Cai, and Y wang, "Evaluation of the interfacial bonding between fibrous substrate and sputter coated copper," *Surface & Coatings Technology*, vol. 202, pp. 4673–4680, 2008.

[118] J.M Lackner, W waldhauser, R Major, B Major, and F Bruckert, "Hemocompatible pulsed laser deposited coatings on polymers," *Biomedical Technology*, vol. 55, pp. 57-64, 2010.

[119] W.A Daoud, J.H Xin, Y.H Zhang, and C.L Mak, "Pulsed laser deposition of superhydrophobic thin Teflon films on cellulosic fibers," *Thin Solid Films*, vol. 515, pp. 835–837, 2006.

[120] A.C Popescu et al., "Radical modification of the wetting behavior of textiles coated with ZnO thin films and nanoparticles when changing the ambient pressure in the pulsed laser deposition process," *Journal of Applied Physics*, vol. 110, pp. 1-8, 2011.

[121] A Krämer, C Kunz, S Gräf, and F.A Müller, "Pulsed laser deposition of anatase thin films on textile substrates," *Applied Surface Science*, vol. 353, pp. 1046–1051, 2015.

[122] D Dellasega et al., "Nanostructured Ag4O4 films with enhanced antibacterial activity," *Nanotechnology*, vol. 19, p. 6, 2008.

[123] D Salz, R Lamber, M Wark, A Baalmann, and N Jaeger, "Metal clusters in plasma polymer matrices Part II.Silver clusters," *Physical Chemistry and Chemical Physics*, vol. 1, pp. 4447-4451, 1999.

[124] T Peter et al., "Metal/polymer nanocomposite thin films prepared by plasma polymerization and high pressure magnetron sputtering," *Surface & Coatings Technology*, vol. 205, pp. S38–S41, 2011.

[125] B Despax and P Raynaud, "Deposition of ''Polysiloxane'' thin films containing silver particles by an RF asymmetrical discharge.," *Plasma processes and polymers*, vol. 4, pp. 127-134, 2007.

[126] E Korner et al., "Formation and distribution of silver nanoparticles in a functional plasma polymer matrix and related agr release properties," *Plasma Processes and Polymers*, vol. 7, pp. 619-625, 2010.

[127] P Hlı´dek, H Biederman, A Choukourov, and D Slavı´nska´, "Behavior of polymeric matrices containing silver inclusions, 2 – oxidative aging of nanocomposite Ag/C:H and Ag/C:H:O films," *Plasma Processes and Polymers*, vol. 6, pp. 34-44, 2009.

[128] W.E Marton and J.W.S Hearle, *Physical properties of textile fibers*. Cambridge, England: Woodhead Publishing Limited, 2008.

[129] K.A Asanovic, D.D Cerovic, T.V Mihailovic, M.M Kostic, and M Reljic, "Quality of clothing fabrics in terms of their comfort propertie," *Indian journal of fiber and textile research*, vol. 40, pp. 363-372, 2015.

[130] S Rebouillat, J.C.M Peng, and J-B Donnet, "Surface structure of Kevlar fiber studied by atomic force microscopy and inverse gas chromatography," *Polymer*, vol. 40, pp. 7341–7350, 1999.

[131] J.Z Wang, D.A Dillard, and T.C Ward, "Temperature and Stress Effects in the Creep of Aramid Fibers Under Transient Moisture Conditions and Discussions on the Mechanisms," *Journal of Polymer Science: Part B: Polymer Physics*, vol. 30, pp. 1391-1400, 1992.

[132] J Lim, J.Q Zheng, K Masters, and W.W Chen, "Effects of gage length, loading rates, and damage on the strength of PPTA fibers," *International Journal of Impact Engineering*, vol. 38, pp. 219-227, 2011.

[133] T Ai, R Wang, and W Zhou, "Effect of grafting alkoxysilane on the surface properties of kevlar fiber," *Polymer Composites*, vol. 28, pp. 412-416, 2007.

[134] [Online].   http://www.dupont.com/products-and-services/fabrics-fibers-nonwovens/fibers/uses-and-applications/aerospace-marine-rail.html

[135] Y.S Lee, E.D Wetzel, and N.J Wagner, "The ballistic impact characteristics of Kevlar woven fabrics impregnated with a colloidal shear thickening fluid," *Journal of Materials Science*, vol. 38, pp. 2825–2833, 2003.

[136] D Cadogan, C Sandy, and M Grahne, "Development and evaluation of the mars pathfinder inflatable airbag landing system," *Acta Astronautica*, vol. 50, pp. 633–640, 2002.

[137] Y Liu et al., "Structural evolution and degradation mechanism of Vectran fibers upon exposure to UV-radiation," *Polymer Degradation and Stability*,

vol. 98, pp. 1744-1753, 2013.

[138] C.K Saw, G Collins, J Menczel, and M Jaffe, "Thermally induced reorganization in LCP fibers - Molecular origin of mechanical strength," *Journal of Thermal Analysis and Calorimetry*, vol. 93, pp. 175–182, 2008.

[139] D.E Beers and J.E Ramirez, "Vectran high-performance fibre," *The Journal of textile Institute*, vol. 81, pp. 561-574, 1990.

[140] D.A Shockey, R.S Piascik, B.J Jensen, and L.S, Sutter, J.K Hewes, "Textile Damage in Astronaut Gloves," *J Fail. Anal. and Preven.*, vol. 13, pp. 748–756, 2013.

[141] http://www.vectranfiber.com/.

[142] M Tanaka and Y Moritaka, "Single bumper shields based on Vectran fibers," *Advances in Space Research*, vol. 34, pp. 1076–1079, 2004.

[143] C Balagna et al., "Antibacterial coating on polymer for space application," *Materials Chemistry and Physics*, vol. 135, pp. 714-722, 2012.

[144] M.R.C Marques, R Loebenberg, and M Almukainzi, "Simulated Biological Fluids with Possible Application in Dissolution Testing," *Dissolution Technologies*, vol. 18, pp. 15-28, 2011.

[145] "National Committee for Clinical Laboratory Standard Performance Standards for Antimicrobial Disk Susceptibility Tests, Approved Standard, NCCLS M2-A9,9th ed., Clinical and Laboratory Standards Institute, Wayne, PA, USA, 2006,".

[146] "AATCC 195-2011, Liquid Moisture Management Properties of Textile Fabrics".

[147] M Irfan et al., "Antimicrobial functionalization of cotton fabric with silver nanoclusters/silica composite coating via RF co-sputtering technique," *Cellulose*, vol. 24, pp. 2331–2345, 2017.

[148] C Balagna et al., "Characterization of antibacterial silver nanocluster/silica composite coating on high performance Kevlar® textile," *Surface & Coatings Technology*, vol. 321, pp. 438–447, 2017.

[149] S Sun, J Sun, L Yao, and Y Qiu, "Wettability and sizing property improvement of raw cotton yarns treated with He/O2 atmospheric pressure plasma jet," *Applied Surface Science*, vol. 257, pp. 2377–2382, 2011.

[150] D Mihailović et al., "Functionalization of cotton fabrics with corona/air RF plasma and colloidal TiO2 nanoparticles," *Cellulose*, vol. 18, pp. 811–825, 2011.

[151] R Rahal, T Pigot, D Foix, and S Lacombe, "Photocatalytic efficiency and self-cleaning properties under visible light of cotton," *Applied Catalysis B: Environmental*, vol. 104, pp. 361–372, 2011.

[152] N.Y Hebalkar, S Acharya, and T.N Rao, "Preparation of bi-functional silica particles for antibacterial and self cleaning surfaces," *Journal of Colloid and Interface Science*, vol. 364, pp. 24-30, 2011.

[153] Y.W Lu et al., "Formation and luminescent properties of face-centered-cubic Si nanocrystals in silica matrix by magnetron sputtering with substrate bias," *Applied physics letters*, vol. 90, pp. 1-4, 2007.

[154] N.D Jayram et al., "Highly monodispersed Ag embedded SiO2 nanostructured thin filmfor Sensitive SERS substrate: Growth, characterization and Detection of dye moloecules," *RSC advances*, vol. 5, pp. 46229-46239, 2015.

[155] M Periolatto, A Basit, A Ferri, and B Roberta, "Wettability and comfort of cellulosic materials modified by photo grafting of non-fluorinated oligomers," *Cellulose*, vol. 23, pp. 1447–1458, 2016.

[156] Q Wang, S Kaliacuine, and A Ait-kadi, "Catalytic crafting: a new technique for polymer-fiber composites. III. polyethylene-plasma-treated kevlar fibers composites: analysis of the fiber surface," *Journal of Applied Polymer Science*, vol. 48, pp. 121-136, 1993.

[157] L Xing et al., "Enhanced interfacial properties of domestic aramid fiber-12 via high energy gamma ray irradiation," *Composites: Part B*, vol. 69, pp. 50–57, 2015.

[158] M Su, A Gu, G Liang, and L Yuan, "The effect of oxygen-plasma treatment on Kevlar fibers and the properties of Kevlar fibers/bismaleimide composites," *Applied Surface Science*, vol. 257, pp. 3158–3167, 2011.

[159] F Guo, Z-Z Zhang, W-M Liu, F-H Su, and H-J Zhang, "Effect of plasma treatment of Kevlar fabric on the tribological behavior of Kevlar fabric/phenolic composites," *Tribology International*, vol. 42, pp. 243–249, 2009.

[160] B Thalmann, A Voegelin, B Sinnet, E Morgenroth, and R Kaegi, "Sulfidation Kinetics of Silver Nanoparticles Reacted with Metal Sulfides," *Environ. Sci. Technol.*, vol. 48, p. 4885−4892, 2014.

[161] C.L Doolettea, M.J McLaughlin, J.K Kirby, and D.A Navarro, "Bioavailability of silver and silver sulfide nanoparticles to lettuce(Lactuca sativa): Effect of agricultural amendments on plant uptake," *Journal of Hazardous Materials*, vol. 300, pp. 788–795, 2015.

[162] M Ferraris et al., "Effect of thermal treatments on sputtered silver nanocluster/silica composite coatings on soda-lime glasses: ionic exchange and antibacterial activity," *Journal of Nanoparticle Research*, vol. 14, pp. 1-19, 2012.

[163] J Liu, J Liu, W Song, F Wang, and Y Song, "The role of electronic interaction in the use of Ag and Mn3O4 hybrid nanocrystals covalently coupled with carbon as advanced oxygen reduction electrocatalysts," *Journal of Materials Chemistry A*, vol. 2, pp. 17477–17488, 2014.

[164] F.P Van Der Zee, I.A.E Bisschops, and G Lettinga, "Activated carbon as an electron acceptor and redox mediator during the anaerobic biotransformation of azo dyes," *Environmental Science & Technology*, vol. 37, pp. 402-408, 2003.

[165] M.Y, Resch, S Bashouti et al., "Functionalization of silver nanowires surface using Ag−C bonds in a, sequential reductive method," *Applied Materials and Interfaces*, vol. 7, p. 21657−21661, 2015.

[166] X Song et al., "Surface activated carbon nanospheres for fast adsorption of silver ions from aqueous solutions," *Journal of Hazardous Materials*, vol. 194, pp. 162–168, 2011.

[167] A Bras et al., "Infl uence of the nanotechnological process of chemical modifi cation on the antimicrobial activity and biodegradability of textile fi bres," *Tekstilec*, vol. 60, pp. 14-24, 2017.

[168] K Jamuna-Thevi, S.A Bakar, S Ibrahim, N Shahab, and M.R.M Toff, "Quantification of silver ion release, in vitro cytotoxicity and antibacterial properties of nanostuctured Ag doped TiO2 coatings on stainless steel deposited by RF magnetron sputtering," *Vacuum*, vol. 86, pp. 235-241, 2011.

[169] R George, S Merten, T.T Wang, P Kennedy, and P Maitz, "In vivo analysis of dermal and systemic absorption of silver nanoparticles through healthy human skin," *Australasian Journal of Dermatology*, vol. 55, pp. 185-190, 2014.

[170] C Bianco et al., "In vitro percutaneous penetration and characterization of silver from silver-containing textiles," *International Journal of Nanomedicine*, vol. 10, pp. 1899–1908, 2015.

[171] A.K Suresh et al., "Silver nanocrystallites: Biofabrication using shewanella oneidensis, and an evaluation of their comparative toxicity on Gram-negative and Gram-positive bacteria," *Environ. Sci. Technol.*, vol. 44, pp. 5210–5215, 2010.

[172] C Losasso et al., "Antibacterial activity of silver nanoparticles: sensitivity of different Salmonella serovars," *Frontiers in Microbiology*, vol. 5, pp. 1-9, 2014.

[173] M Ferraris et al., "Chemical, mechanical, and antibacterial properties of

silver nanocluster–silica composite coatings obtained by sputtering," *Advanced engineering materials*, vol. 12, pp. B276-B282, 2010.

[174] M Ferraris et al., "Antibacterial silver nanocluster/silica composite coatings on stainless steel," *Applied Surface Science*, vol. 396, pp. 1546–1555, 2017.

[175] A Gao et al., "The effects of titania nanotubes with embedded silver oxide nanoparticles on bacteria and osteoblasts," *Biomaterials*, vol. 35, pp. 4223-4235, 2014.